JPL PUBLICATION 86-21

Centroid Tracking With Area Array Detectors

T. A. Glavich

June 1, 1986

Prepared for
U.S. Department of Defense
and
National Aeronautics and
Space Administration
by
Jet Propulsion Laboratory
California Institute of Technology
Pasadena, California

The research described in this publication was carried out by the Jet Propulsion Laboratory, California Institute of Technology, and was sponsored by the U.S. Department of Defense and the National Aeronautics and Space Administration.

SUMMARY

This report presents a summary of the development of a computer program (ALGEVAL) to simulate the position estimating behavior of a centroid estimator algorithm using data typical of optical point spread function data recorded by an area array detector.

Typical results are shown in a primarily graphical format of varying detector properties and optical point spread function types. The program will generate point spread functions typical of those generated by most optical systems such as radially symmetric and elliptical Gaussian functions from laser systems, Airy functions from refractive systems, Sinc^2 functions from systems with retangular apertures, as well as functions defined by radial polynomials. Point spread functions typical of obscured systems may also be generated.

The detector parameters currently available for study include: read noise mean value, dark current mean value and spatial variation, charge transfer efficiency and point spread function location, saturation level, signal level and pixel size.

The program is capable of calculating any order centroid using an array size from 2 x 2 to 15 x 15 pixels. Prior to calculating the centroid the program is capable of subtracting a threshold value based on a user selected value, rms or maximum noise or signal value.

The output of the program is either a performance map, showing performance variation in a pixel, or histogram data showing performance of a number of cases as a user selected parameter (such as matrix size or a detector parameter) is varied. Tabular output showing detailed statistical behavior is also available.

Conclusions reached as a result of this work include:

1. Nonlinear position estimate bias results from a matrix size that is smaller than the point spread function. However, this bias is deterministic and can be calibrated.

2. Dark current and read noise introduce bias errors in addition to contributing to the variance of the estimate.

3. Thresholds reduce the effect of additive noise sources by converting part of the variance to a deterministic bias which can then be removed or calibrated.

4. The program has been successful in allowing the exploration of the sensitivity of position estimate bias and variance to noise sources, thresholds and point spread function types.

5. A capability now exists for doing optical system-detector parameter trade-offs during the system design stage and optimizing both to achieve acceptable system performance at minimum cost.

A number of further developments are recommended. The noise models used must be verified and improved, bias removal techniques need to be better defined, additional algorithm types need to be investigated, and the detector system model needs to be expanded to include additional noise sources.

Contents

Tables

ABSTRACT

A computer program (ALGEVAL) has been developed to simulate the position estimating behavior of a centroid estimator algorithm using data typical of optical point spread function data recorded by an area array detector. Typical results are shown of varying detector properties and optical point spread function types. The detector parameters currently available for study include read noise mean value, dark current mean value and spatial variation, charge transfer efficiency and point spread function location, saturation level, signal level and pixel size. The program is capable of calculating any order centroid using an array size from 2 x 2 to 15 x 15 pixels. The output of the program is either a performance map, histogram data or tabular data. A number of further developments are recommended.

I. Introduction

This report contains the results of the development of a program to simulate the performance of an optical array detector used to estimate the centroid position of an optical point spread function. The program was written to provide a basis for defining the performance of area array tracking systems; for providing a test bed to allow exploration of the effects of optical system and detector property design trade-offs; and to allow the development of advanced tracking performance algorithms.

A. Development History

The effort described in this report occurred from July 1985 to January 1986 and was supported primarily by the HIBREL effort of the Acquisition, Tracking and Pointing Project at the Jet Propulsion Laboratory. A large part of the software development relies on previous simulation efforts performed in support of the Space Infrared Telescope Facility (SIRTF). Simulation efforts of similar but simpler problems are documented in Reference 1. These efforts were devoted primarily to developing adaptive algorithms that would maximize pointing accuracy in the presence of an unknown point spread function.

B. Problem Statement

The problem is to simulate the behavior of a detector array viewing an arbitrary point spread function to determine which properties of the detector and optical system limit the accuracy of some measure of the point spread function position on the detector array. There is a substantial history of efforts to determine the best point spread function form and size for a given detector size as well as efforts to determine and improve those detector parameters that limit the estimate bias and variance (Refs. 1-5).

The general problem attacked in this simulation is the determination of the bias and variance of an estimate of the centroid of an arbitrary but known point spread function whose centroid is at a known location on a pixel in an area array detector in the presence of various types of noise and detector nonlinearities. The point spread function size is defined to be much larger than a single pixel. The chief area of interest is point spread functions with a diameter of about 10 pixels.

The point spread function is defined by an array of 150 x 150 points. The detector array is defined as a 15 x 15 array of pixels, any number of which may be used.

The program varies signal level, signal noise properties and all relevant detector properties. The details of available properties are defined in the body of the report. The output of the program is either a map showing actual versus estimated location or graphical and tabular data showing the statistical performance of a set of estimates.

II. Program Description

This section contains a description of the principal segments of the program, the point spread function model, the detector model, the noise generation routines, the position estimation algorithms, and the data output generation routines.

A. Point Spread Function Model Generation

Point Spread Functions (PSF) are generated from a user selected functional form with selectable coefficients. The available functional forms are listed in Table 1.

The PSF is defined as an array of 150 by 150 points. A data file is created by the generating program (PSFGEN) which consists of the point spread function type, the generating coefficients, field location coordinates (currently set to zero but will be used with Optical Analysis Programs such as ACCOS V and CODE V) and the PSF values at all points in the array.

B. Detector Model

The detector is modeled as a 15 x 15 array of pixels centered at an arbitrary (user specified) point in a larger array. The program assumes that charge is read down a column to a serial register and along the serial register to the output amplifier located at (0,0). The following parameters are user selectable and program modifiable:

1. Read Noise - The read noise mean and variance are user selectable parameters. The mean and variance are used as input to a Gaussian Random Number generator. A read noise value is calculated for each pixel every time the detector is accessed.

2. Dark Current - The dark current is defined by its mean (variance is set equal to the mean) and a set of eight shading coefficients. These shading coefficients allow the individual pixel dark current means to vary from the overall mean in a nonrandom pattern. This phenomenon is often encountered in actual array detectors. After the selection of the mean and shading coefficients by the user or subroutines that change the mean, an array that contains the pixel means is initialized. The pixel means are determined by a Gaussian Random Number generator using the overall mean and shading coefficients as inputs. The results are truncated at zero for pixel means that are less than zero.

   New dark current values are calculated for each detector access from the local pixel means, again using a Gaussian random number generator.

3. Response Irregularity - This is modeled in a similar manner as the dark current. The user specifies a variance (the mean is assumed 1) and shading coefficients. An array containing all pixel relative responsivity values is generated. In all subsequent operations each pixel input is weighted by this value, until the

pixel array is reinitialized. The pixel response array is a nonrandom array once it has initially been generated.

4. Charge Transfer Efficiency - The detector type assumed by the program is a Charge Coupled Device. Charge is transferred along a column to a serial register and then along a serial register to an output amplifier. Charge Transfer is specified by the column and row number of the central 15 x 15 pixel and column and serial transfer efficiencies. After the efficiencies are selected by the user, two vectors containing the column and serial efficiencies for each pixel are calculated. Transfer is performed from the highest pixel number to the lowest, with the untransferred charge added to the charge in the following pixel.

5. Saturation Level, Signal Level and Signal Correlation Factor - The signal level defines the mean number of electrons produced by the signal over the entire array.

   The signal in each pixel is calculated by summing the intensity values of those points within the pixel. Then if the signal correlation factor is zero, the value of each pixel is used to define the mean and variance inputs to a Gaussian random number generator. The output of the Gaussian random number generator is the current pixel value. If the signal correlation factor is one, the total input signal level is used for the mean and variance input to the Gaussian Random Number Generator and all pixels are weighted by their proportional value. The total signal is the sum of the deterministic and random portions of the signal.

   These pixel values are multiplied by the responsivity matrix values; the dark current is then added. Each pixel is checked against the saturation level. If the pixel value is greater than the saturation level, equal amounts of the excess are added to the pixels above and below, until the boundary of the pixel array is reached. Any charge spilling over the boundary is lost. It is assumed that the row charge barriers are larger than the column barriers and that no row blooming occurs. The serial register is assumed larger than the pixels so that no row blooming ever occurs.

6. Pixel Size - The pixel size is defined by the user. Currently only square pixels are accommodated; a future update may accommodate rectangular pixels.

   Table 2 lists the program default values for all detector and noise values.

C. System Model

The system model, Figure 1, consists of a point spread function-electron generation program, which incorporates the detector quantum efficiency and optical system. The output of this block is fed to the detector block. The detector block uses previously specified noise and detector characteristics to produce a set of electron values for a 15 x 15 matrix of pixels. Following the detector is the algorithm evaluation. This block consists of a threshold setting algorithm to modify the detector data, a user selectable estimator algorithm, and a set of performance measures.

1. Threshold Types

   There are 6 types of thresholds definable by the user. They are listed in Table 3.

2. Algorithm Types

   The only algorithm type currently in the program is a centroid type. The user selects the centroid order and the matrix size to be used.

III. Simulation Results

A. Interpretation of Simulator Output

The output of the simulation program is almost always graphical in nature and generally is plotted in one of three forms:

1. Pixel Performance Map

   Figure 4 is the first example of this format. For algorithms using an odd number of pixels, a pixel center is defined by the intersection of two center lines. A dotted boundary defines the edge of the pixel. A series of plus (+) marks are plotted at 0.1 pixel coordinates across the pixel. The point spread function centroid is moved to each of the "plus" positions. In turn, the program signal and noise contributions for each pixel are calculated, and the centroid position estimate is determined. The results are plotted as a line starting at the "plus" and ending at the calculated centroid position.

   When noise is present, arrays are initialized once for pixel dark current and response irregularity means but new values of dark current, shot noise, and read noise are calculated for each calculation "plus" position.

   For algorithms using an even number of pixels, the center line intersection defines the intersection of four pixels and the outer boundary, the midpoint of each pixel. This allows the bias plots of odd and even algorithms to have the same general appearance for easy comparison.

   Plot annotation is at the right of the map and is generally self-explanatory. All plots in this report have Algorithm type 2 which is a simple centroid. The threshold type number corresponds to those listed in Table 3.

2. Performance vs. Matrix Size Histogram

These plots (Figure 8 is an example) are histograms showing the position estimate bias and variance for a particular location in the pixel. The pixel location, in fractions of a pixel, used for the calculation is listed in the lower right hand corner of the plot. The statistical data is based on twenty trials for each matrix size. The solid line is the radial position estimate and variance, the broken line shows the y position estimate and the dotted line the x position estimate.

3. Performance vs. Detector Parameter Plots

These plots (Figure 13 is an example) are plots of performance versus some detector parameter, again at a user specified pixel location. They are also based on twenty samples for each parameter variation. As with the histogram data, a solid line is used for the radial estimate, a broken line for the y estimate, and a dotted line for the x estimate.

B. Centroid Performance with Gaussian Point Spread Functions

1. Point Spread Function Definition

The data in this report is grouped by point spread function type. All data following a line spread function plot uses the same point spread function until a new line spread function plot appears.

Figure 2 shows a Gaussian point spread function generated by PSFGEN with the coefficients:

$$a_0 = 1$$
$$a_1 = -1$$
$$a_2 = 5$$
$$a_3 = 0$$

where

$$I = a_0 + a_1 \exp[-a_2(r - a_3)^2]$$

This function has been used as the input point spread function to evaluate the effects of various detector properties and noise types.

Figure 3 shows the line spread functions in x and y and a cross section through the origin.

2. Algorithm Performance - No Noise

Figure 4 shows the behavior of a 15 by 15 first order centroid algorithm in the absence of noise and with no threshold.

Figure 5 shows the results for the same conditions using a 10 x 10 algorithm, Figure 6, for a 7 x 7 algorithm and Figure 7 for a 3 x 3 algorithm. Figure 8 shows a plot of the algorithm position estimate as a function of pixel size when the true centroid location is (0.2, 0.3). A variance is also plotted but in this case there are no random quantities and the variance is uniformly zero. The pixel plots of Figures 4 through 7 give a feel for the magnitude and direction of the errors throughout the CCD. They show the effect of taking small differences of large numbers in the smaller algorithm matrix sizes and that for this PSF a matrix size of 15 gives a nearly bias free estimate in the absence of noise. Figure 8 shows the continuing improvement up to the full 15 x 15 matrix.

These plots demonstrate the importance of having the entire signal within the bounds of the algorithm matrix. The bias in these plots is caused by the "lost" energy in the signal.

3. Influence of Signal Level and Shot Noise

Figure 9 shows a matrix size of 15 tracking in the presence of signal and shot noise only, with a total signal level of 100,000e^-. Figure 10 shows the same with a signal level of 10,000e^- and Figure 11 with 1,000e^-. Figure 12 is a plot of performance versus matrix size for a signal level of 10,000 electrons. Figure 13 is the performance at pixel location (0.2, 0.3) as a function of the signal level. These figures show that quite respectable performance can be obtained even with very low signal levels, if the remaining noise sources can be kept small.

4. Influence of Dark Current on Algorithm Performance

Figure 14 is a full pixel plot of a 15 x 15 algorithm run for the same point spread function as the previous cases with 10 electrons mean dark current, 10^5 electrons total signal, and no threshold. The performance is still good, with the RMS errors being quite small. Figure 15 shows the same with a 10 x 10 algorithm. The algorithm error would dominate for any smaller matrix size. Figure 16 is a plot of the RMS errors and variances of twenty cases as a function of matrix size, again at location (0.2, 0.3). This figure can be compared to the no noise case of Figure 8. The estimate value and bias are virtually the same, but the variance is no longer zero.

Figures 17 and 18 show the effect of increasing the dark current mean to 50 electrons for a 15 x 15 matrix and a 10 x 10 matrix. Figure 19 and 20 are the same for 100 electrons, and Figures 21 and 22 are the same for 200 electrons dark current mean. Adding dark current is the same as adding a constant term plus additional noise to the signal. This creates a bias error towards the origin and increases the estimate variance. This is demonstrated in Figures 23 and 24 which are plots of the RMS errors and variance for position (0.2, 0.3) as a function of dark current mean for matrix sizes 15 and 10.

5. Influence of Read Noise

Figures 25 and 26 show algorithm performance with 10 electrons mean read noise for matrix sizes 15 and 10. Figure 27 shows the effect of increasing the read noise mean, using a matrix size of 15, and Figure 28 shows the same for a matrix size of 10. The read noise acts much like dark current, as far as affecting the bias and variance of the estimate.

6. Influence of Response Irregularity

Figure 29 shows the effect of response irregularity on algorithm performance as a function of matrix size. Figure 30 shows the effect of varying response irregularity on performance for a matrix size of 15. The effect of response irregularity is to impose an additional random and unknown weight on the signal level in each pixel. Random irregularity can be essentially removed by prior calibration. Comparison of these plots to Figure 8, the noise free case, will allow the response irregularity to be specified, or the accuracy of the response irregularity calibration to be calculated. Typical values of pixel response irregularity specifications for CCDs are on the order of 5%. Calibration by multiple flat field reads can bring the uncalibrated random irregularity well below 1%.

7. Influence of Charge Transfer Efficiency

Figure 31 shows the effects of charge transfer efficiency for pixel locations 200 and 300. Decreasing the charge transfer efficiency introduces a bias into the pointing estimate. Typical charge transfer efficiencies are 0.99995 to 0.99999, making this a minor effect except for the most accurate systems using very large arrays.

8. Nominal Performance of a "Good" CCD

Figure 32 shows the nominal performance of a good CCD, operated cold. Figure 33 shows the nominal performance of a CCD being read at a high data date in a relatively noisy environment. Table 4 lists the "Good" CCD and "Noisy" specifications used for the remainder of the report. The Good Case is typical of a slow readout scientific CCD, while the Noisy case is typical of a high bandwidth tracking sensor.

9. Influence of Point Spread Function Size

Figure 34 shows the effect of reducing the point spread function size on the line spread and profiles. Figure 35 shows the effect of a matrix size on the position estimate when the good CCD is used. The estimate bias is a constant for all matrix sizes above 9, but the variance increasees slightly. Figure 36 shows the same data using the noisy CCD. In this case the bias decreases as the matrix grows.

Figure 37 shows the effect of increasing the point spread function size on the line spread and profiles. Figures 38 and 39 are plots of performance versus matrix size for the good and noisy cases. The estimate continues to improve as the matrix size increases for both the good and noisy cases. This set of data demonstrates the importance of the matrix being large enough to encompass the entire point spread function.

C. Centroid Performance as a Function of Point Spread Function Shape

1. Pillbox Point Spread Functions

Figure 40 shows the line spread functions and profiles of a pill box point spread function.

Figure 41 shows the performance of a single pixel using a matrix size of 15 while Figures 42 and 43 show the performance as a function of matrix size for the good and noisy CCD cases. The position estimates of pillbox point spread functions show much greater sensitivity to matrix size than the Gaussian cases.

2. Conical Point Spread Function

Figures 44 through 47 are the same as above for a conical point spread function. The performance is similar to that of the Gaussian point spread function.

3. Airy Function Point Spread Function

This function is what would be expected at best focus of a diffraction limited refractive optical system illuminated by a monochromatic plane wave. Figure 48 shows the line spread function and point spread function profiles. Figure 49 shows a single pixel performance map using the good CCD and a matrix size of 15. Figures 50 and 51 show the performance as a function of matrix size for the good and noisy cases. It appears that for this type of point spread function we are better off operating on the central peak only rather than the central peak in addition to part of the first diffraction ring. If the matrix extended to cover the entire diffraction ring, performance results equal to or better than the matrix size of five would result.

4. Obscured System Point Spread Function

These point spread functions are typical of those at best focus of an optical system with a central obscuration, again illuminated by a monochromatic plane wave. Figures 52-55 show the results for a linear obscuration ratio of 10% and Figures 56-59 for 50%.

This series of plots, along with the Airy function shown previously, shows previously unsuspected behavior. The existence of a central obscuration has an affect on the pointing performance achievable with a given matrix size, if all other parameters are held constant. This program can be used in the design of future systems to optimize the design and permit design trades between optical system design parameters and detector parameters such as matrix size and dark current.

5. Sinc^2 Point Spread Function

Figures 60-63 show the results of a set of sinc^2 point spread functions that are unequal in x and y. These point spread functions are typical of those at best focus of an unobscured optical system with a rectangular entrance pupil illuminated by a monochromatic plane wave.

6. Comparison of Results

Table 5 is a comparison of good CCD results and Table 6 is a comparison of Noisy CCD results. A review of these tables shows that there is an optimum matrix size for each point spread function type and that this matrix size is not significantly affected by the amount of noise. The biases vary significantly but the variances do not.

D. Effect of Thresholds

1. Constant Thresholds

Thresholds are user defined levels subtracted from the value of all pixel counts. Thresholds can be used to remove some of the effects of noise. In Figures 14 through 28, we showed that a dark current or read noise mean created a nonlinear bias towards the algorithm origin in addition to increasing the variance of the position estimate. This bias can be removed or reduced by estimating or measuring the noise mean contribution and subtracting the contribution from the signal.

Figure 64 shows the results of a threshold equal to the dark current mean applied to the good CCD case with a matrix size of 15 viewing the Gaussian point spread function of Figure 2. The results of this figure can be compared directly with Figure 32. Figure 65 shows the effect of changing the threshold from zero to 5 times the dark current mean. Figure 66 shows the same for the Noisy CCD. Figure 67 shows the same for a matrix size of 10. Table 7 shows a typical single point calculation using a threshold.

2. Guard Band Thresholds

Figure 68 shows the effect of using a guard band threshold, the threshold set to the RMS value of an outer ring of pixels for matrix size 10. (This cannot be done for matrix sizes of 14 and 15 due to program storage limitations.) Figure 69 shows this effect as a function of the threshold factor and Figure 70 shows the result as a function of matrix size for a factor of 1. Figure 71 shows the effect of the threshold when the threshold is set to the maximum of the guard band.

3. Matrix Derived Thresholds

Figures 72, 73, and 74 are the same as the guard band threshold cases, except that the threshold base is derived from the outer band of the matrix.

4. Summary of Threshold Performance

Table 8 shows a summary of the threshold performance. This table shows that the best threshold types, based on the maximum value of a guard band, reduce the variance by a factor of 2. The best reduced the bias as well by a factor of almost 10. The effect of thresholds on variance, bias, and stability is an area that needs further work. The results of a threshold at a single point can be misleading as shown in a comparison of Figure 30 (the Gaussian Pixel Map with no threshold) and of Figures 64 and 68 (the same Pixel Map with constant and Guard band threshold).

IV. Conclusions

A. Current Program Utility

1. The program development has been successful to date. The program is proving useful not only in simulating point spread function and detector behavior, but in providng insights into unexpected coupling of detector and optical properties. It will be a valuable system design tool.

2. The program provides the capability of obtaining quantitative limits on tracking performance given a point spread function and a set of detector parameters.

3. System tolerance capabilities are now possible by using the detector parameter variation subroutine.

4. Optimum matrix sizes for any level of bias and variance can be obtained by using the matrix size variation subroutine.

5. Threshold type and value can be determined from the detector characterization data and point spread function information in this program.

6. The program can be used as a valuable tool in developing detector specifications.

B. Tracking Simulation

1. Nonlinear tracking bias results from tracking with a matrix that is smaller than the point spread functions. The bias is deterministic and is removable by calibration.

2. Dark current and read noise introduce bias errors as well as contribute to the tracking position variance. It is important to minimize both of these contributions.

3. Detector response irregularity contributes little to tracking variance but affects the bias so that the apparent tracking algorithm origin is offset from the actual origin. Flat field calibration can remove almost all of this effect.

4. Charge transfer efficiency should not be a significant effect with today's detectors. The effect of slight inefficiencies (less than 1×10^{-5}) is a small pointing bias, with no contribution to the pointing estimate variance.

5. Although no examples were shown, saturation causes entirely erroneous pointing results. The error is nonrecoverable.

6. Thresholds are a useful method of reducing the effects of dark current and noise. The optimum threshold is near the sum of dark current and read noise contribution means. The major effect of a threshold is to convert a portion of the variance into a deterministic bias. This bias can be calibrated or determined by the use of ALGEVAL and removed. Thresholds must be used with great care. The evaluation of the effect of thresholds is not complete.

7. Point Spread Function shape is not a significant factor in pointing performance, as long as the extreme cases such as the pillbox point spread function are avoided.

8. Centroid algorithms yield stable, predictable, pointing estimates. Pointing accuracies of 0.01 pixel or less do not appear to be a significant problem with large point spread functions such as the ones used in this report.

C. Continued Developments

A number of developments need to be added to the program.

1. Noise Models

   The current noise models are based on Gaussian random number generation. The models need to be verified and improved.

2. Bias Removal

   References 1 to 3 discuss techniques of bias removal that were incorporated into other programs. These subroutines need to be added to ALGEVAL for a full analysis capability.

3. Program Accuracy Verification

   The program is based on the use of point spread function values calculated at discrete points. Validation of the technique needs to be performed analytically by integration of the function over pixel boundaries for point spread functions defined by functional forms.

4. Additional Algorithm Types

References 6 and 7 describe a number of other algorithm types, fast algorithms based on less than the full complement of pixels, optimum pointing algorithms, and robust algorithms. These algorithms need to be coded and added to the program for comparison to the centroid algorithm.

5. Detector Model Improvements

The current detector model consists of an array of square pixels. The model needs to be upgraded to allow rectangular pixels with dead bands between pixels. The quantum efficiency needs to be better modeled as does the charge transfer efficiency. Both of these properties are signal dependent. The effect of quantum efficiency hysteresis should also be included.

6. Threshold Evaluation

Further efforts need to be taken in the design and evaluation of thresholds. Overall pixel pointing performance appears to improve with a properly chosen threshold, but only at the expense of the performance at some pixel locations.

V. References

1. Glavich, T. A., An Adaptive Interpolator Algorithm for Area-array Fine Guidance Sensors, SPIE Vol. 485, May 2, 1984.

2. Salomon, P. M. and Glavich, T. A. Image Signal Processing in Subpixel Accuracy Star Trackers, SPIE Vol. 252, P. 64, August 1, 1980.

3. Dennison, E. W. and Stanton, R. H. Ultra-Precise Star Tracking Using Charge Coupled Devices (CCDs), SPIE Vol. 252, P. 54, August 1, 1980.

4. Grossman, S. B. Fine Guidance Sensor Design Optimization for Space Infrared Telescope Facility, SPIE Vol. 500, P. 76, 1984.

5. Grossman, S. B. and Emmons, R. B. Performance Analysis and Size Optimization of Focal Planes for Point-Source Tracking Algorithm Applications, Optical Engineering, Vol. 23, P. 167, March/April 1984.

6. Nowakowski, J. and Elbaum, M. Fundamental Limits in Estimating Light Pattern Position, JOSA 73, P. 1744.

7. Andrews, D. F., Bickel, P. S., Hempel, F. R., Huber, P. J., Rogers, W. H., and Tukeg, J. W. Robust Estimates of Location, 1972, Princeton University Press, Princeton.

Table 1

Point Spread Functional Forms

1. I = A0 + A1*R + A2*R**2 + A3*R**3 + A4*R**4 + A5*R**5
2. I = A0 + A1*X + A2*X**2 + A3*X**3 + A4*X**4 + A5*X**5
   B1*Y + B2*Y**2 + B3*Y**3 + B4*Y**4 + B5*Y**5
3. I = A0 + A1*EXP(-A2*(R-A3)**2)
4. I = A0 + [A1*EXP(-A2*(X-A3)**2)]*[A4*EXP(-A5*(Y-A6)**2)]
5. I = A0 + A1*[J1(2*PI*A3*R)/(2*PI*A3*R)]**2
6. I = A0 + A1*2*[J1(2*PI*A2*R)/(2.*PI*A2*R]**2 -
   2.*A3**2*[J1(2*PI*A3*R)/(2.*PI*A3*R)]**2
7. I = A0 + A1*[SINC(2*PI*A2*X)]**2 + A3*[SINC(2*PI*A4*Y)]**2
8. I(R>A0) = 0
9. I(X>A0) = 0
10. I(Y>A0) = 0
11. DO A POINT BY POINT ADD WITH THE NEXT FUNCTION.
12. DO A POINT BY POINT MULTIPLY WITH THE NEXT FUNCTION

Table 2

DETECTOR AND NOISE DEFAULT VALUES

1. READ NOISE MEAN 10.0000
2. READ NOISE VARIANCE 10.0000
3. DARK CURRENT MEAN 10.0000
4. DARK CURRENT VERTICAL CONSTANTS 0.0000 0.0000 1.0000 8
5. DARK CURRENT HORIZONTAL CONSTANTS 0.0000 0.0000 1.0000 8
6. RESPONSE IRREGULARITY VARIANCE 0.0100
7. RESPONSE VERTICAL SHADING COEFFICIENTS 0.0000 0.0000 1.0000 8
8. RESPONSE HORIZONTAL SHADING COEFFICIENTS 0.0000 0.0000 1.0000 8
9. CHARGE TRANSFER EFFICIENCY - COLUMN 0.999990
10. CHARGE TRANSFER EFFICIENCY - SERIAL 0.999990
11. LOCATION OF PIXEL (8,8) 200, 300
12. SATURATION LEVEL 0.2500E+06
13. SIGNAL LEVEL 0.1000E+06
14. SIGNAL CORRELATION FACTOR 0.0000
15. PIXEL SIZE 15.0000

SHADING EQUATION FORM: K1(I-M)**2 + K2(I-M) + K3

TABLE 3

THRESHOLD MENU

1. NO THRESHOLD
2. USER SUPPLIED NUMBER
3. RMS VALUE OF GUARD BAND TIME USER SUPPLIED FACTOR
4. MAXIMUM VALUE OF GUARD BAND TIMES USER'S SUPPLIED FACTOR
5. RMS VALUE OF MATRIX OUTER BAND TIMES USER SUPPLIED FACTOR
6. MAXIMUM VALUE OF MATRIX OUTER BAND TIMES USER SUPPLIED FACTOR
7. PRINT CURRENT TYPE AND FACTOR

Table 4

Good and Noisy CCD Specifications

Good CCD

Read Noise Mean	$10e^-$
Dark Current Mean	$10e^-$
Response Irregularity	0.01

Noisy CCD

Read Noise Mean	$100e^-$
Dark Current Mean	$50e^-$
Response Irregularity	0.03

Table 5

Good CCD Results at Location 0.2, 0.3

Point Spread Function	**Value at Minimum Bias**	**Minimum Bias**	**Variance at Minimum Bias**	**Matrix Size**	**Fig. No.**
Gaussian	.3376	-.0230	2.2×10^{-5}	15	30
Gaussian - Small	.3128	-.0478	6.1×10^{-6}	10	35
Gaussian - Large	.3145	-.0461	2.4×10^{-5}	15	38
Pillbox	.3709	.0103	2.4×10^{-5}	12	42
Conical	.3587	-.0018	1.8×10^{-5}	9	46
Airy	.3287	-.0319	1.7×10^{-5}	15	50
0.1 Obscured	.3323	-.0283	7.8×10^{-6}	8	54
0.5 Obscured	.3223	-.0383	9.6×10^{-6}	6	58
Sinc^2	.3396	.0210	8.5×10^{-6}	8	62

Table 6

Noisy CCD Results at Location 0.2, 0.3

Point Spread Function	**Value at Minimum Bias**	**Minimum Bias**	**Variance at Minimum Bias**	**Matrix Size**	**Fig. No.**
Gaussian	.3105	.3606	2.8×10^{-3}	14	
Gaussian - Small	.3207	-.0399	1.4×10^{-5}	9	36
Gaussian - Large	.2824	-.0782	4.5×10^{-5}	15	39
Pillbox	.3468	-.0138	1.9×10^{-5}	12	43
Conical	.3531	-.0076	1.5×10^{-5}	11	47
Airy	.3693	.0087	1.0×10^{-5}	8	51
0.1 Obscured	.3191	-.0416	1.1×10^{-5}	8	55
0.5 Obscured	.3478	-.0128	9.2×10^{-6}	6	59
Sinc^2	.3297	-.0307	7.3×10^{-6}	8	63

Table 7
Noise, Signal and Threshold Data

PIXEL ENERGY DISTRIBUTION (PIXMAT)

	1	2	3	4	5	6	7	8
1	0	0	0	0	0	0	0	0
2	0	0	0	0	0	0	0	0
3	0	0	0	0	0	3	15	25
4	0	0	0	0	20	89	210	297
5	0	0	0	21	155	608	1432	2039
6	0	0	5	98	640	2497	5888	8379
7	0	0	20	244	1586	6191	14589	20762
8	0	0	33	364	2373	7268	21835	31067
9	0	0	29	329	2146	8379	19741	28090
10	0	0	13	180	1172	4575	10781	15344
11	0	0	1	59	386	1509	3557	5060
12	0	0	0	7	76	298	705	1005
13	0	0	0	0	5	34	85	119
14	0	0	0	0	0	0	1	6
15	0	0	0	0	0	0	0	0

	9	10	11	12	13	14	15
1	0	0	0	0	0	0	0
2	0	0	0	0	0	0	0
3	20	8	0	0	0	0	0
4	257	133	41	3	0	0	0
5	1753	909	284	53	2	0	0
6	7202	3740	1173	220	22	0	0
7	17848	9268	2907	547	63	0	0
8	26710	13872	4349	821	94	2	0
9	24150	12542	3932	741	86	1	0
10	13190	6848	2149	404	45	0	0
11	4350	2260	707	134	12	0	0
12	863	447	140	24	0	0	0
13	104	53	14	0	0	0	0
14	3	0	0	0	0	0	0
15	0	0	0	0	0	0	0

SHOT NOISE

	1	2	3	4	5	6	7	8
1	0	0	0	0	0	0	0	0
2	0	0	0	0	0	0	0	0
3	0	0	0	0	0	5	12	23
4	0	0	0	0	22	105	189	283
5	0	0	0	16	186	600	1467	2064
6	0	0	4	82	624	2477	5979	8461
7	0	0	19	238	1624	6242	14424	20811
8	0	0	26	381	2383	9386	21769	30837
9	0	0	27	329	2174	8258	19774	28018
10	0	0	6	156	1171	4716	10735	15444
11	0	0	0	55	418	1510	3524	5080
12	0	0	0	5	75	273	672	973
13	0	0	0	0	11	33	72	121
14	0	0	0	0	0	0	1	7
15	0	0	0	0	0	0	0	0

Table 7 (contd)

	9	10	11	12	13	14	15
1	0	0	0	0	0	0	0
2	0	0	0	0	0	0	0
3	24	14	0	0	0	0	0
4	276	151	42	8	0	0	0
5	1781	909	290	54	3	0	0
6	7139	3798	1178	243	26	0	0
7	17822	9280	2904	584	63	0	0
8	26643	14013	4502	801	114	2	0
9	24313	12588	3971	742	92	1	0
10	13188	6928	2174	353	51	0	0
11	4282	2241	696	123	9	0	0
12	860	443	131	24	0	0	0
13	121	67	16	0	0	0	0
14	3	0	0	0	0	0	0
15	0	0	0	0	0	0	0

DARK CURRENT MEAN VARIATION

	1	2	3	4	5	6	7	8
1	45	56	46	59	50	44	52	42
2	54	33	43	40	56	50	53	53
3	50	36	46	50	45	57	59	48
4	49	40	54	56	37	49	47	36
5	44	54	42	48	45	54	50	41
6	49	52	44	51	49	56	51	56
7	46	58	62	46	47	46	60	38
8	48	40	50	52	60	36	51	56
9	45	59	48	59	58	43	47	43
10	49	61	49	52	52	59	30	48
11	47	55	51	40	59	50	50	50
12	52	48	43	49	49	42	54	66
13	50	55	41	48	52	56	56	52
14	48	42	46	57	43	48	55	53
15	58	39	45	45	39	40	48	55

	9	10	11	12	13	14	15
1	47	60	51	49	42	46	45
2	54	45	43	49	52	38	49
3	36	54	53	46	52	44	43
4	55	44	39	44	52	46	36
5	53	60	51	61	54	52	48
6	39	56	38	60	54	43	59
7	55	47	54	43	57	43	44
8	49	45	60	56	47	39	67
9	36	45	48	58	52	54	53
10	39	57	63	58	33	46	48
11	53	42	54	48	47	38	62
12	52	46	45	55	52	52	47
13	46	41	43	49	52	54	42
14	48	52	55	58	47	44	57
15	57	47	42	48	60	39	56

Table 7 (contd)

DARK CURRENT CONTRIBUTION

	1	2	3	4	5	6	7	8
1	43	44	48	64	54	57	53	50
2	51	40	39	41	46	59	60	52
3	52	37	53	51	48	59	66	52
4	58	40	52	64	27	54	44	46
5	50	50	38	43	58	45	42	47
6	60	47	37	48	38	59	57	59
7	57	53	67	41	44	48	76	27
8	47	43	52	45	86	44	46	54
9	40	62	56	53	52	33	48	46
10	47	67	49	60	60	61	31	55
11	54	62	59	39	79	47	50	51
12	52	41	49	59	47	55	59	65
13	51	54	24	40	54	74	44	61
14	59	36	39	58	48	39	45	48
15	73	40	36	49	35	43	50	51

	9	10	11	12	13	14	15
1	44	56	47	45	44	63	43
2	44	41	49	47	60	34	51
3	33	60	61	43	43	51	47
4	58	55	43	45	49	46	39
5	53	62	51	61	59	46	53
6	38	48	28	52	62	42	54
7	61	32	62	45	60	42	41
8	39	44	51	61	38	33	66
9	33	50	40	63	48	42	55
10	41	58	72	56	39	46	55
11	63	38	54	60	53	38	63
12	60	61	43	58	40	56	46
13	49	38	51	48	47	41	48
14	46	48	53	55	43	50	55
15	61	47	36	40	62	40	58

PIXEL RESPONSE IRREGULARITY

	1	2	3	4	5	6	7	8
1	1.27E+00	9.92E-01	7.94E-01	9.54E-01	9.75E-01	1.05E+00	9.88E-01	9.76E-01
2	1.03E+00	8.64E-01	8.75E-01	1.02E+00	8.77E-01	9.59E-01	9.83E-01	8.60E-01
3	9.30E-01	8.88E-01	1.17E+00	9.51E-01	1.10E+00	9.52E-01	1.10E+00	9.75E-01
4	1.02E+00	9.82E-01	1.05E+00	9.73E-01	1.04E+00	9.86E-01	8.19E-01	9.33E-01
5	9.03E-01	9.25E-01	1.00E+00	9.33E-01	9.56E-01	9.78E-01	9.20E-01	1.02E+00
6	1.03E+00	1.06E+00	1.10E+00	9.76E-01	9.26E-01	9.19E-01	1.03E+00	1.05E+00
7	1.14E+00	6.92E-01	7.95E-01	1.00E+00	1.11E+00	8.41E-01	9.78E-01	8.91E-01
8	1.04E+00	9.45E-01	1.01E+00	9.79E-01	1.01E+00	1.05E+00	1.11E+00	9.67E-01
9	1.02E+00	1.02E+00	8.40E-01	1.11E+00	1.15E+00	1.13E+00	9.68E-01	8.77E-01
10	9.56E-01	1.02E+00	9.37E-01	1.08E+00	8.55E-01	9.07E-01	1.12E+00	1.06E+00
11	1.04E+00	8.38E-01	1.10E+00	1.03E+00	1.17E+00	8.90E-01	8.68E-01	8.99E-01
12	1.05E+00	9.32E-01	1.19E+00	9.99E-01	9.49E-01	1.02E+00	1.03E+00	9.26E-01
13	9.94E-01	1.03E+00	1.04E+00	1.05E+00	8.95E-01	8.98E-01	1.08E+00	9.99E-01
14	9.74E-01	1.09E+00	9.61E-01	9.49E-01	9.65E-01	9.08E-01	8.26E-01	1.19E+00
15	1.20E+00	8.78E-01	9.83E-01	1.14E+00	8.23E-01	1.02E+00	8.50E-01	1.02E+00

Table 7 (contd)

	9	10	11	12	13	14	15
1	9.27E-01	9.61E-01	1.14E+00	9.93E-01	1.20E+00	1.06E+00	1.09E+00
2	8.56E-01	9.62E-01	1.08E+00	9.21E-01	1.13E+00	9.49E-01	1.13E+00
3	1.03E+00	1.04E+00	1.17E+00	1.01E+00	8.66E-01	1.06E+00	9.82E-01
4	1.06E+00	1.02E+00	9.31E-01	9.13E-01	1.09E+00	8.94E-01	1.02E+00
5	7.94E-01	1.12E+00	9.54E-01	8.94E-01	9.98E-01	9.04E-01	9.67E-01
6	9.63E-01	1.10E+00	9.57E-01	1.09E+00	1.10E+00	9.42E-01	1.01E+00
7	9.77E-01	1.04E+00	8.59E-01	1.15E+00	9.77E-01	7.45E-01	1.03E+00
8	1.05E+00	9.24E-01	8.92E-01	1.04E+00	9.49E-01	9.90E-01	9.43E-01
9	8.18E-01	1.00E+00	9.59E-01	9.08E-01	9.41E-01	9.12E-01	1.13E+00
10	9.62E-01	9.54E-01	9.28E-01	9.07E-01	1.05E+00	8.86E-01	1.05E+00
11	1.04E+00	8.84E-01	9.98E-01	9.69E-01	1.18E+00	1.07E+00	1.06E+00
12	9.62E-01	1.02E+00	1.03E+00	1.03E+00	1.01E+00	7.91E-01	1.17E+00
13	9.62E-01	1.09E+00	8.87E-01	1.07E+00	1.04E+00	9.36E-01	1.16E+00
14	9.62E-01	8.91E-01	8.96E-01	1.03E+00	1.14E+00	9.70E-01	1.04E+00
15	1.11E+00	9.73E-01	1.02E+00	1.01E+00	8.93E-01	9.53E-01	1.02E+00

PIXEL RESPONSE VARIATION

	1	2	3	4	5	6	7	8
1	1.27E+00	9.92E-01	7.94E-01	9.54E-01	9.75E-01	1.05E+00	9.88E-01	9.76E-01
2	1.03E+00	8.64E-01	8.75E-01	1.02E+00	8.77E-01	9.59E-01	9.83E-01	8.60E-01
3	9.30E-01	8.88E-01	1.17E+00	9.51E-01	1.10E+00	9.52E-01	1.10E+00	9.75E-01
4	1.02E+00	9.82E-01	1.05E+00	9.73E-01	1.04E+00	9.86E-01	8.19E-01	9.33E-01
5	9.03E-01	9.25E-01	1.00E+00	9.33E-01	9.56E-01	9.78E-01	9.20E-01	1.02E+00
6	1.03E+00	1.06E+00	1.10E+00	9.76E-01	9.26E-01	9.19E-01	1.03E+00	1.05E+00
7	1.14E+00	6.92E-01	7.95E-01	1.00E+00	1.11E+00	8.41E-01	7.78E-01	8.91E-01
8	1.04E+00	9.45E-01	1.01E+00	9.79E-01	1.01E+00	1.05E+00	1.11E+00	9.67E-01
9	1.02E+00	1.02E+00	8.40E-01	1.11E+00	1.15E+00	1.13E+00	9.68E-01	8.77E-01
10	9.56E-01	1.02E+00	9.37E-01	1.08E+00	8.55E-01	9.07E-01	1.12E+00	1.06E+00
11	1.04E+00	8.38E-01	1.10E+00	1.03E+00	1.17E+00	8.90E-01	8.68E-01	8.99E-01
12	1.05E+00	9.32E-01	1.19E+00	9.99E-01	9.49E-01	1.02E+00	1.03E+00	9.26E-01
13	9.94E-01	1.03E+00	1.04E+00	1.05E+00	8.95E-01	8.98E-01	1.08E+00	9.99E-01
14	9.74E-01	1.09E+00	9.61E-01	9.49E-01	9.65E-01	9.08E-01	8.26E-01	1.19E+00
15	1.20E+00	8.78E-01	9.83E-01	1.14E+00	8.23E-01	1.02E+00	8.50E-01	1.02E+00

	9	10	11	12	13	14	15
1	9.27E-01	9.61E-01	1.14E+00	9.93E-01	1.20E+00	1.06E+00	1.09E+00
2	8.56E-01	9.62E-01	1.08E+00	9.21E-01	1.13E+00	9.49E-01	1.13E+00
3	1.03E+00	1.04E+00	1.17E+00	1.01E+00	8.66E-01	1.06E+00	9.82E-01
4	1.06E+00	1.02E+00	9.31E-01	9.13E-01	1.09E+00	8.94E-01	1.02E+00
5	7.94E-01	1.12E+00	9.54E-01	8.94E-01	9.98E-01	9.04E-01	9.67E-01
6	9.63E-01	1.10E+00	9.57E-01	1.09E+00	1.10E+00	9.42E-01	1.01E+00
7	9.77E-01	1.04E+00	8.59E-01	1.15E+00	9.77E-01	7.45E-01	1.03E+00
8	1.05E+00	9.24E-01	8.92E-01	1.04E+00	9.49E-01	9.90E-01	9.43E-01
9	8.18E-01	1.00E+00	9.59E-01	9.08E-01	9.41E-01	9.12E-01	1.13E+00
10	9.62E-01	9.54E-01	9.28E-01	9.07E-01	1.05E+00	8.86E-01	1.05E+00
11	1.04E+00	8.84E-01	9.98E-01	9.69E-01	1.18E+00	1.07E+00	1.06E+00
12	9.62E-01	1.02E+00	1.03E+00	1.03E+00	1.01E+00	7.91E-01	1.17E+00
13	9.62E-01	1.09E+00	8.87E-01	1.07E+00	1.04E+00	9.36E-01	1.16E+00
14	9.62E-01	8.91E-01	8.96E-01	1.03E+00	1.14E+00	9.70E-01	1.04E+00
15	1.11E+00	9.73E-01	1.02E+00	1.01E+00	8.93E-01	9.53E-01	1.02E+00

SIGNAL, DARK CURRENT AND NOISE

	1	2	3	4	5	6	7	8
1	43	44	48	64	54	57	53	50
2	51	40	39	41	46	59	60	52
3	52	37	53	51	48	64	79	75
4	58	40	52	64	50	158	199	311
5	50	50	38	59	236	632	1392	2151
6	60	47	42	128	616	2335	6241	8944
7	57	53	82	280	1842	5295	14183	18560
8	47	43	79	418	2496	9938	24155	29870
9	40	62	79	420	2563	9401	19197	24620
10	47	67	55	228	1062	4340	12029	16362
11	54	62	60	96	570	1392	3110	4619
12	52	41	49	64	119	333	750	967
13	51	54	24	40	64	105	121	182
14	59	36	39	58	48	39	47	57
15	73	40	36	49	35	43	50	51

Table 7 (contd)

	9	10	11	12	13	14	15
1	44	56	47	45	44	63	43
2	44	41	49	47	60	34	51
3	58	75	61	43	43	51	47
4	350	210	82	53	49	46	39
5	1468	1085	329	110	62	46	53
6	6911	4217	1156	317	91	42	54
7	17469	9673	2558	720	122	42	41
8	28106	12985	4067	890	146	36	66
9	19928	12670	3849	737	135	43	55
10	12725	6668	2091	377	93	46	55
11	4528	2018	749	180	65	38	63
12	888	513	178	84	40	56	46
13	166	112	66	48	47	41	48
14	49	48	53	55	43	50	55
15	61	47	36	40	62	40	58

CHARGE TRANSFER EFFICIENCIES

ROW	SERIAL
0.9970	0.9980
0.9970	0.9980
0.9970	0.9980
0.9970	0.9980
0.9971	0.9980
0.9971	0.9981
0.9971	0.9981
0.9971	0.9981
0.9971	0.9981
0.9971	0.9981
0.9971	0.9981
0.9971	0.9981
0.9971	0.9981
0.9971	0.9981
0.9972	0.9981

SIGNAL AFTER TRANSFERS

	1	2	3	4	5	6	7	8
1	43	44	48	64	54	57	53	50
2	51	40	39	41	46	59	60	52
3	52	37	53	51	48	64	80	76
4	58	40	52	64	51	159	202	317
5	50	50	38	59	238	639	1408	2170
6	60	47	42	129	623	2352	6269	8968
7	57	53	83	283	1850	5325	14220	18591
8	47	43	80	422	2511	9964	24151	29850
9	40	62	79	423	2572	9405	19186	24587
10	48	67	56	229	1067	4346	12012	16321
11	54	62	60	97	570	1392	3106	4608
12	52	41	49	64	119	333	749	965
13	51	54	24	40	64	105	121	181
14	59	36	39	58	48	39	47	57
15	73	40	36	49	35	43	50	51

Table 7 (contd)

	9	10	11	12	13	14	15
1	44	56	47	45	45	63	43
2	45	41	50	47	60	34	51
3	59	75	61	43	43	51	47
4	353	212	83	53	49	46	39
5	1483	1092	331	110	62	46	53
6	6937	4227	1159	318	91	42	54
7	17485	9669	2559	720	122	42	41
8	28053	12967	4060	888	146	36	66
9	19893	12636	3838	735	135	43	55
10	12690	6646	2084	376	93	46	55
11	4513	2012	746	179	65	38	63
12	885	511	178	84	40	56	46
13	165	112	66	48	47	42	47
14	49	48	53	55	43	50	54
15	61	46	36	40	62	40	57

READ NOISE

	1	2	3	4	5	6	7	8
1	108	96	110	98	107	112	82	79
2	94	77	94	104	111	94	104	91
3	98	106	87	103	105	83	93	91
4	100	93	91	91	108	101	108	100
5	103	110	90	126	121	96	103	101
6	94	103	103	95	109	87	107	88
7	112	96	93	97	102	91	94	117
8	93	97	104	80	97	92	107	106
9	104	114	90	108	111	99	91	100
10	91	92	116	95	100	76	110	103
11	107	101	100	89	107	97	118	91
12	102	110	93	109	98	112	100	112
13	88	103	98	98	88	82	96	100
14	112	120	107	79	98	94	104	98
15	92	92	117	110	91	100	79	87

	9	10	11	12	13	14	15
1	93	91	105	100	104	86	94
2	86	115	92	88	98	102	107
3	94	101	102	120	95	98	100
4	99	91	103	93	106	121	104
5	86	101	110	101	112	96	107
6	86	103	98	125	102	95	91
7	86	93	98	96	105	103	95
8	118	95	112	104	99	100	112
9	101	88	109	109	98	105	93
10	95	92	104	85	87	108	98
11	81	100	89	97	78	100	95
12	109	102	107	87	97	106	91
13	101	94	104	109	119	83	101
14	104	102	91	80	88	91	114
15	77	100	89	100	100	106	89

Table 7 (contd)

FINAL SIGNAL AND NOISE

	1	2	3	4	5	6	7	8
1	152	141	159	163	162	169	136	130
2	146	117	134	145	158	153	164	143
3	150	143	140	154	154	147	173	167
4	158	133	143	155	159	261	311	418
5	153	161	128	186	359	735	1512	2271
6	155	150	145	225	732	2439	6376	9057
7	169	149	176	381	1952	5416	14315	18708
8	141	141	184	502	2609	10057	24259	29957
9	145	176	170	531	2683	9504	19278	24687
10	139	160	173	325	1167	4423	12122	16425
11	162	164	160	187	677	1490	3225	4700
12	154	152	142	174	218	445	849	1078
13	139	157	123	139	153	188	217	282
14	171	156	146	137	146	134	151	155
15	165	132	153	160	126	143	130	138

	9	10	11	12	13	14	15
1	137	148	153	146	149	150	137
2	131	157	142	136	158	136	159
3	153	177	164	164	138	149	147
4	452	304	186	147	156	167	143
5	1570	1194	441	212	175	142	161
6	7023	4330	1258	444	193	137	145
7	17571	9763	2657	816	228	145	136
8	28172	13062	4173	993	245	137	178
9	19994	12724	3947	845	233	149	148
10	12786	6739	2188	462	180	155	154
11	4594	2112	836	277	144	138	159
12	994	613	285	171	137	162	137
13	267	206	170	157	166	125	149
14	153	151	144	135	132	141	169
15	138	147	126	141	163	146	147

PIXEL ARRAY AFTER THRESHOLDING

	1	2	3	4	5	6	7	8
1	102	91	109	113	112	119	86	80
2	96	67	84	95	108	103	114	93
3	100	93	90	104	104	97	123	117
4	108	83	93	105	109	211	261	368
5	103	111	78	136	309	685	1462	2221
6	105	100	95	175	682	2389	6326	9007
7	119	99	126	331	1902	5366	14265	18658
8	91	91	134	452	2559	10007	24209	29907
9	95	126	120	481	2633	9454	19228	24637
10	89	110	123	275	1117	4373	12072	16375
11	112	114	110	137	627	1440	3175	4650
12	104	102	92	124	168	395	799	1028
13	89	107	73	89	103	138	167	232
14	121	106	96	87	96	84	101	105
15	115	82	103	110	76	93	80	88

Table 7 (contd)

	9	10	11	12	13	14	15
1	87	98	103	96	99	100	87
2	81	107	92	86	108	86	109
3	103	127	114	114	88	99	97
4	402	254	136	97	106	117	93
5	1520	1144	391	162	125	92	111
6	6973	4280	1208	394	143	87	95
7	17521	9713	2607	766	178	95	86
8	28122	13012	4123	943	195	87	128
9	19944	12674	3897	795	183	99	98
10	12736	6689	2138	412	130	105	104
11	4544	2062	786	227	94	88	109
12	944	563	235	121	87	112	87
13	217	156	120	107	116	75	99
14	103	101	94	85	82	91	119
15	88	97	76	91	113	96	97

CALCULATED COORDINATES: 0.1627 0.2714

PLEASE ENTER A TASK NUMBER

Table 8

Threshold Performance at (0.2, 0.3)

Type	Threshold Factor Value at Minimum Radial Bias	Radial Value	Bias	Variance at Minimum Bias	Matrix Size	Fig. No.
2	50.	0.3306	-0.0300	1.9×10^{-5}	15	65
2	100.	0.3494	- .0112	3.4×10^{-5}	15	66
2	100.	.2638	- .0968	1.8×10^{-5}	10	67
3	2.4	.3123	- .0483	3.9×10^{-5}	10	69
3	1.	.3464	- .0142	1.7×10^{-5}	13	70
4	1.	.3204	- .0402	1.0×10^{-3}	6	71
5	1.	.3507	- .0099	2.0×10^{-5}	15	72
5	1.	.3658	+ .0052	9.5×10^{-5}	6	73
6	1.	.3582	- .0023	1.0×10^{-5}	8	74

Threshold Type

2	Constant Factor
3	Guard Band RMS Value x Constant Factor
4	Guard Band Maximum Value x Constant Factor
5	Matrix Outer Band RMS Value x Constant Factor
6	Matrix Outer Band Max Value x Constant Factor

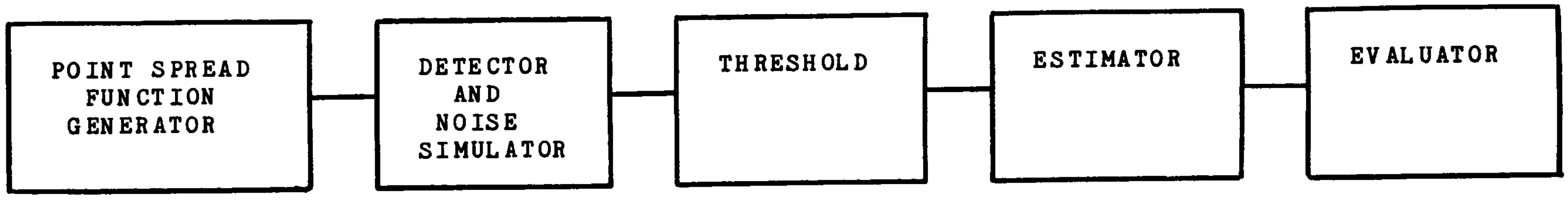

Fig. 1 System Model

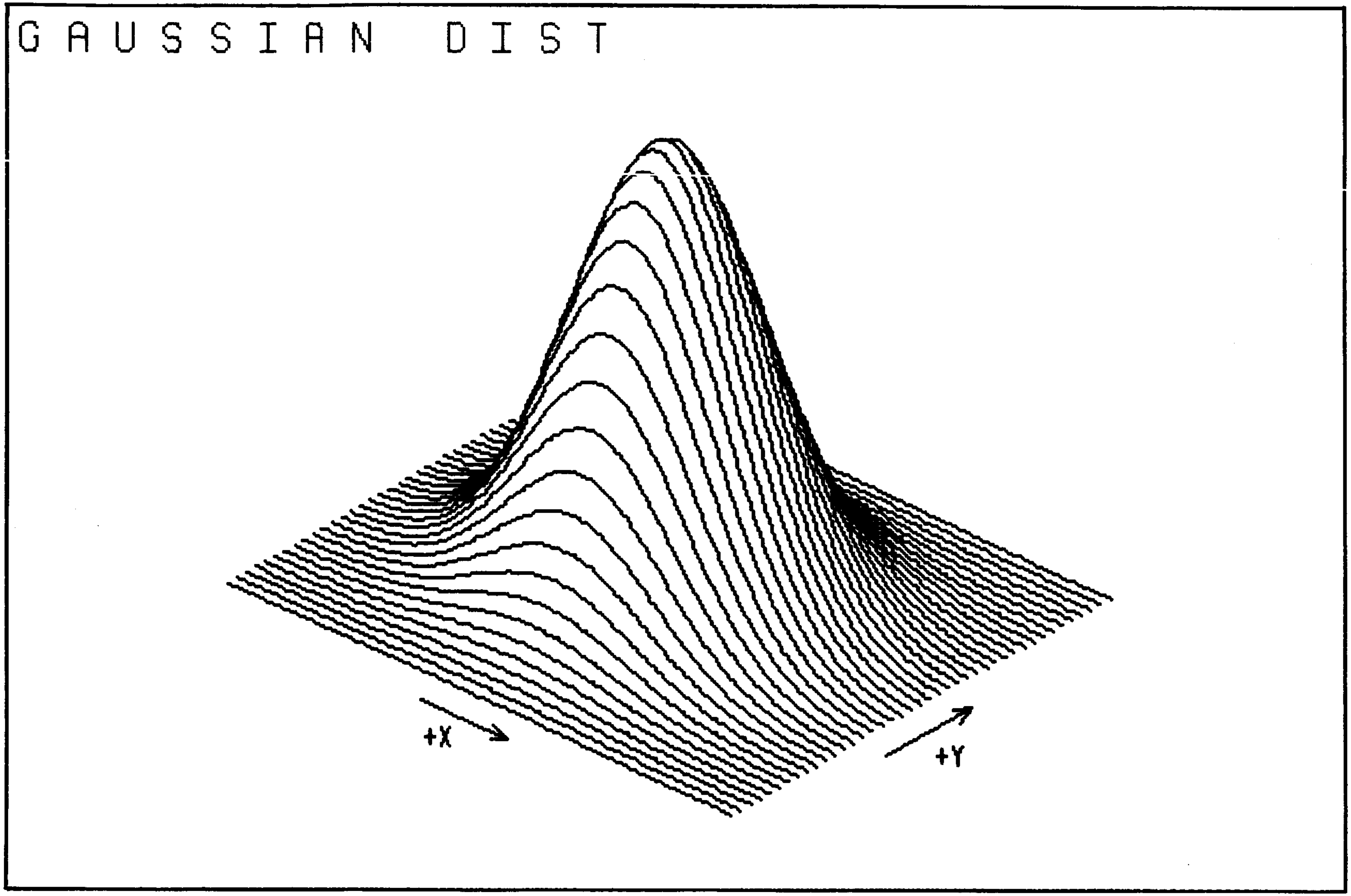

Fig. 2 Gaussian Point Spread Function

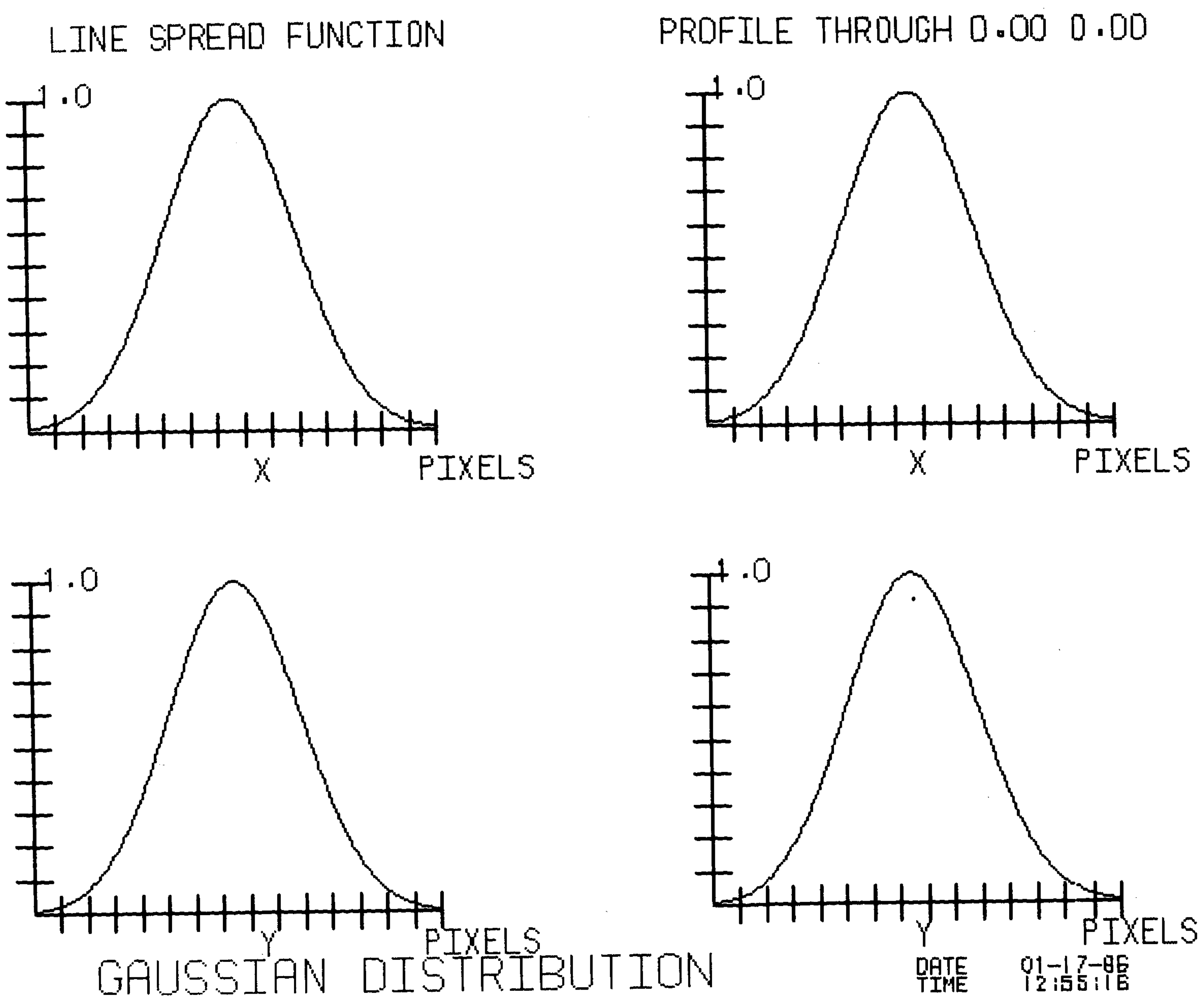

Fig. 3 Gaussian Line Spread Functions

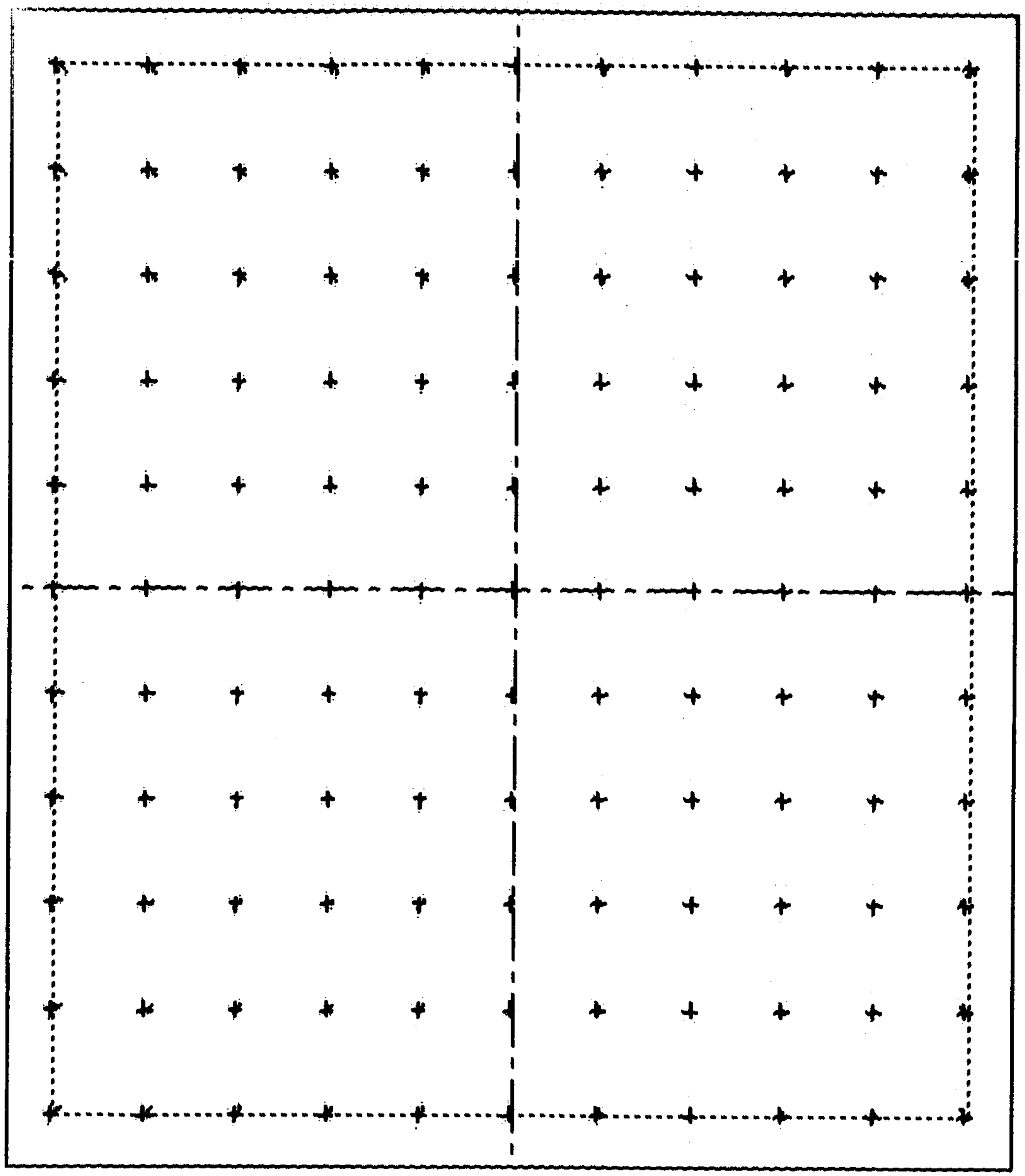

GAUSSIAN DISTRIBUTION
SCALE 1.0
MATRIX SIZE 15
ALGORITHM TYPE 2
CENTROID ORDER 1

RMS ERRORS

X	0.004
Y	0.004
RAD	0.005
ANG	42.405

DETECTOR PARAMETERS
SIGNAL 100000
DARK CURRENT 0
READ NOISE 0
RESP IRREGULARITY 0.000
CTE 1.00000 1.00000
PIXEL LOCATION -1 -1
SATURATION LEVEL 9:00001024
DARK SHADING OFF
RESP SHADING OFF
THRESHOLD TYPE NONE

DATE 01-30-86
TIME 13:38:13

Fig. 4 Pixel Performance Map - Gaussian PSF, Matrix Size 15.

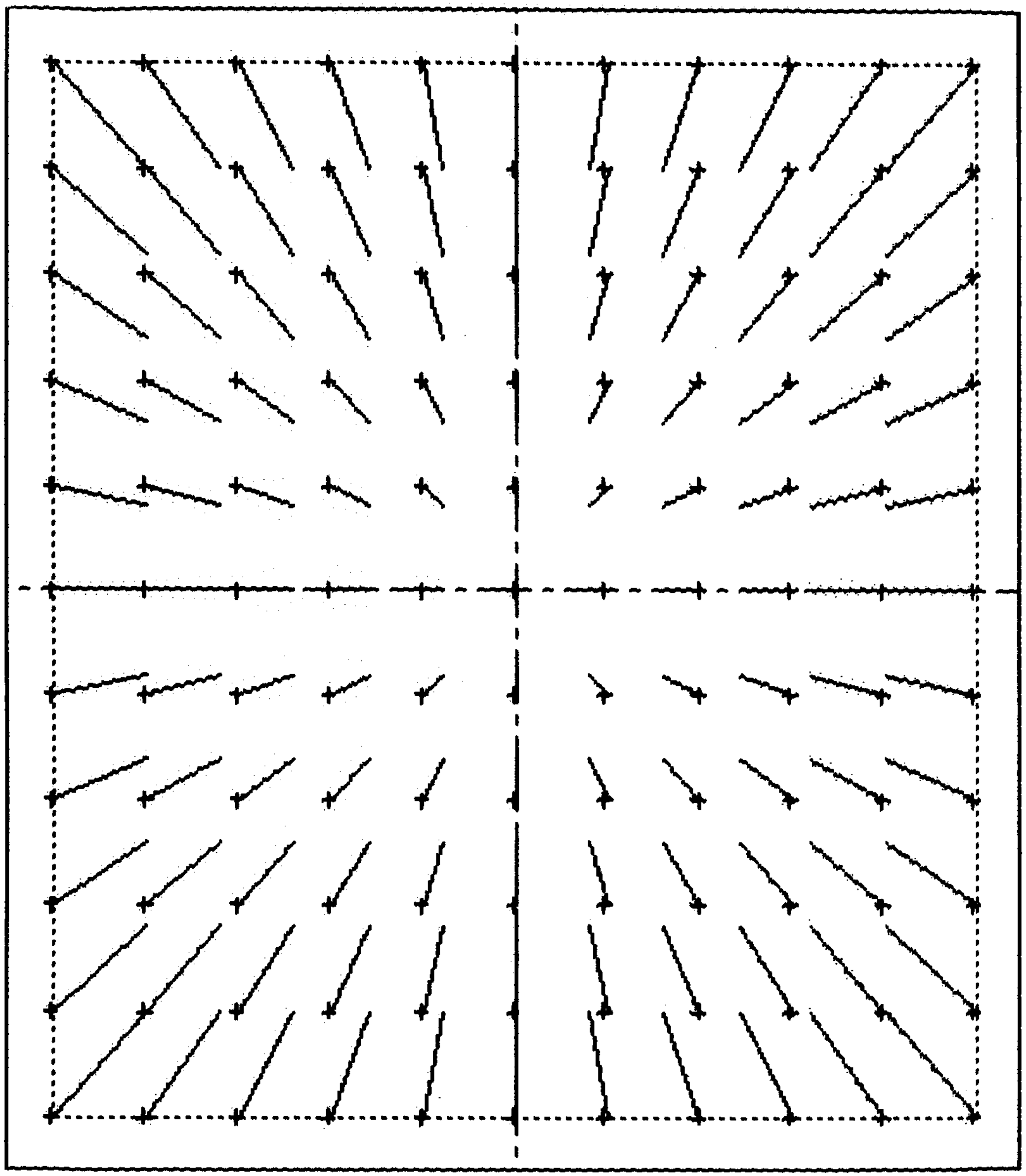

GAUSSIAN DISTRIBUTION
SCALE 1.0
MATRIX SIZE 10
ALGORITHM TYPE 2
CENTROID ORDER 1

RMS ERRORS

X	0.063
Y	0.063
RAD	0.089
ANG	42.211

DETECTOR PARAMETERS
SIGNAL 100000
DARK CURRENT 0
READ NOISE 0
RESP IRREGULARITY 0.000
CTE 1.00000 1.00000
PIXEL LOCATION -1 -1
SATURATION LEVEL 9:00001024
DARK SHADING OFF
RESP SHADING OFF
THRESHOLD TYPE NONE

DATE 01-30-86
TIME 13:51:23

Fig. 5 Pixel Performance Map - Gaussian PSF, Matrix Size 10

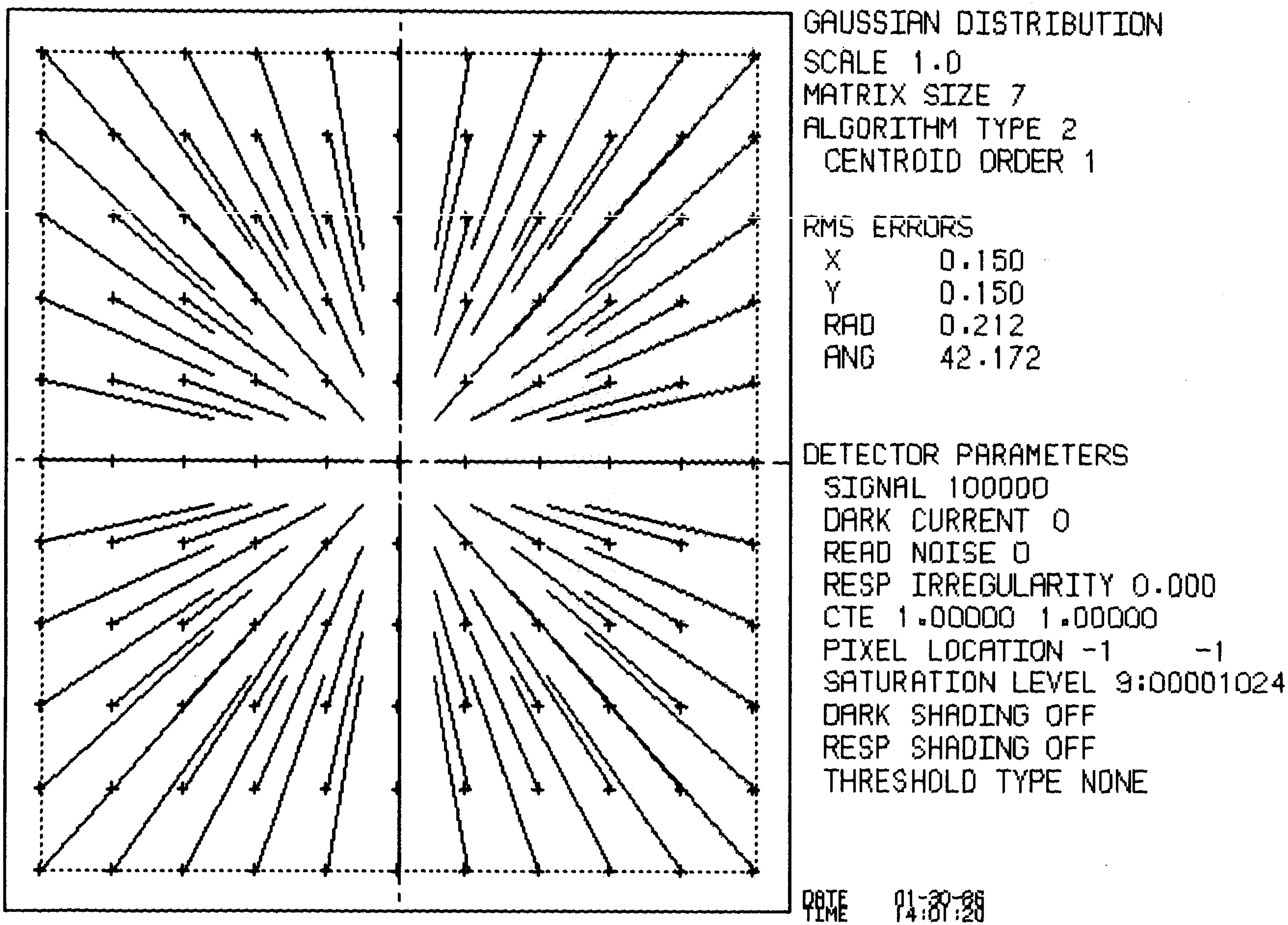

Fig. 6 Pixel Performance Map - Gaussian PSF, Matrix Size 7

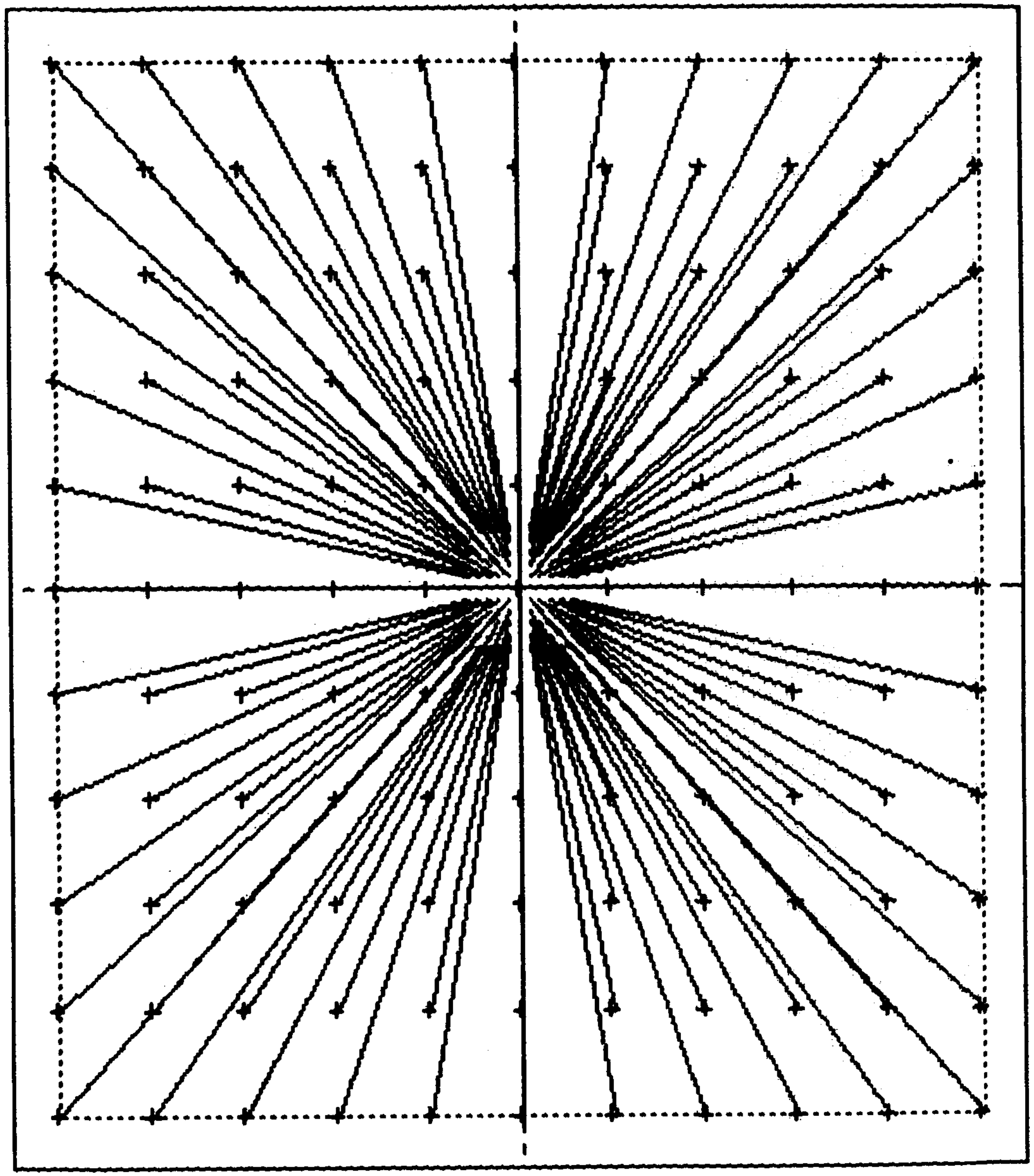

GAUSSIAN DISTRIBUTION
SCALE 1.0
MATRIX SIZE 3
ALGORITHM TYPE 2
CENTROID ORDER 1

RMS ERRORS

X	0.281
Y	0.281
RAD	0.397
ANG	42.065

DETECTOR PARAMETERS
SIGNAL 100000
DARK CURRENT 0
READ NOISE 0
RESP IRREGULARITY 0.000
CTE 1.00000 1.00000
PIXEL LOCATION -1 -1
SATURATION LEVEL 9:00001024
DARK SHADING OFF
RESP SHADING OFF
THRESHOLD TYPE NONE

DATE 01-30-86
TIME 14:16:06

Fig. 7 Pixel Performance Map - Gaussian PSF, Matrix Size 3

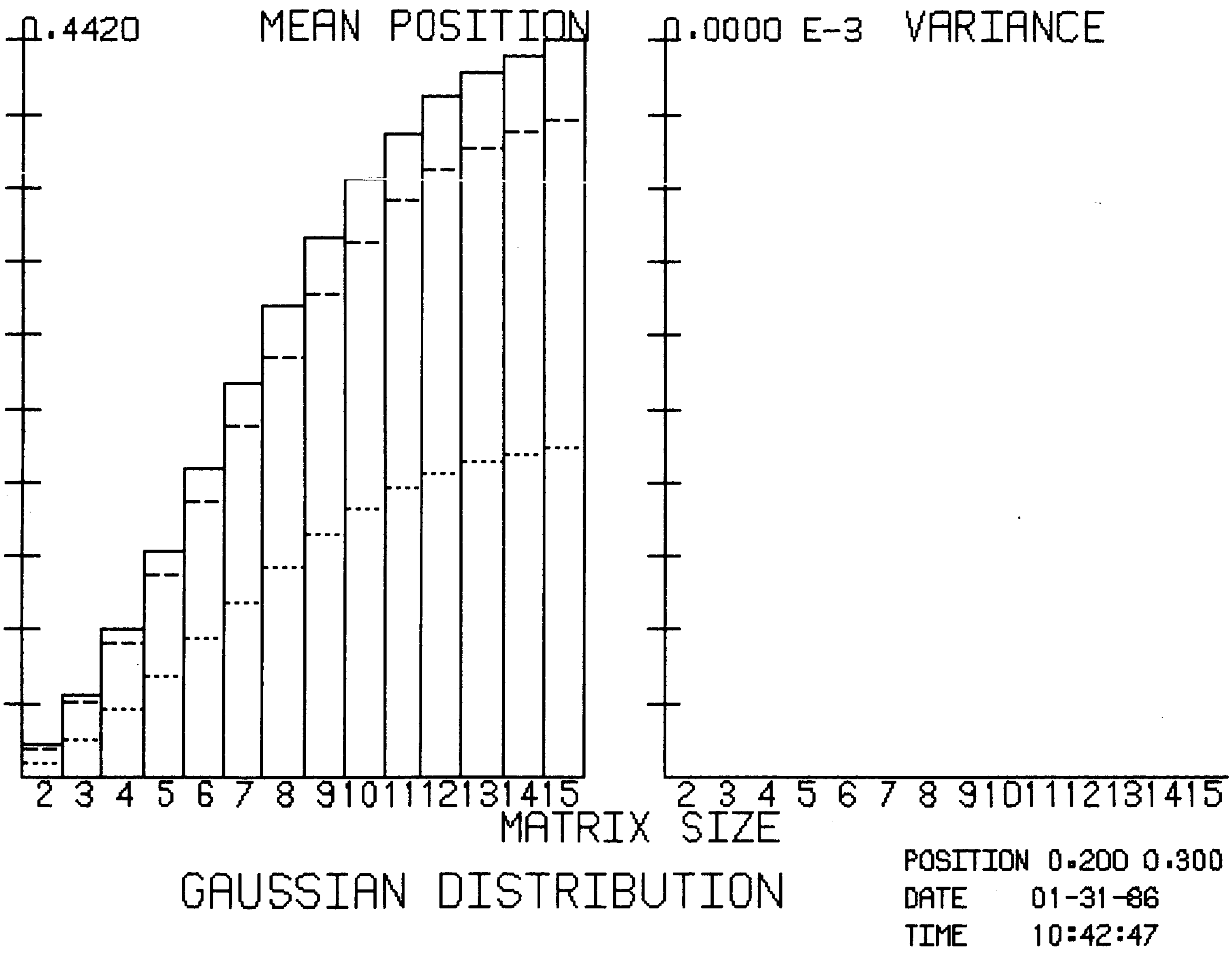

Fig. 8 Position Estimate as a Function of Matrix Size, No Noise

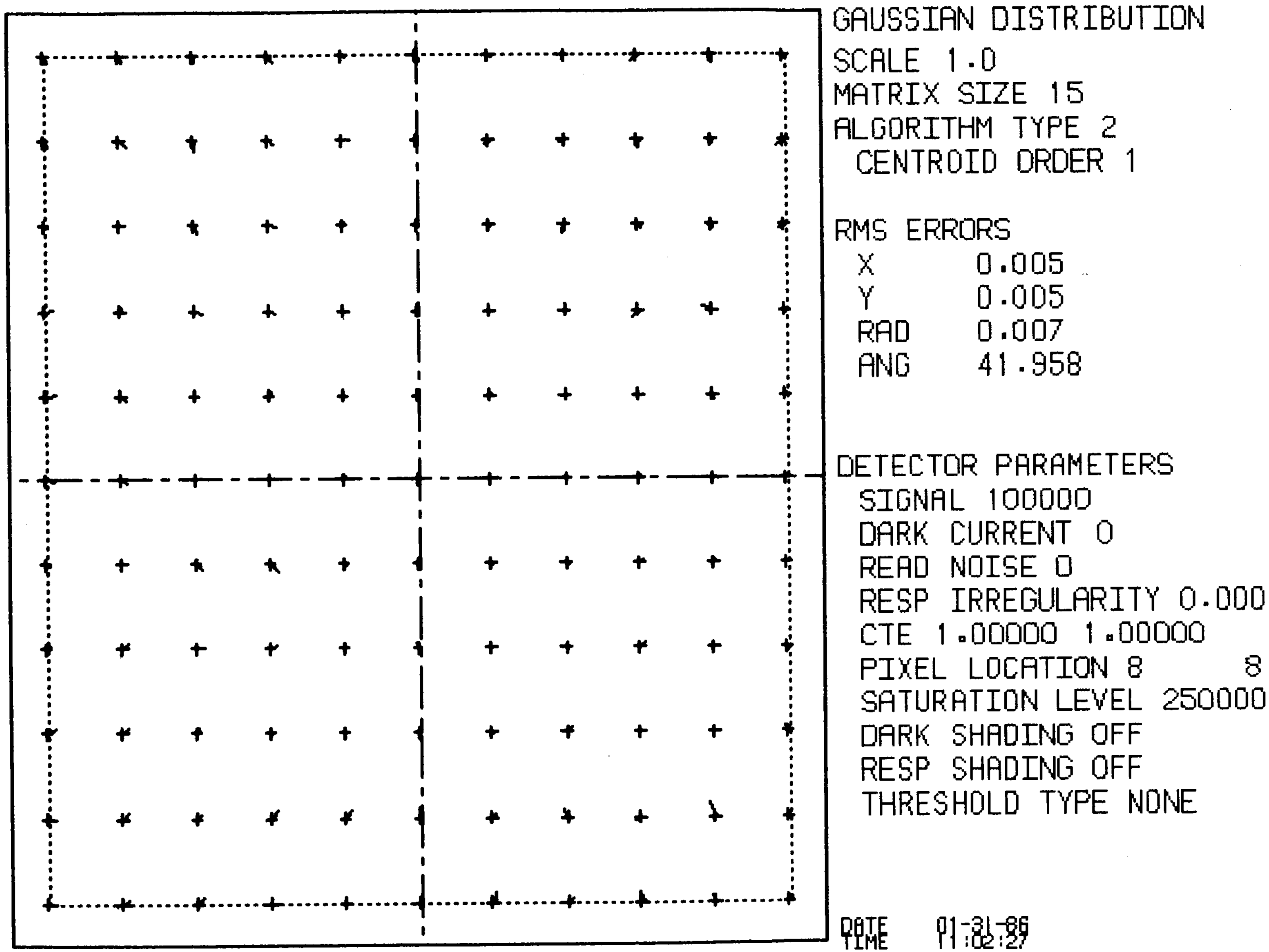

Fig. 9 Pixel Performance Map - Gaussian PSF, Shot Noise, Signal - 100,000e⁻

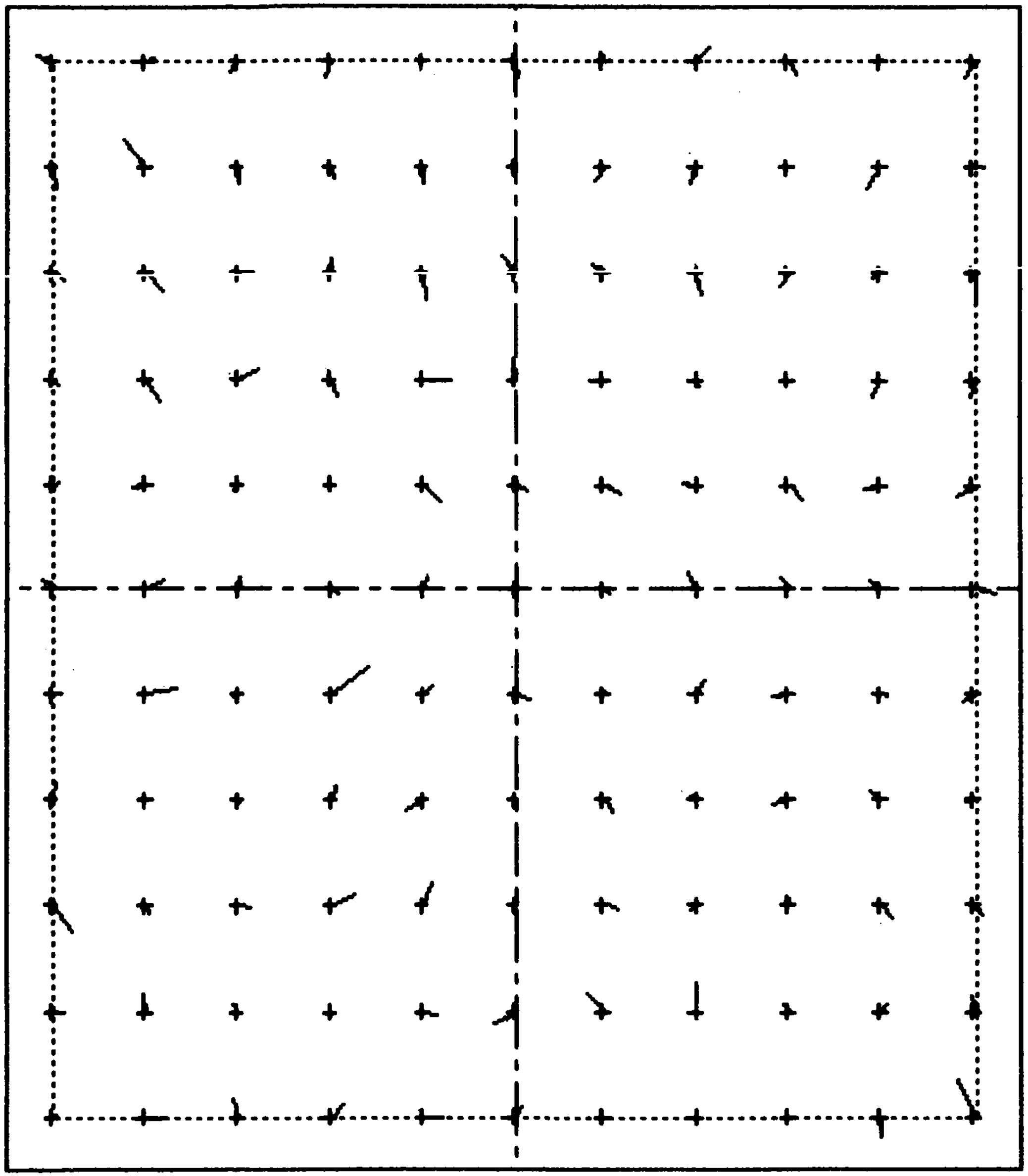

GAUSSIAN DISTRIBUTION
SCALE 1.0
MATRIX SIZE 15
ALGORITHM TYPE 2
CENTROID ORDER 1

RMS ERRORS
X 0.012
Y 0.012
RAD 0.017
ANG 41.942

DETECTOR PARAMETERS
SIGNAL 10000
DARK CURRENT 0
READ NOISE 0
RESP IRREGULARITY 0.000
CTE 1.00000 1.00000
PIXEL LOCATION 8 8
SATURATION LEVEL 250000
DARK SHADING OFF
RESP SHADING OFF
THRESHOLD TYPE NONE

DATE 01-31-86
TIME 11:15:29

Fig. 10 Pixel Performance Map - Gaussian PSF, Shot Noise, Signal = 10,000e^{-}

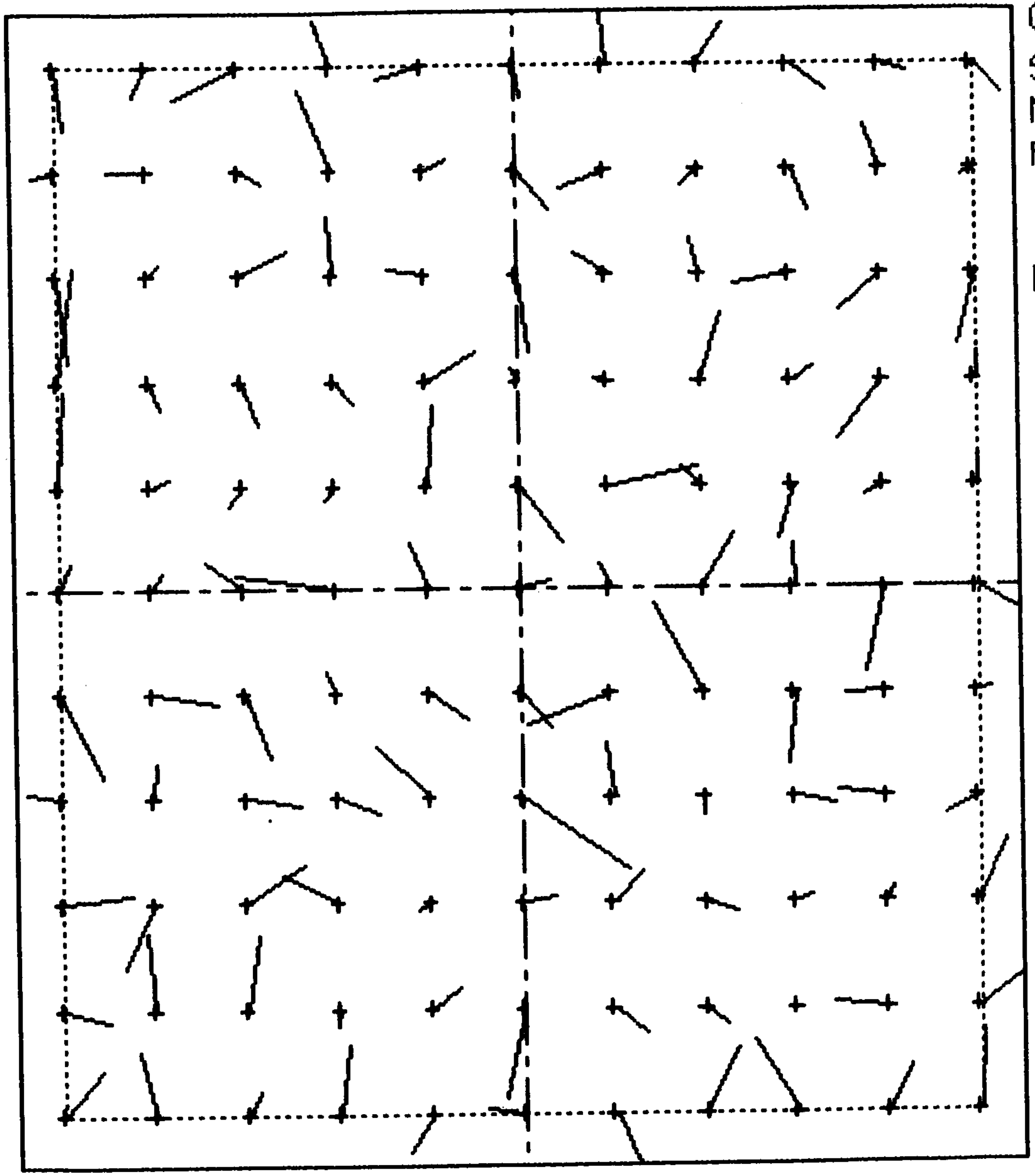

Fig. 11 Pixel Performance Map - Gaussian PSF, Shot Noise, Signal = 1,000e⁻

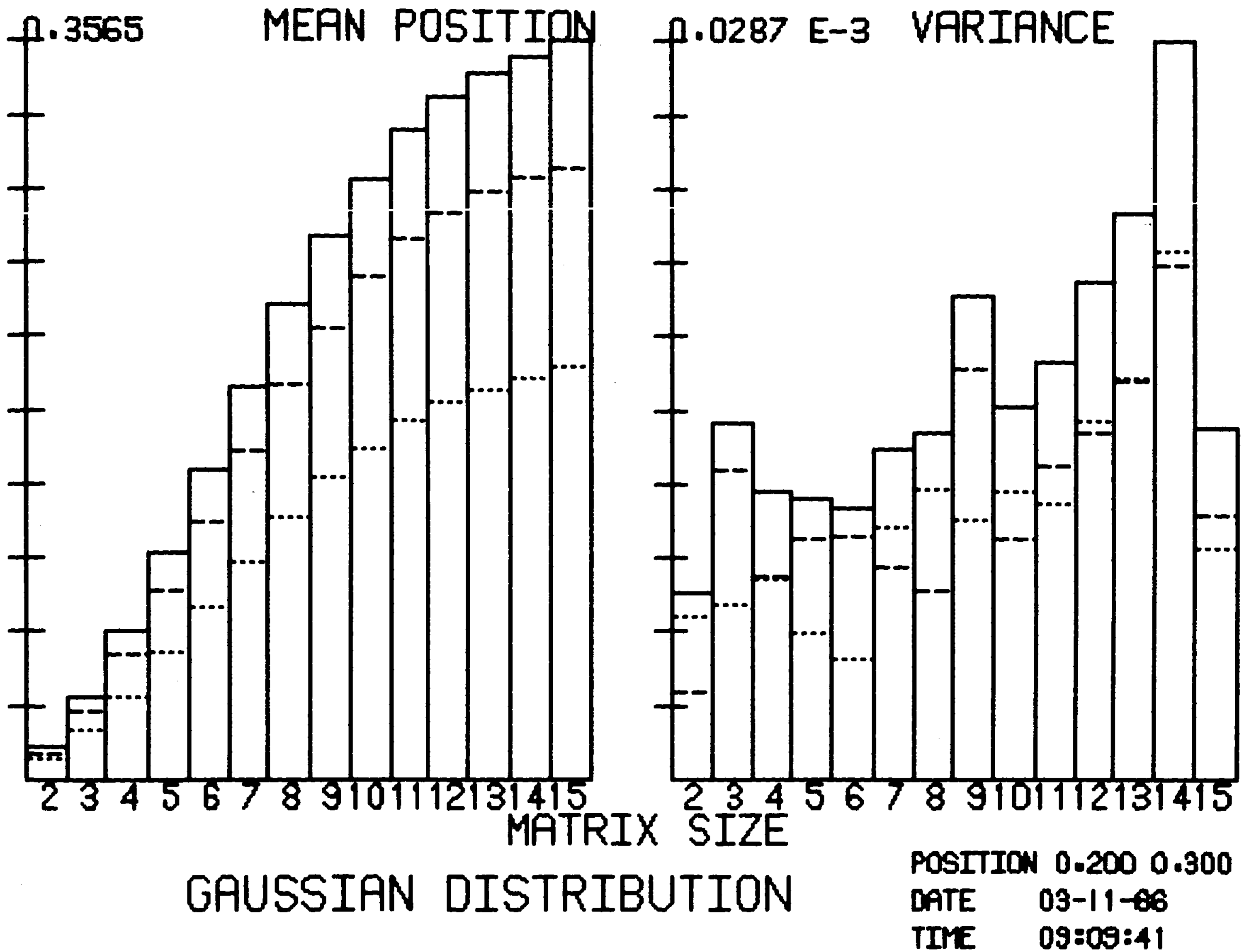

Fig. 12 Position Estimate as a Function of Matrix Size, Gaussian PSF with Shot Noise

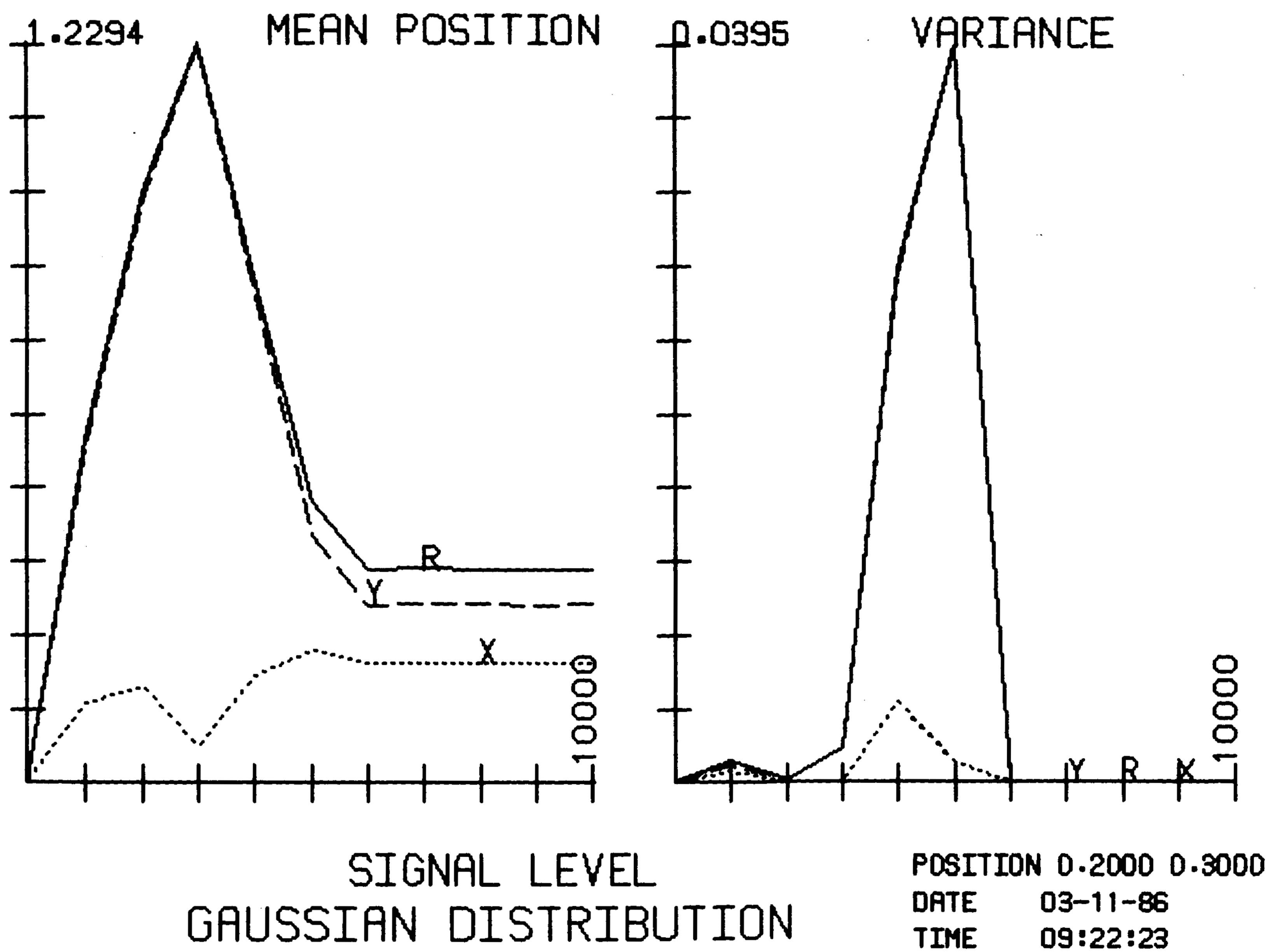

Fig. 13 Position Estimate as a Function of Signal Level, Gaussian PSF with Shot Noise

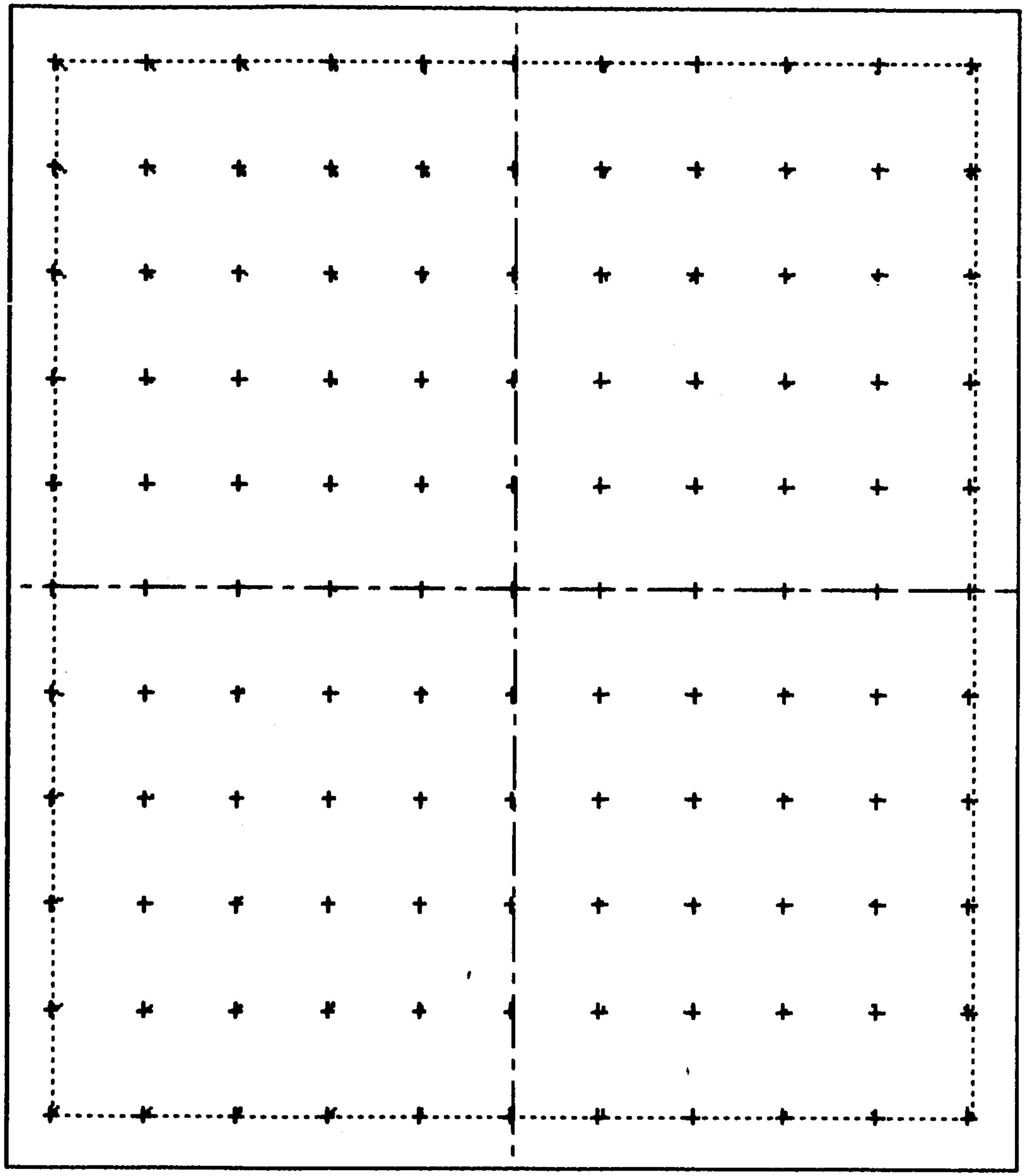

Fig. 14 Pixel Performance Map - Gaussian PSF, Dark Current, Signal = 0

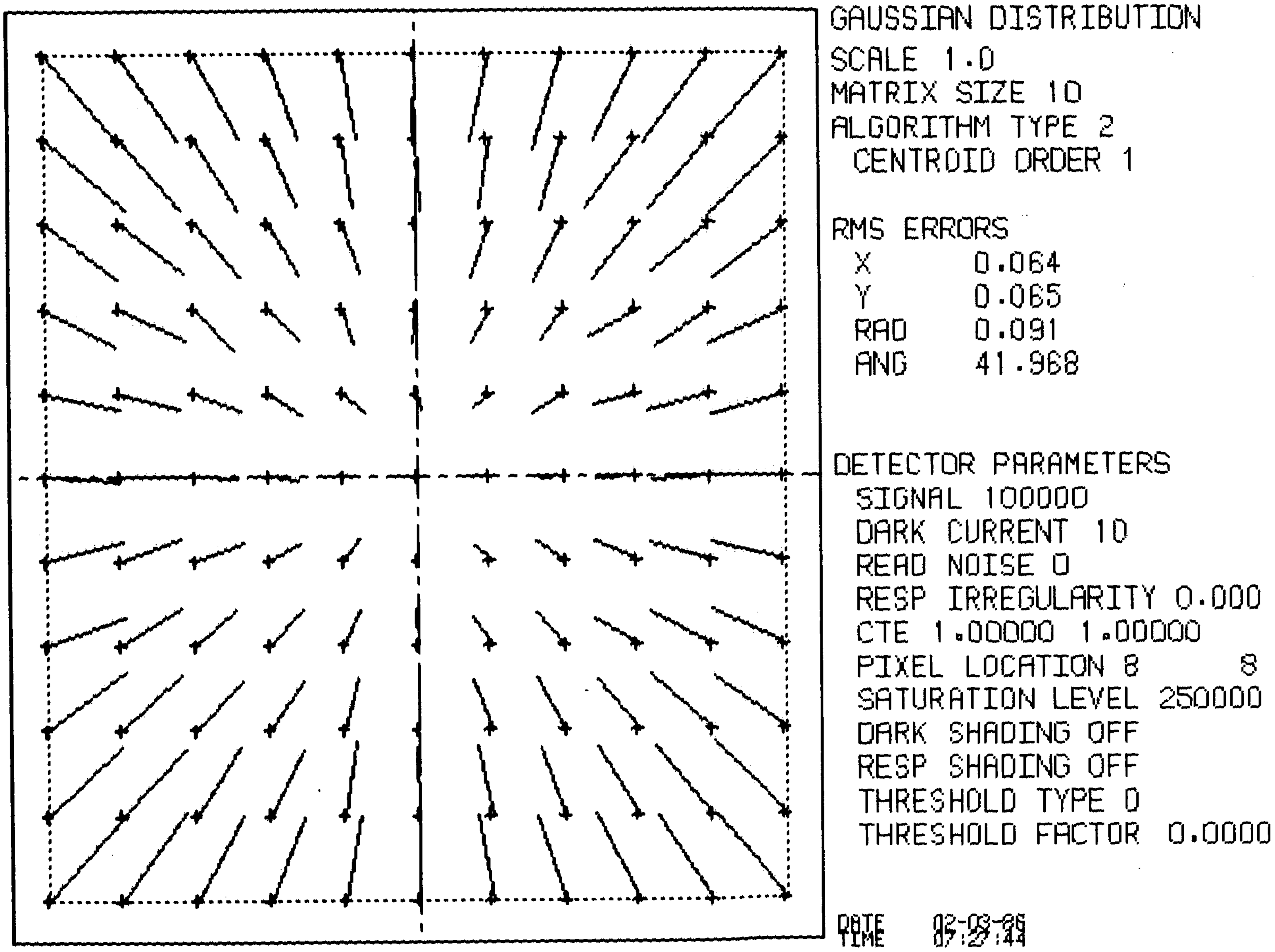

Fig. 15 Pixel Performance Map - Gaussian PSF, Dark Current, Signal = 100,000e⁻

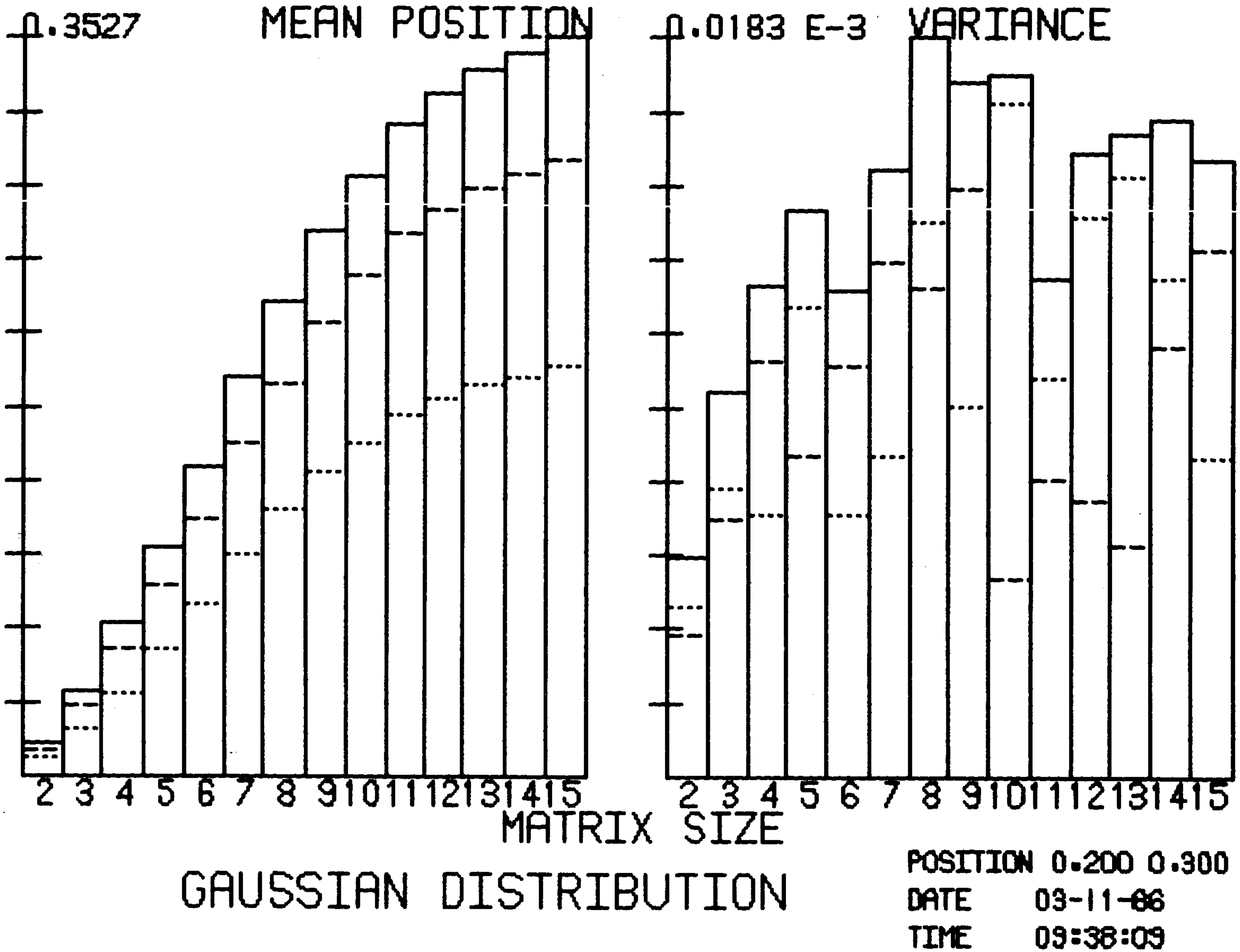

Fig. 16 Position Estimate as a Function of Matrix Size, Gaussian PSF and Dark Current

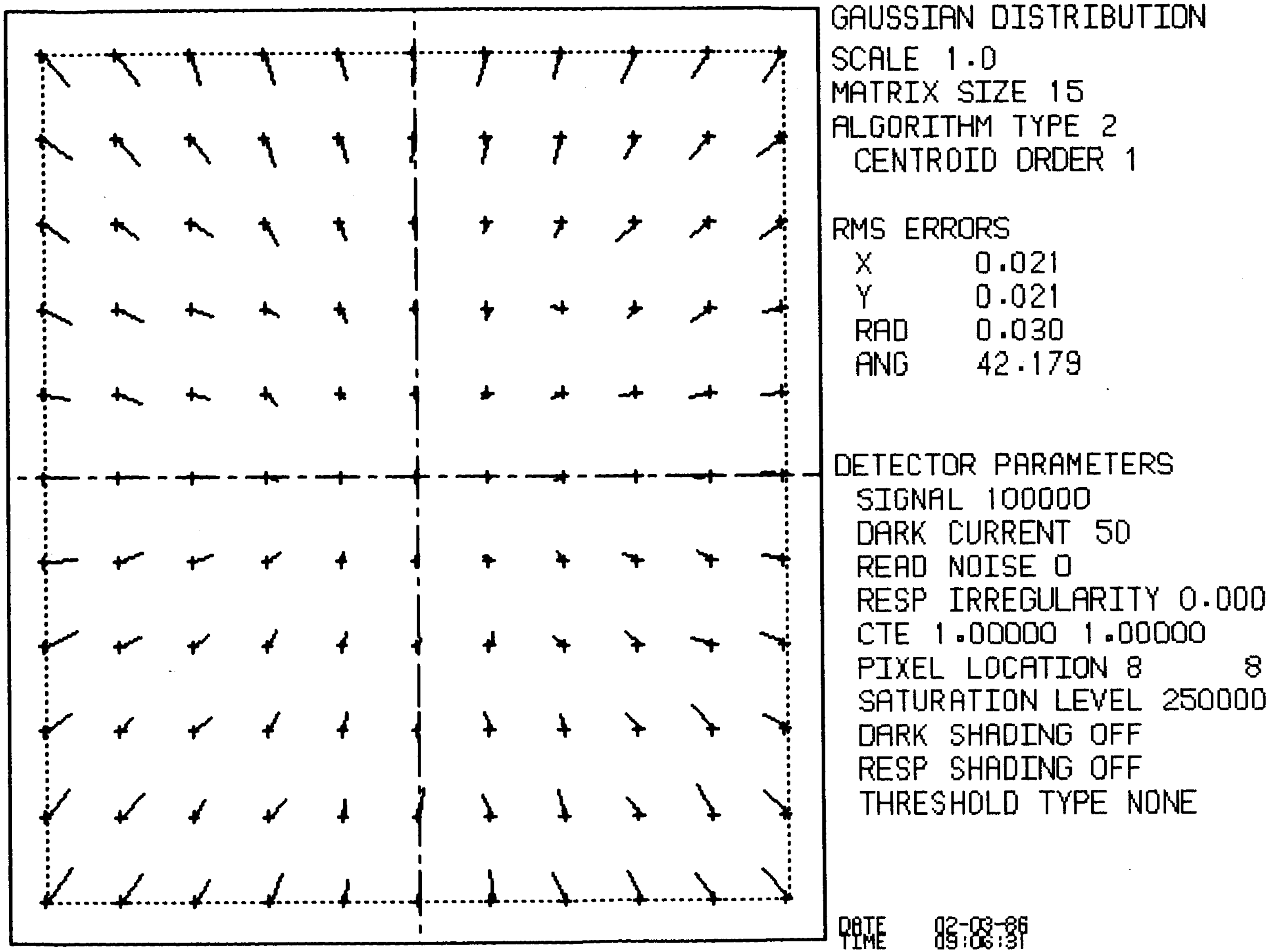

Fig. 17. Pixel Performance Map - Gaussian PSF, 50e⁻ Dark Current, Matrix Size 15

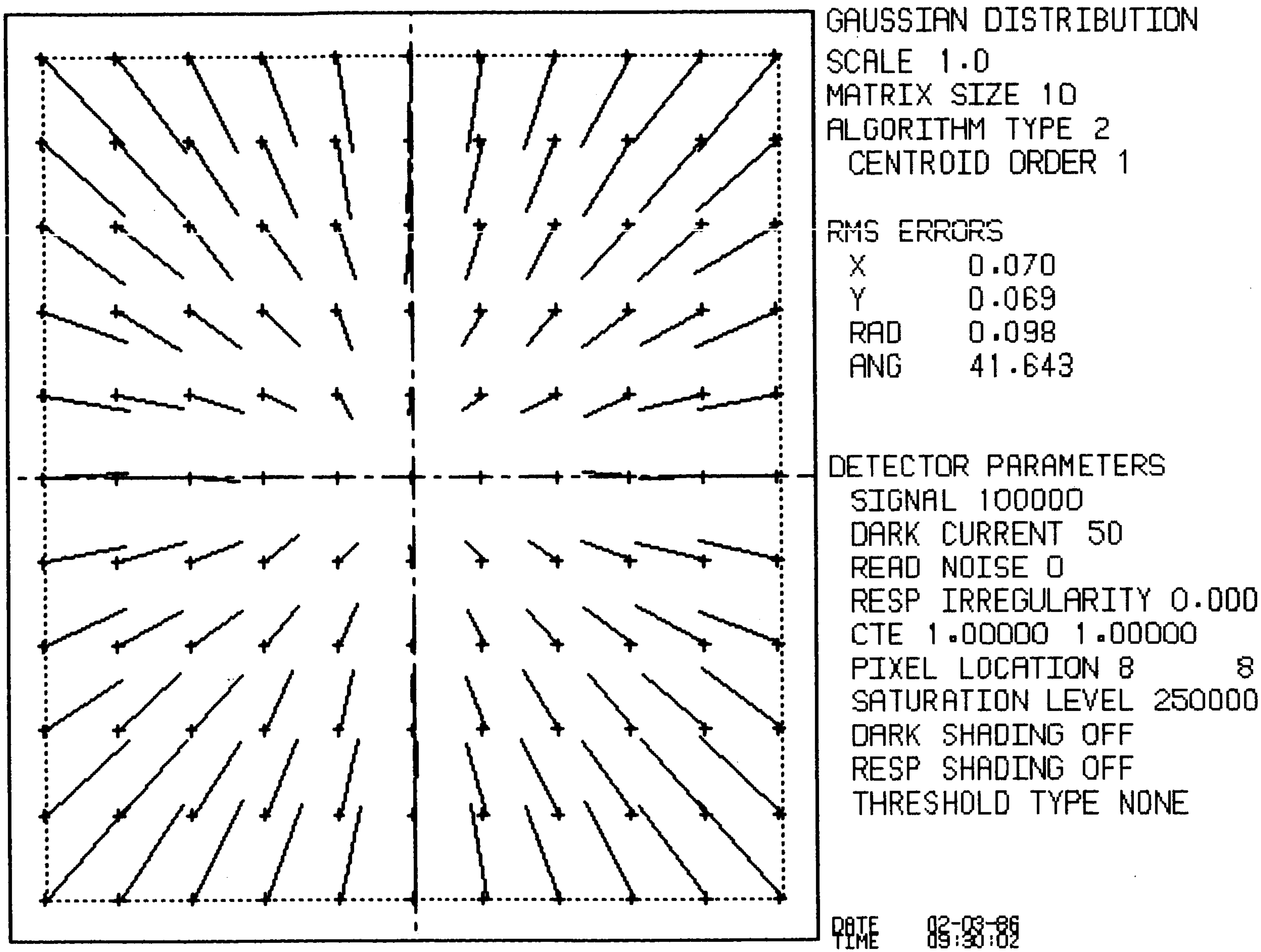

Fig. 18 Pixel Performance Map - Gaussian PSF, 50e$^-$ Dark Current, Matrix Size 10

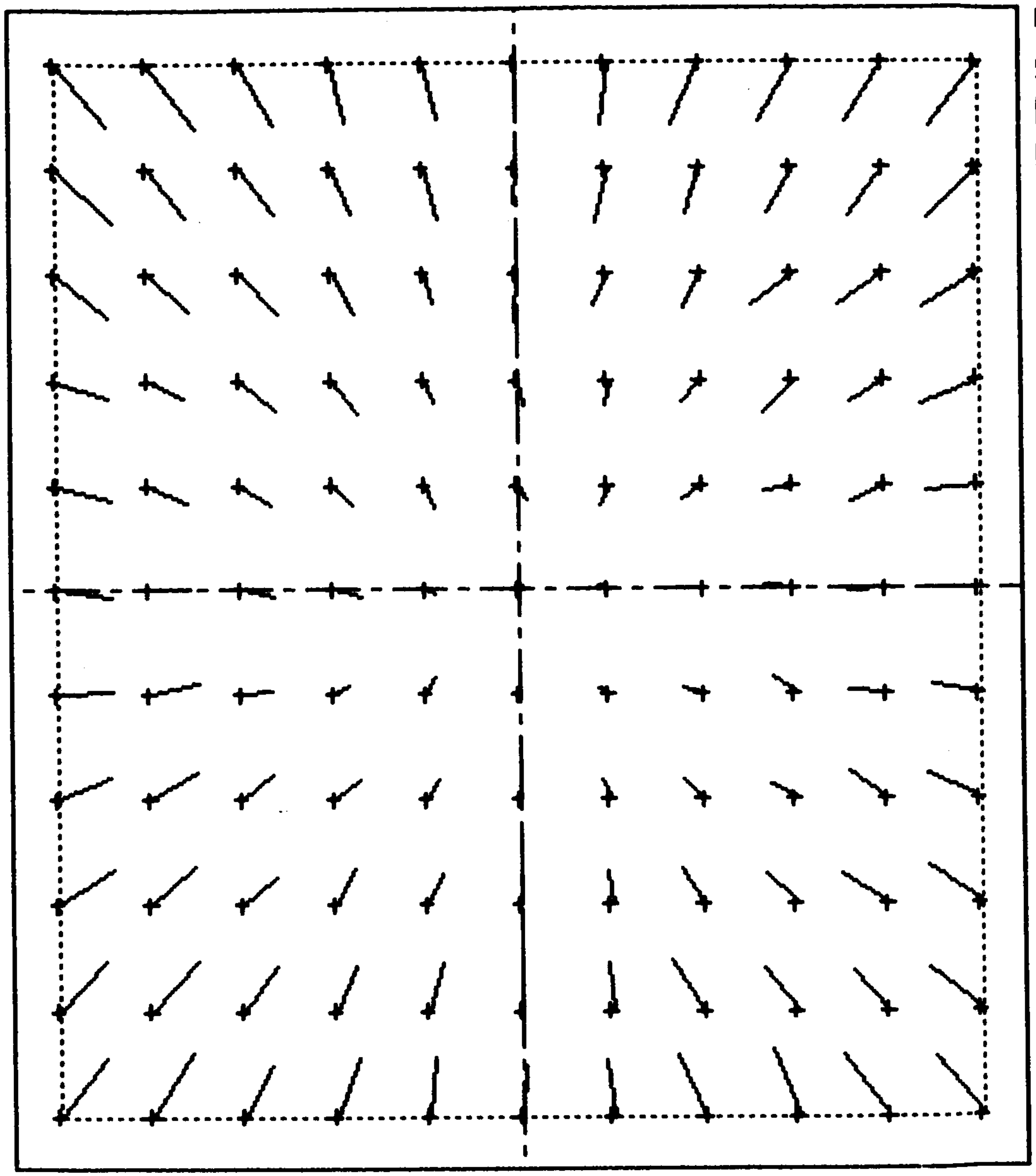

GAUSSIAN DISTRIBUTION
SCALE 1.0
MATRIX SIZE 15
ALGORITHM TYPE 2
CENTROID ORDER 1

RMS ERRORS

X	0.036
Y	0.036
RAD	0.050
ANG	41.878

DETECTOR PARAMETERS
SIGNAL 100000
DARK CURRENT 100
READ NOISE 0
RESP IRREGULARITY 0.000
CTE 1.00000 1.00000
PIXEL LOCATION 8 8
SATURATION LEVEL 250000
DARK SHADING OFF
RESP SHADING OFF
THRESHOLD TYPE NONE

DATE 02-03-86
TIME 09:43:28

Fig. 19 Pixel Performance Map - Gaussian PSF, 100e- Dark Current, Matrix Size 15

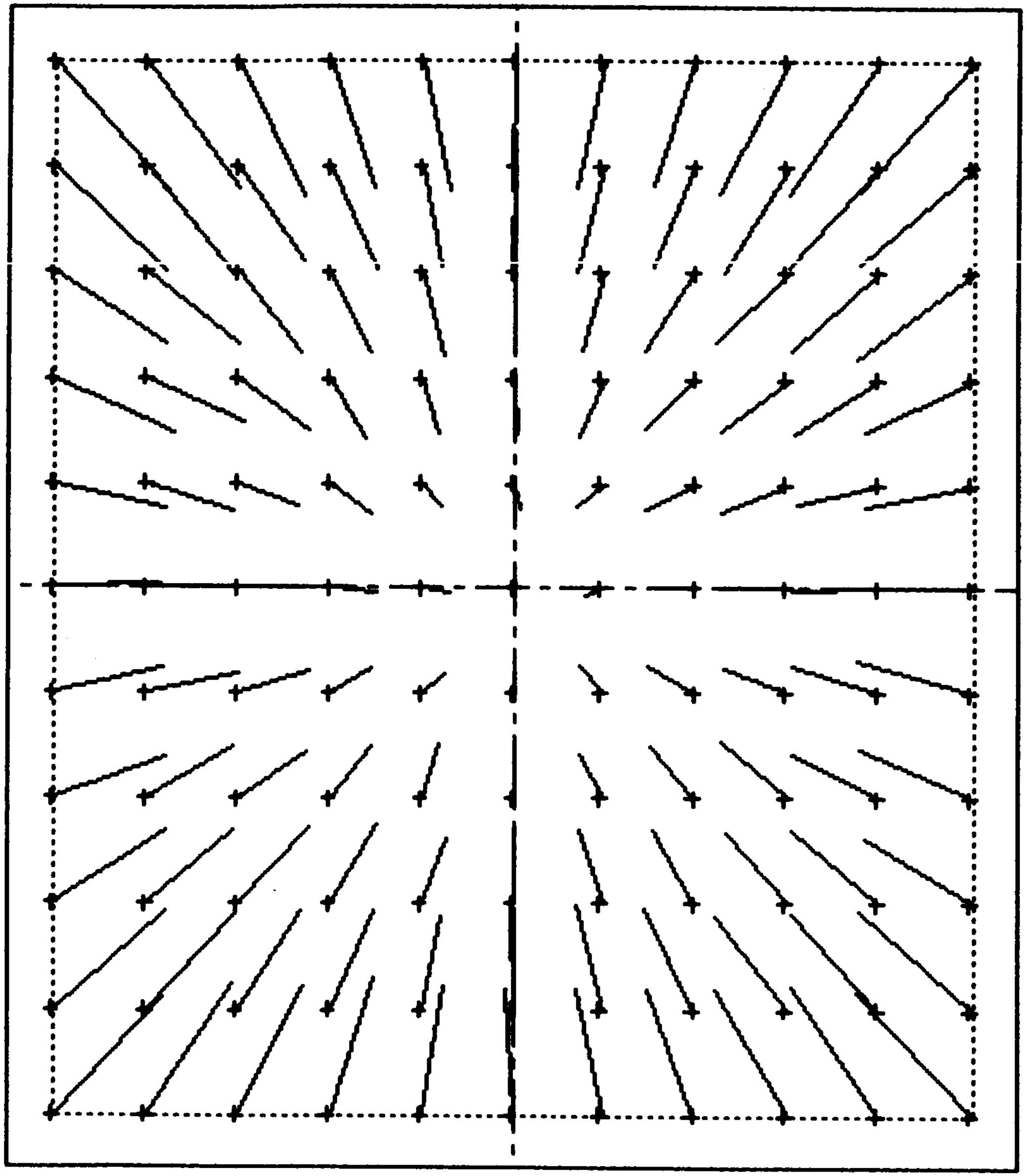

GAUSSIAN DISTRIBUTION
SCALE 1.0
MATRIX SIZE 10
ALGORITHM TYPE 2
CENTROID ORDER 1

RMS ERRORS

X	0.076
Y	0.076
RAD	0.108
ANG	41.902

DETECTOR PARAMETERS
SIGNAL 100000
DARK CURRENT 100
READ NOISE 0
RESP IRREGULARITY 0.000
CTE 1.00000 1.00000
PIXEL LOCATION 8 8
SATURATION LEVEL 250000
DARK SHADING OFF
RESP SHADING OFF
THRESHOLD TYPE NONE

DATE 02-03-86
TIME 09:51:20

Fig. 20 Pixel Performance Map - Gaussian PSF, $100e^-$ Dark Current, Matrix Size 10

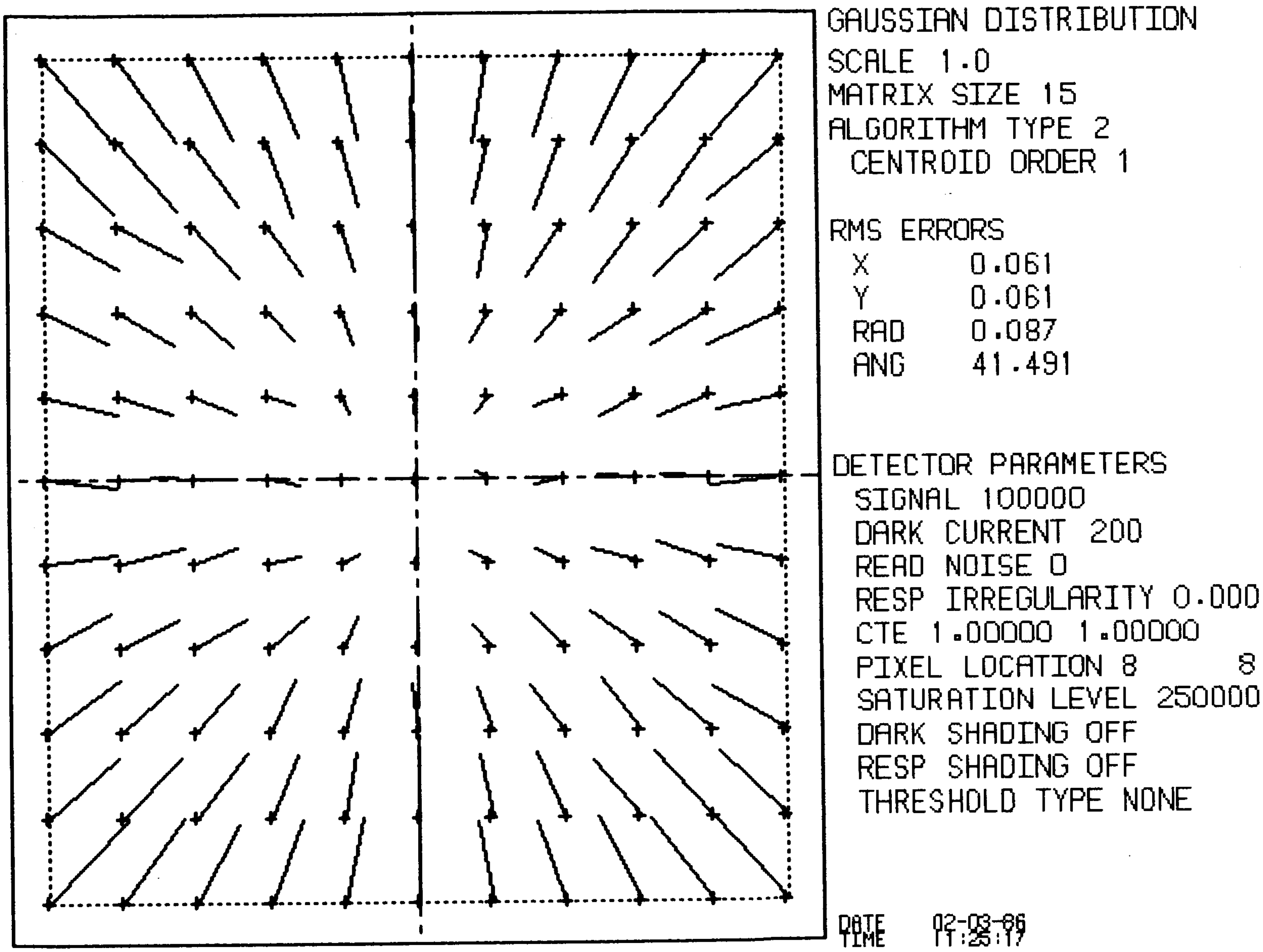

Fig. 21 Pixel Performance Map - Gaussian PSF, 200e⁻ Dark Current, Matrix Size 15

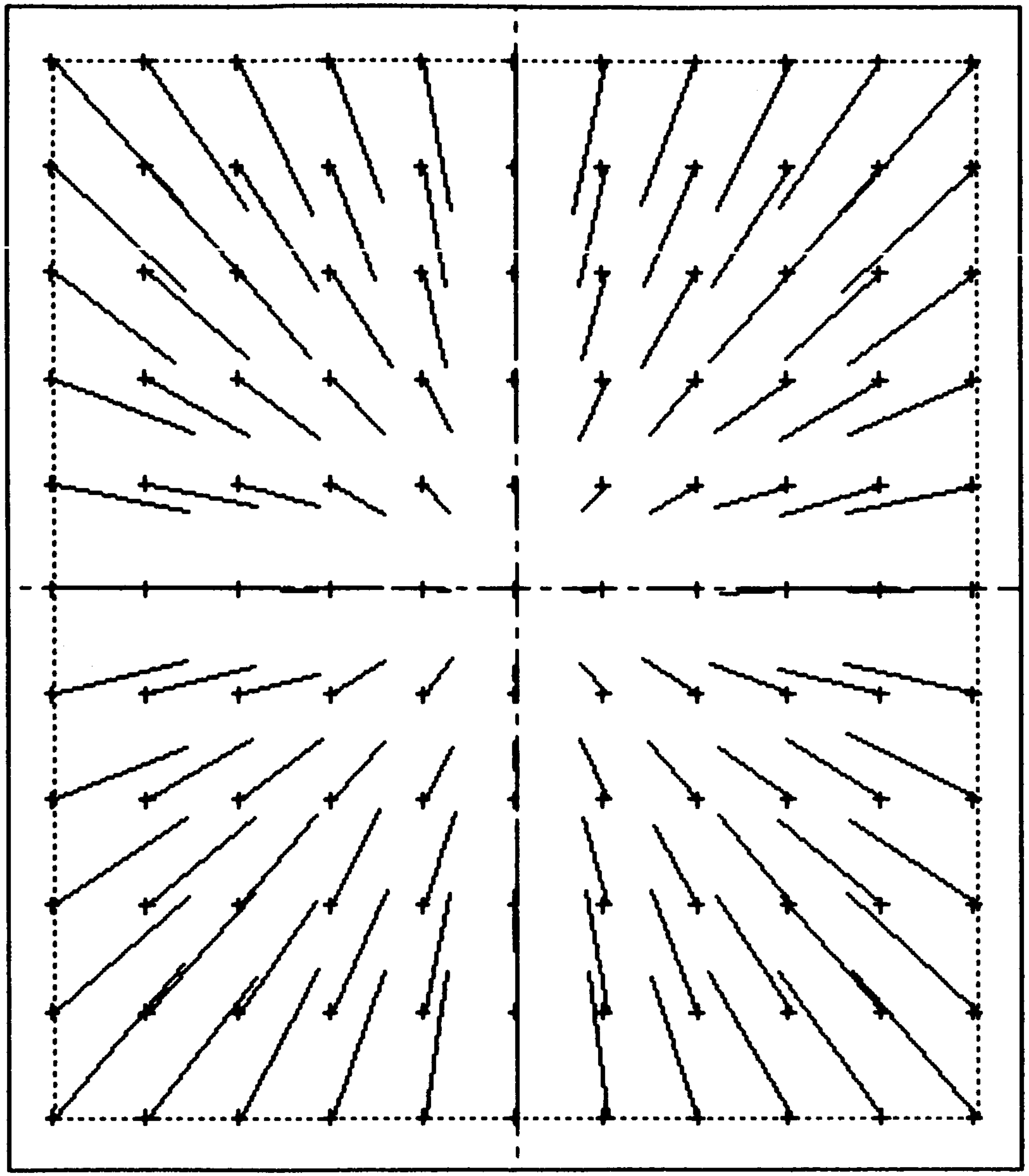

Fig. 22 Pixel Performance Map - Gaussian PSF, 200e⁻ Dark Current, Matrix Size 10

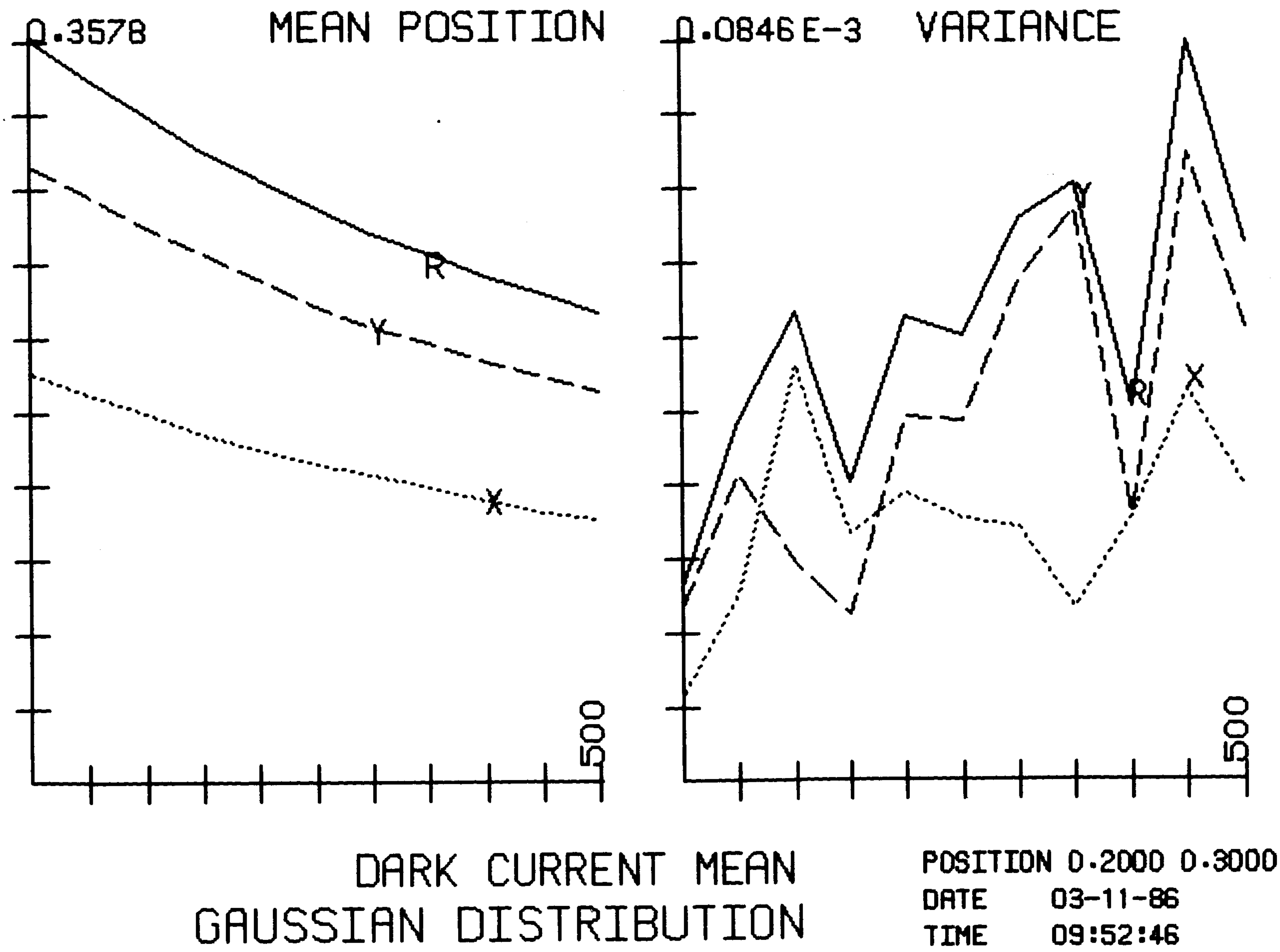

Fig. 23 Position Estimate as a Function of Dark Current, Matrix Size 15

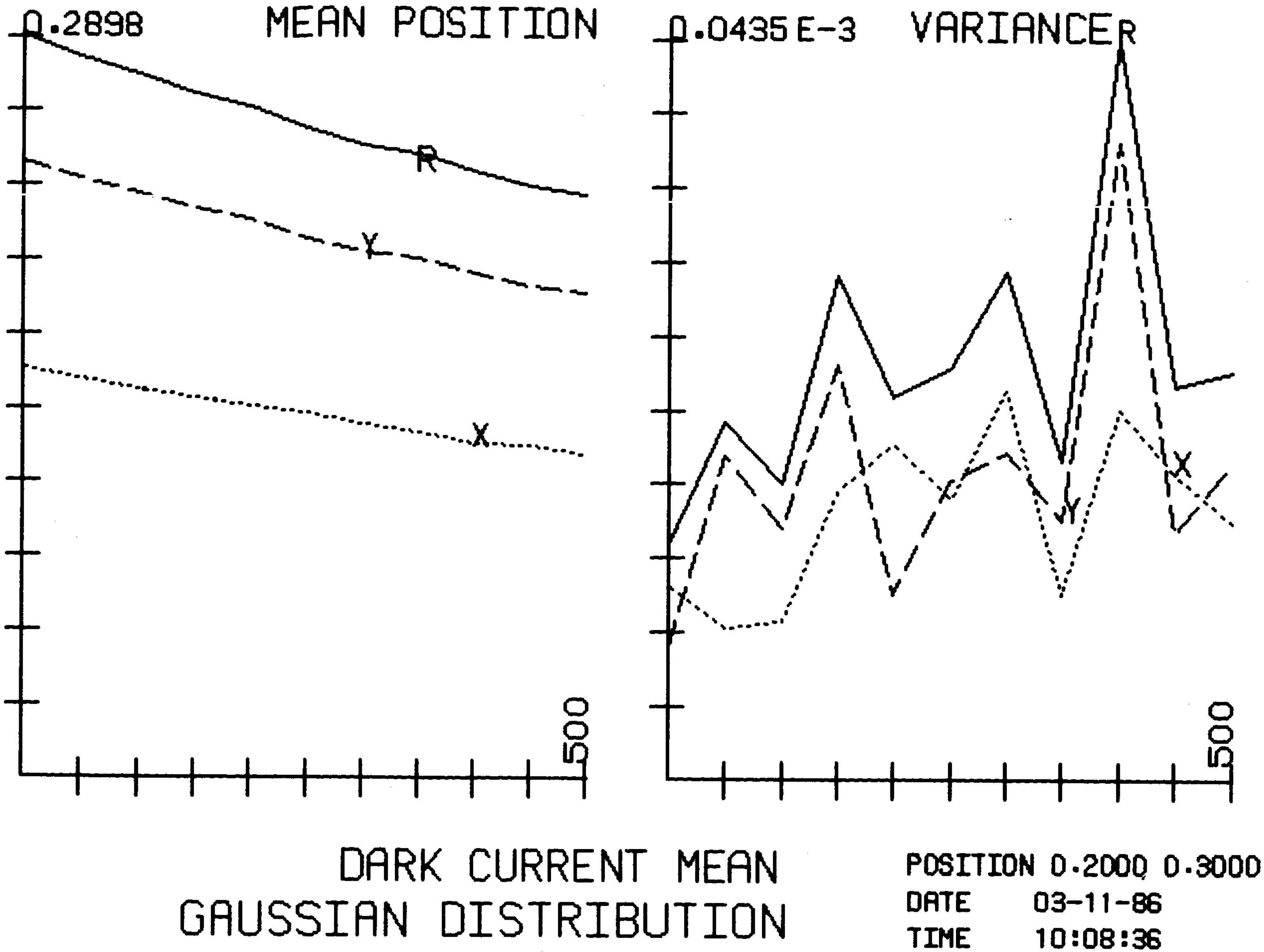

Fig. 24 Position Estimate as a Function of Dark Current, Matrix Size 10

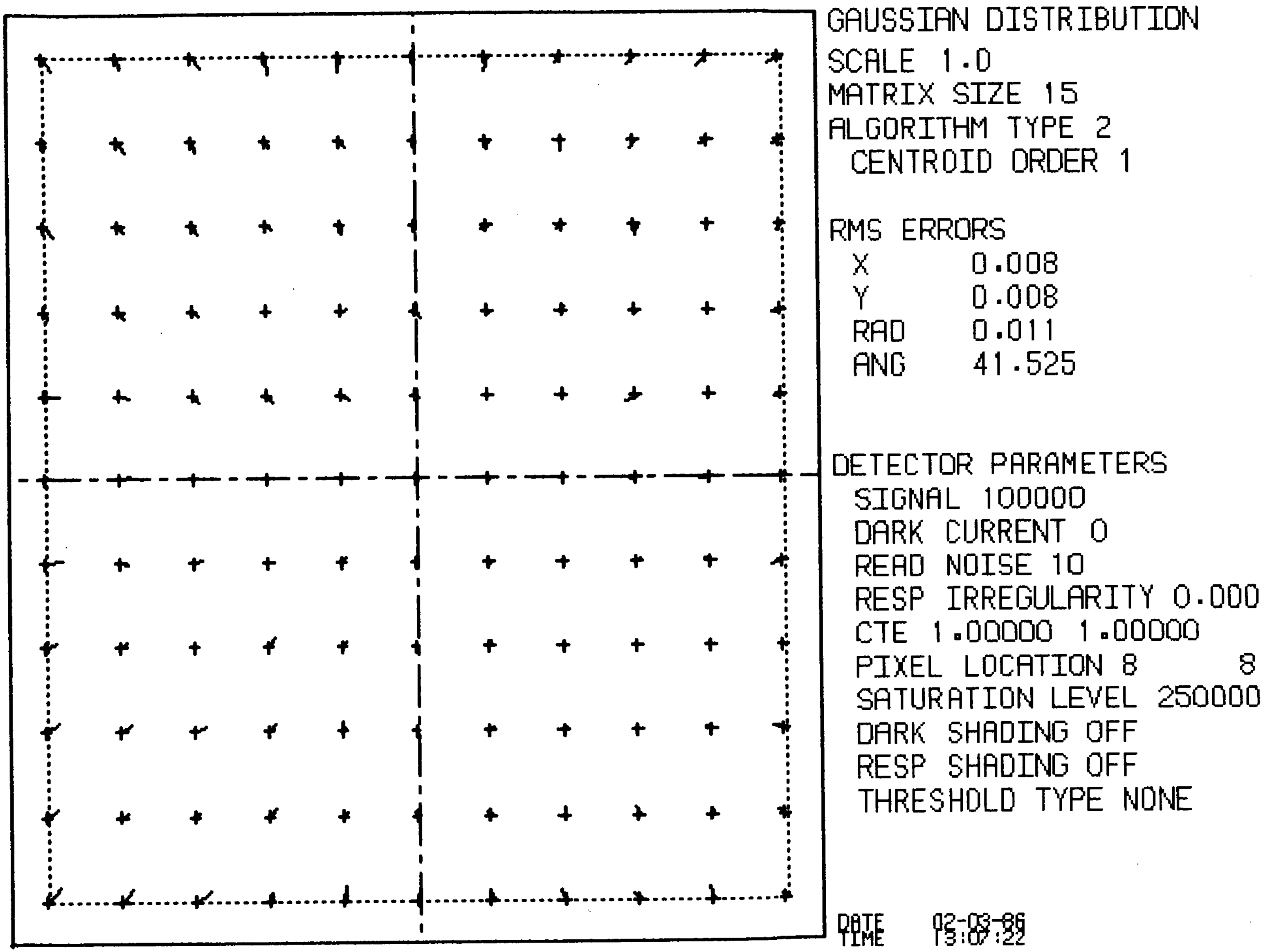

Fig. 25 Pixel Performance Map - Gaussian PSF and Read Noise, Matrix Size 15

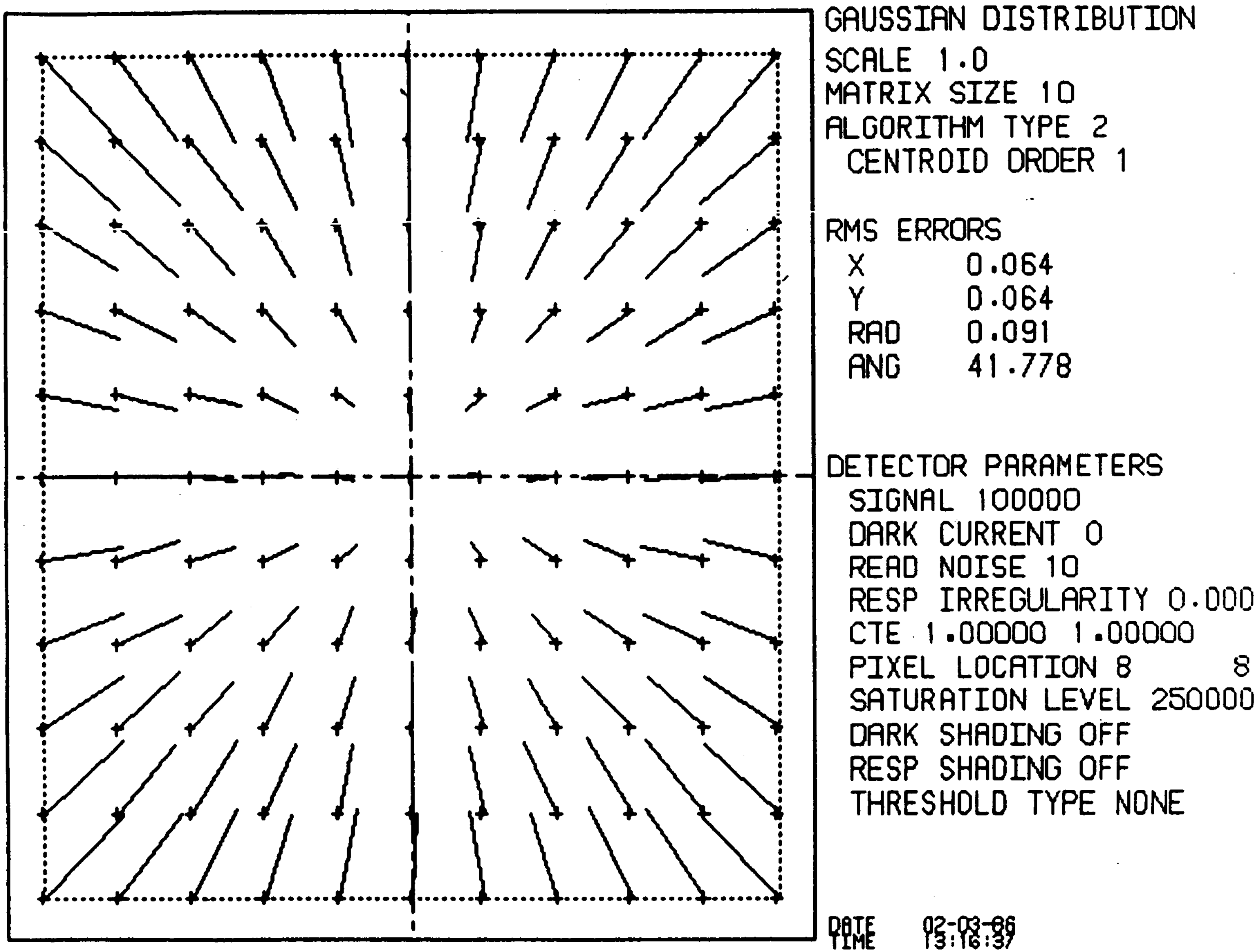

Fig. 26 Pixel Performance Map - Gaussian PSF and Read Noise, Matrix Size 10

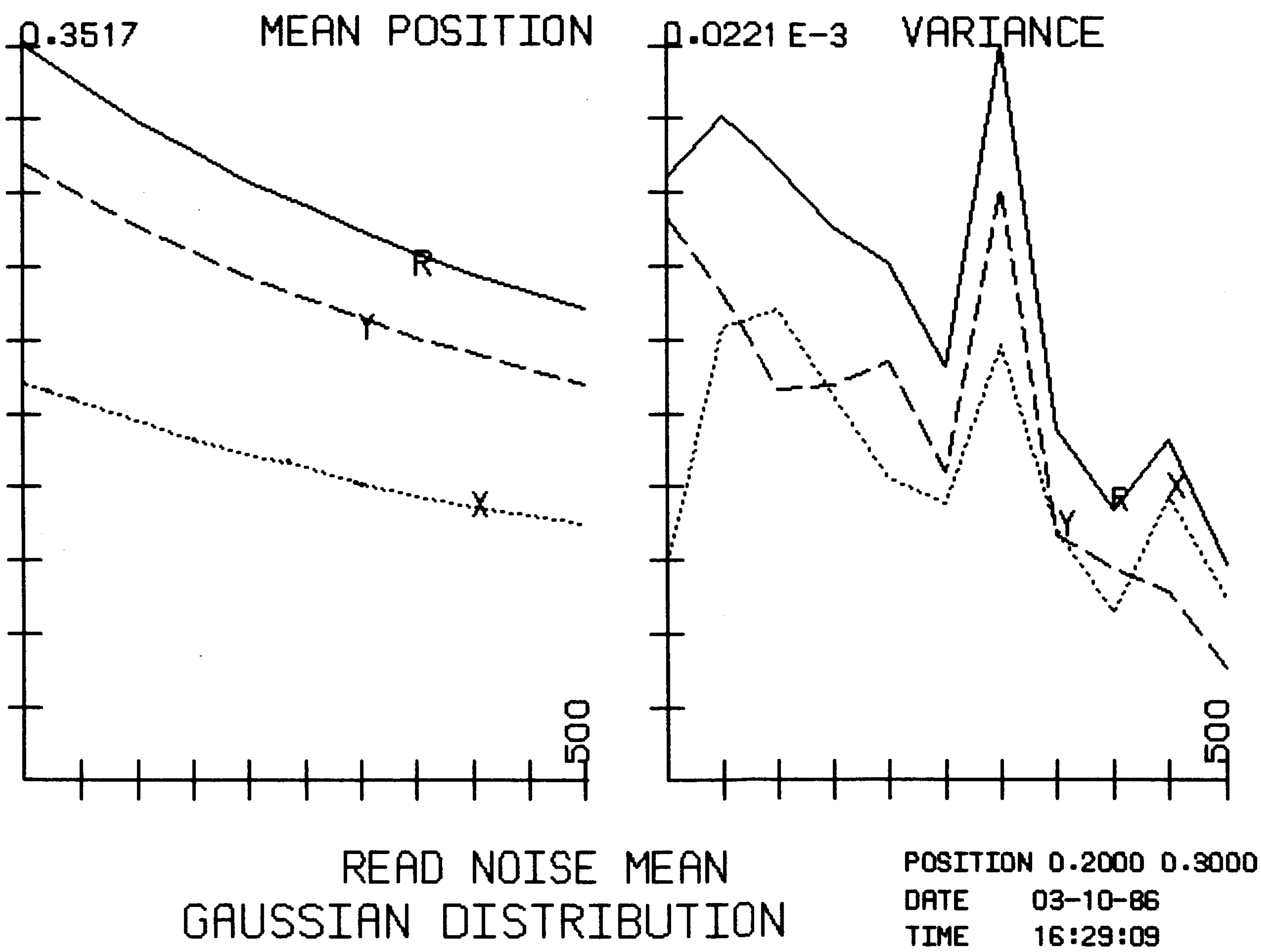

Fig. 27 Position Estimate as a Function of Read Noise, Matrix Size 15

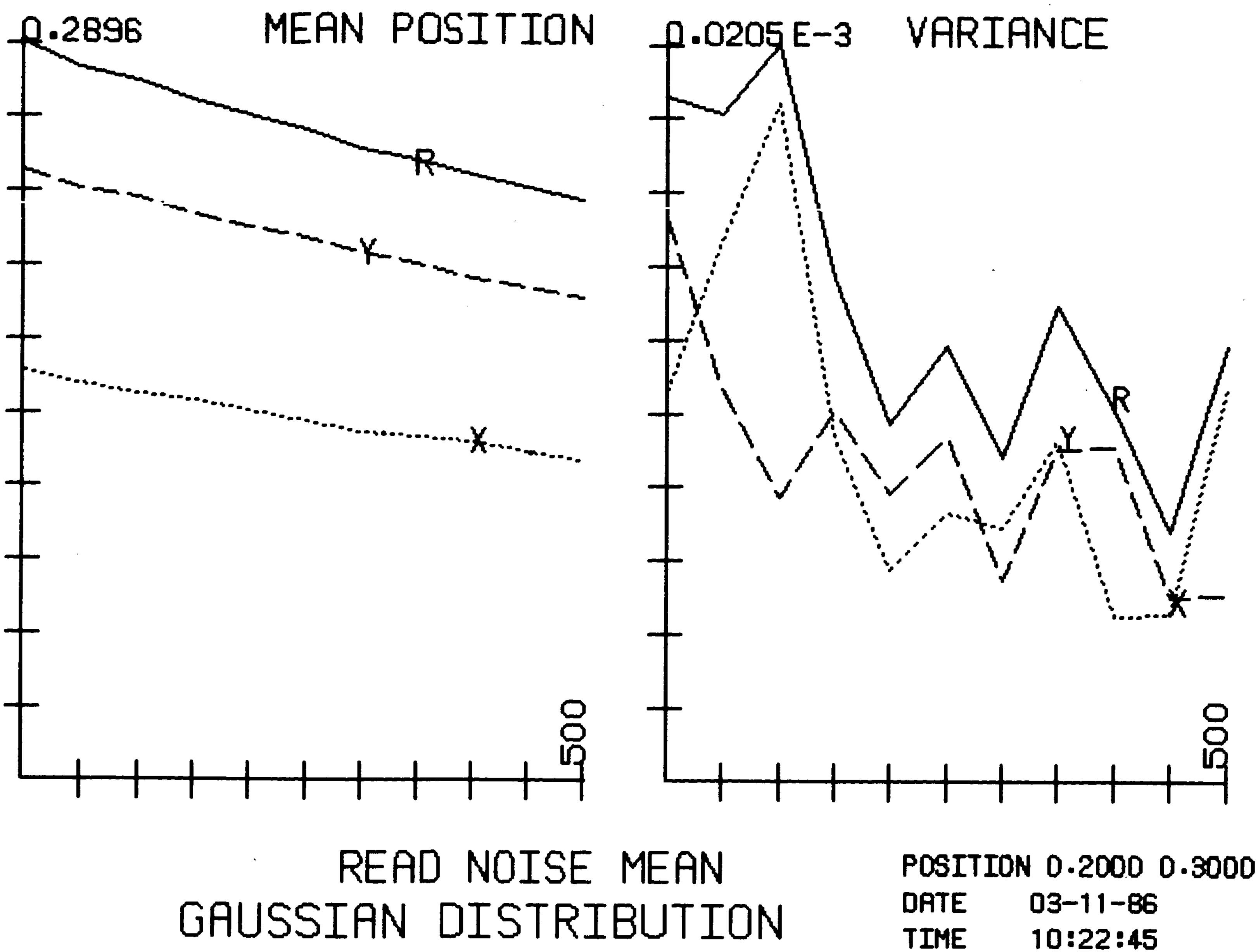

Fig. 28 Position Estimate as a Function of Read Noise, Matrix Size 10

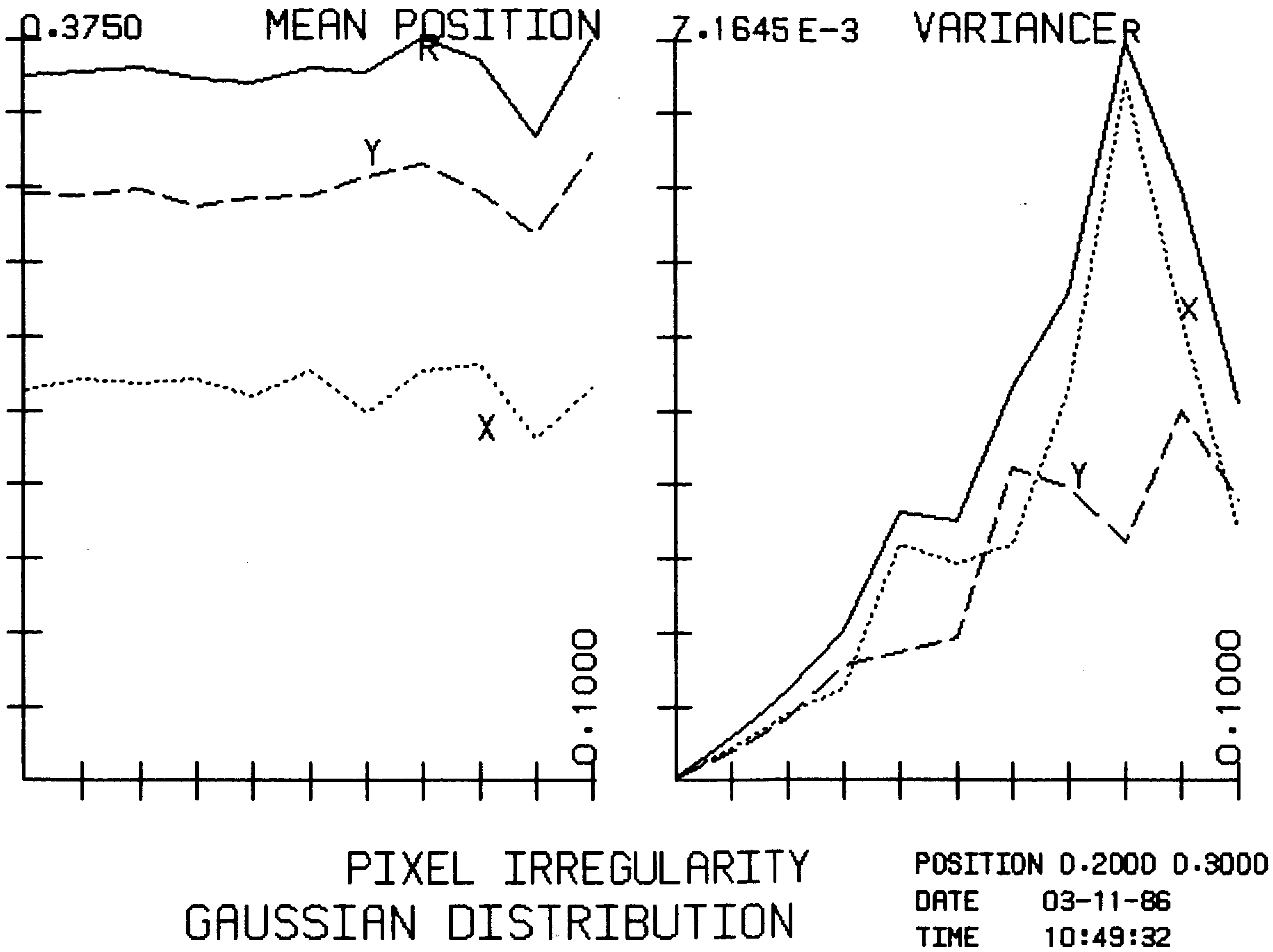

Fig. 29 Position Estimate as a Function of Pixel Irregularity

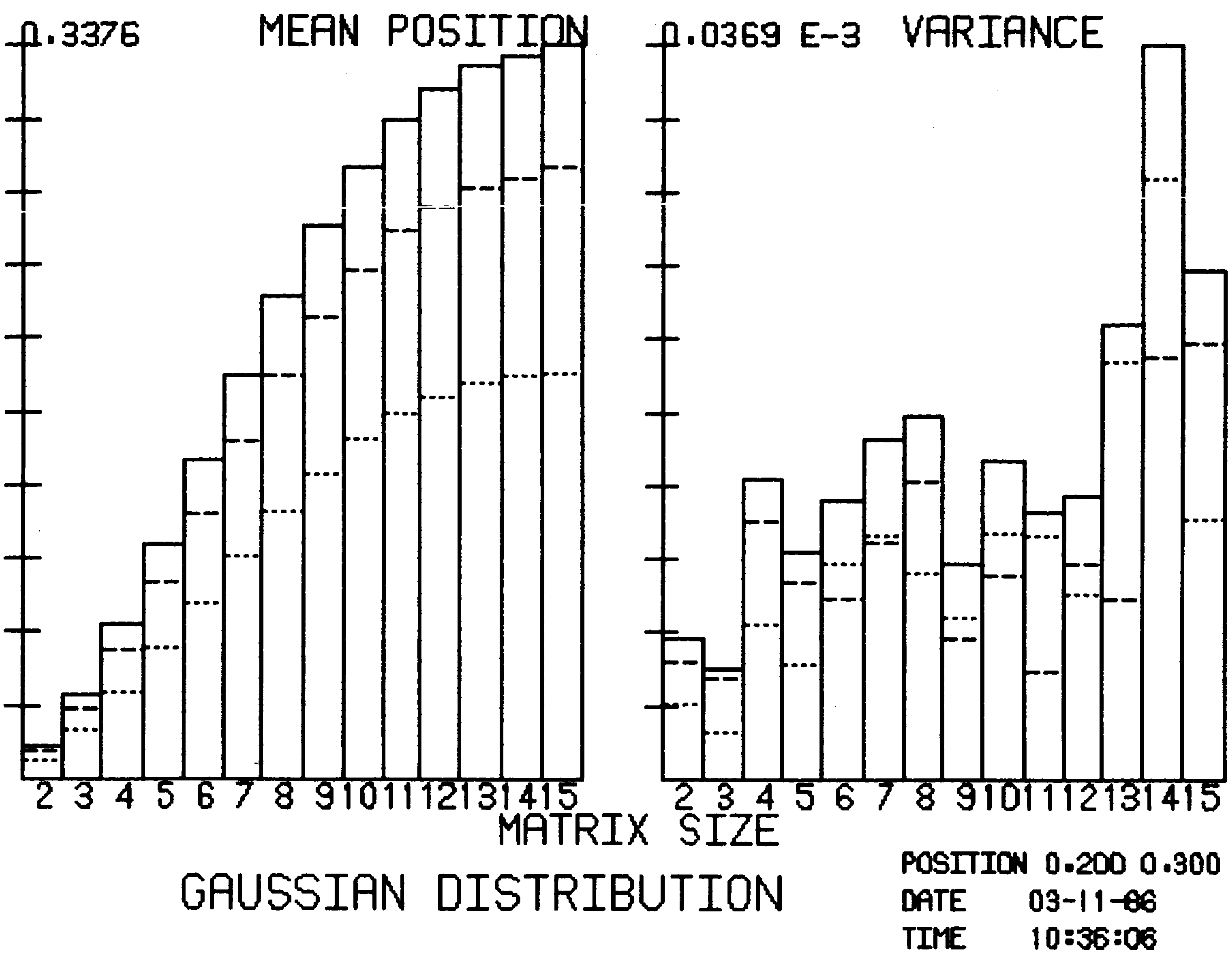

Fig. 30 Position Estimate as a Function of Matrix Size

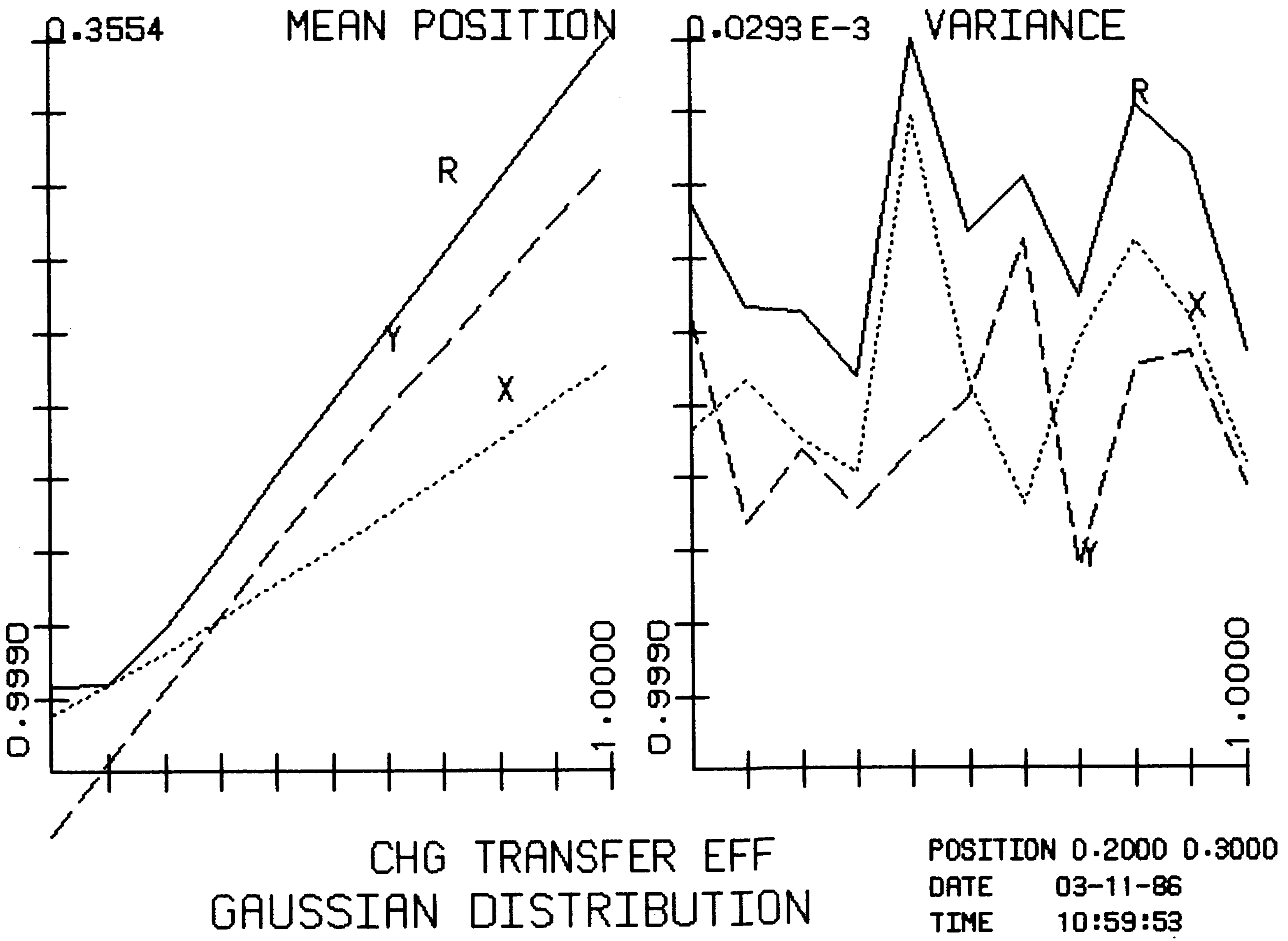

Fig. 31 Position Estimate as a Function of Charge Transfer Efficiency

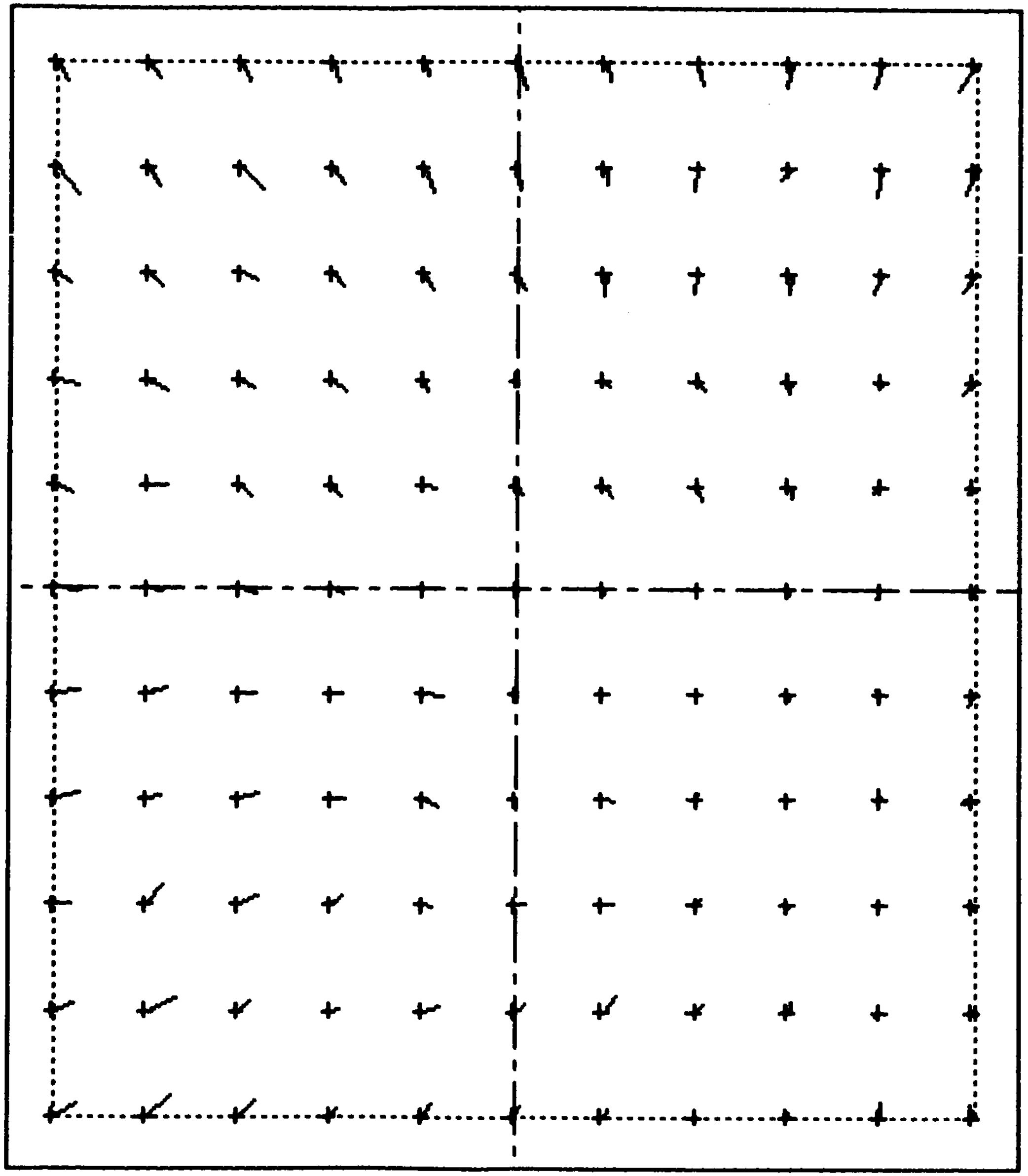

GAUSSIAN DISTRIBUTION
SCALE 1.0
MATRIX SIZE 15
ALGORITHM TYPE 2
CENTROID ORDER 1

RMS ERRORS

X	0.012
Y	0.012
RAD	0.017
ANG	42.275

DETECTOR PARAMETERS
SIGNAL 100000
DARK CURRENT 10
READ NOISE 10
RESP IRREGULARITY 0.010
CTE 0.99999 0.99999
PIXEL LOCATION 200 300
SATURATION LEVEL 250000
DARK SHADING OFF
RESP SHADING OFF
THRESHOLD TYPE NONE

DATE 02-04-86
TIME 09:43:30

Fig. 32 Pixel Performance Map - Good CCD

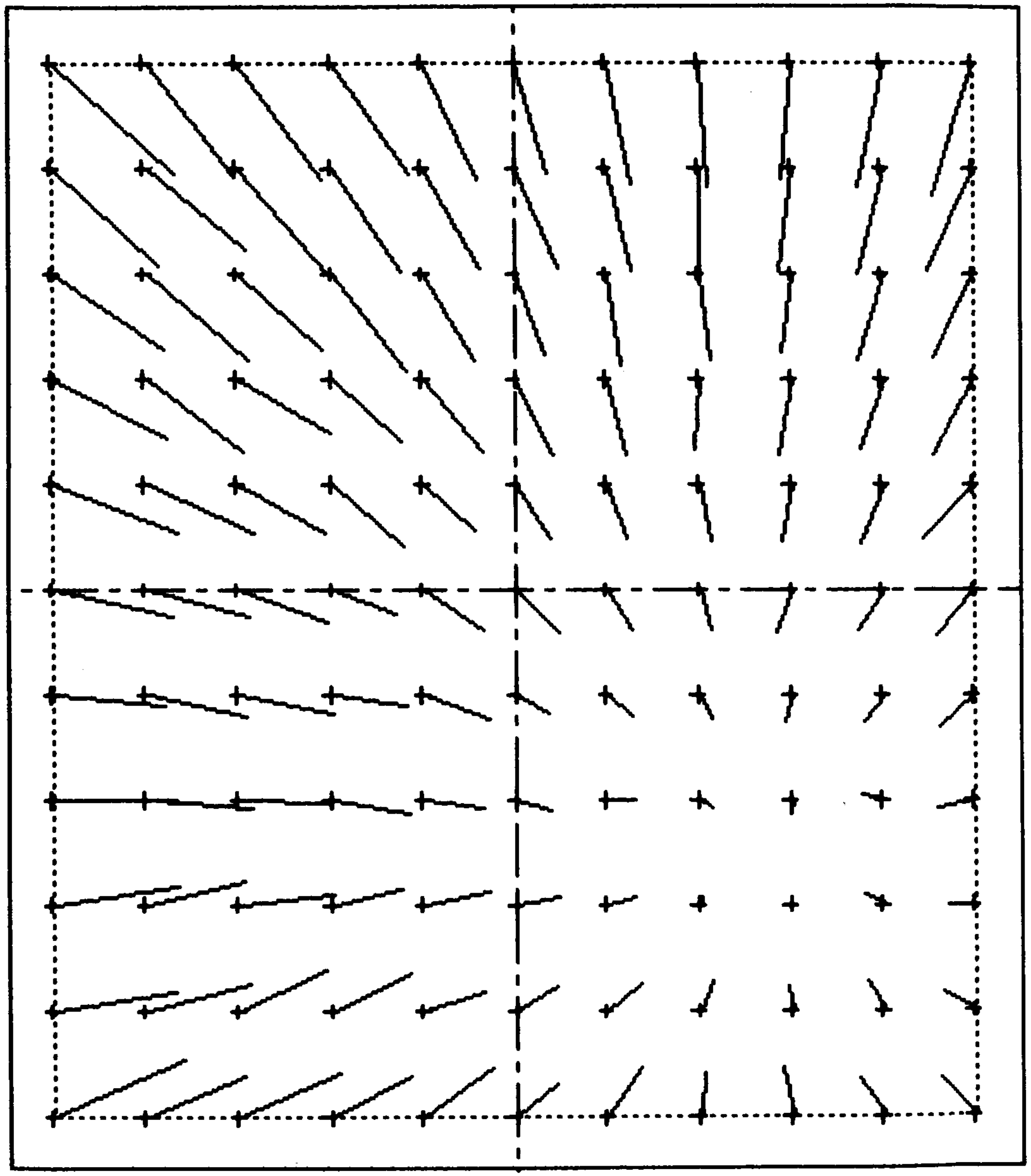

GAUSSIAN DISTRIBUTION

SCALE 1.0
MATRIX SIZE 15
ALGORITHM TYPE 2
CENTROID ORDER 1

RMS ERRORS

X	0.069
Y	0.060
RAD	0.092
ANG	40.807

DETECTOR PARAMETERS
SIGNAL 100000
DARK CURRENT 50
READ NOISE 100
RESP IRREGULARITY 0.030
CTE 0.99999 0.99999
PIXEL LOCATION 200 300
SATURATION LEVEL 250000
DARK SHADING OFF
RESP SHADING OFF
THRESHOLD TYPE NONE

DATE 02-04-86
TIME 10:08:51

Fig. 33 Pixel Performance Map - Noisy CCD

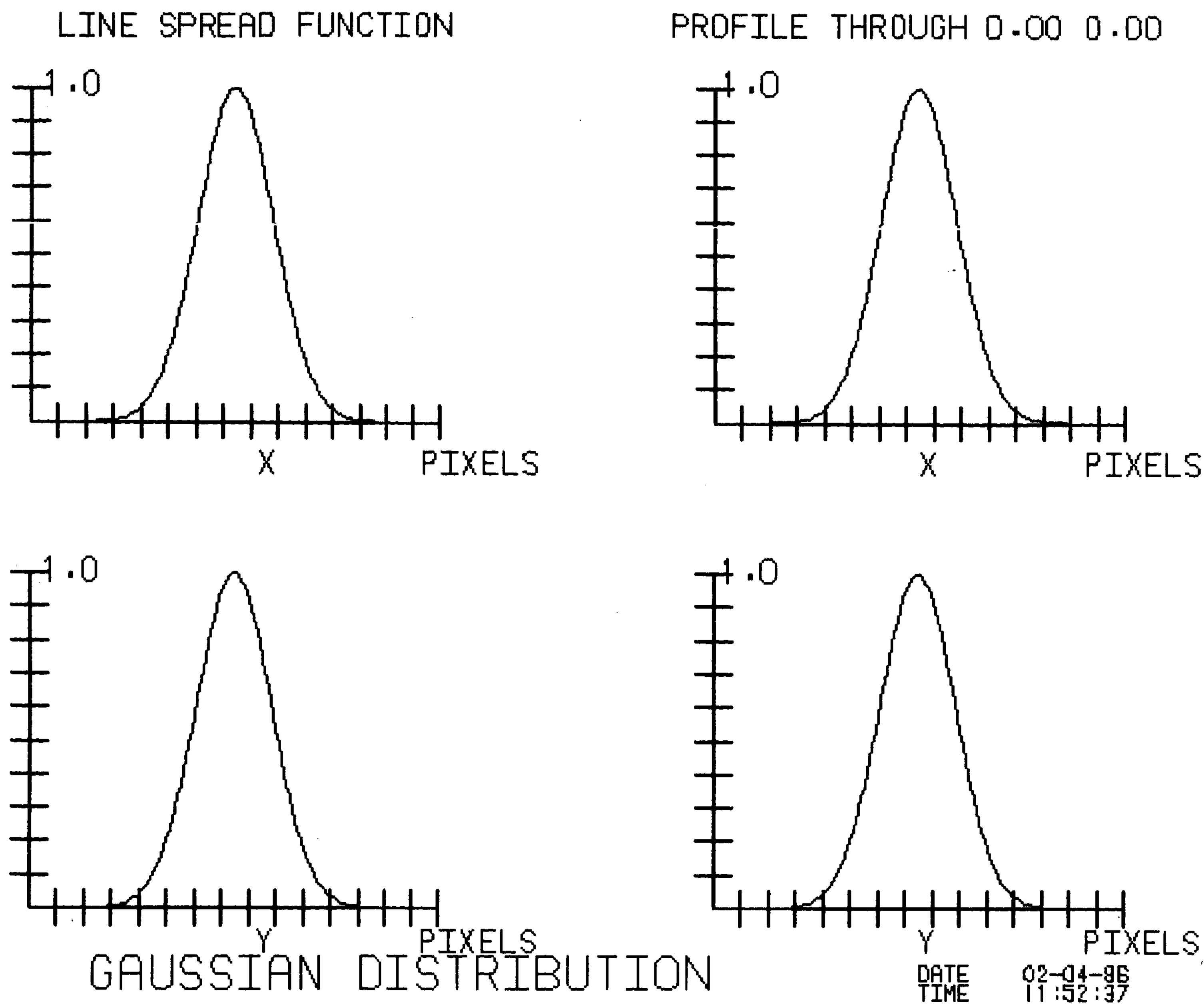

Fig. 34 Line Spread Functions - Small Gaussian PSF

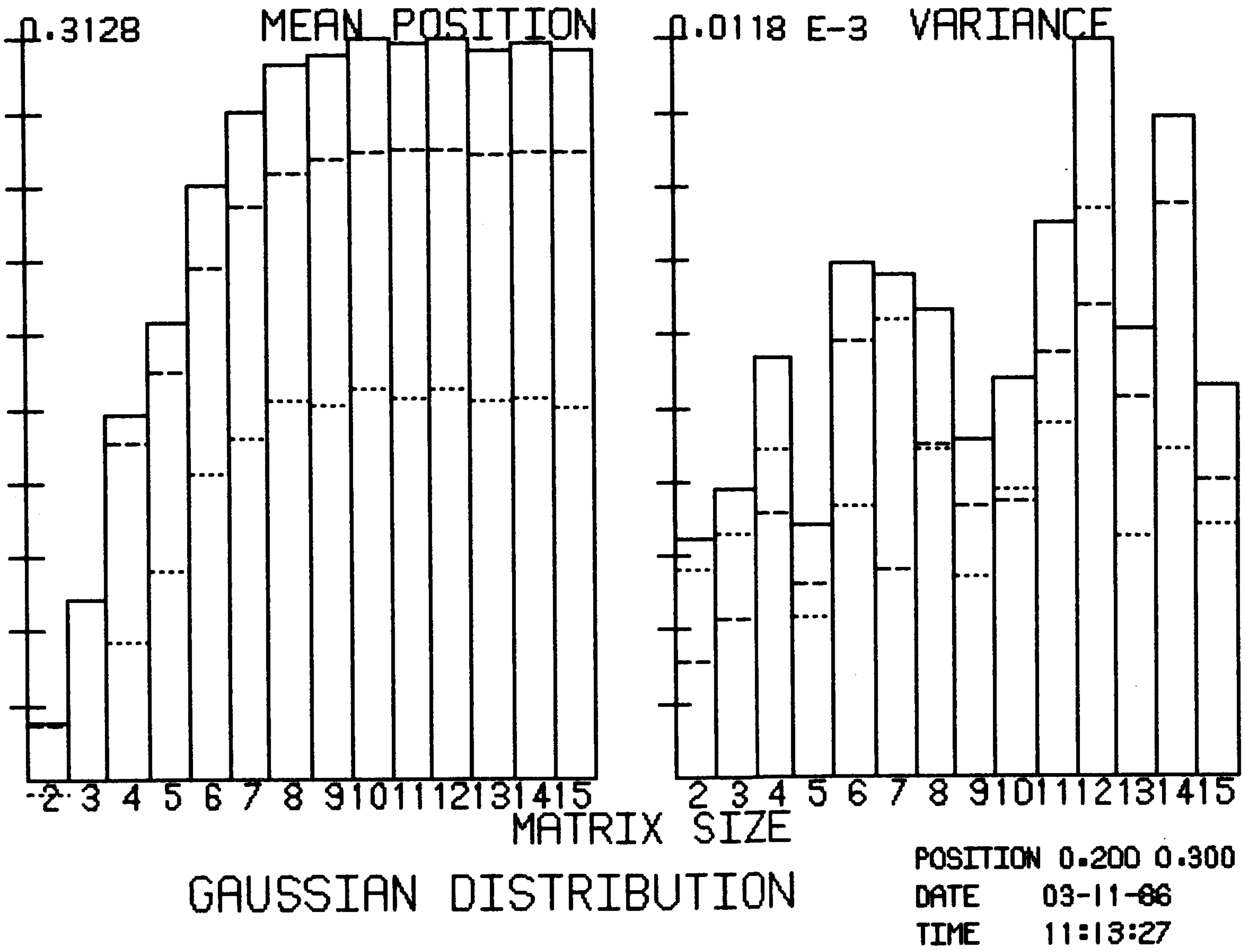

Fig. 35 Position Estimate as a Function of Matrix Size - Good CCD

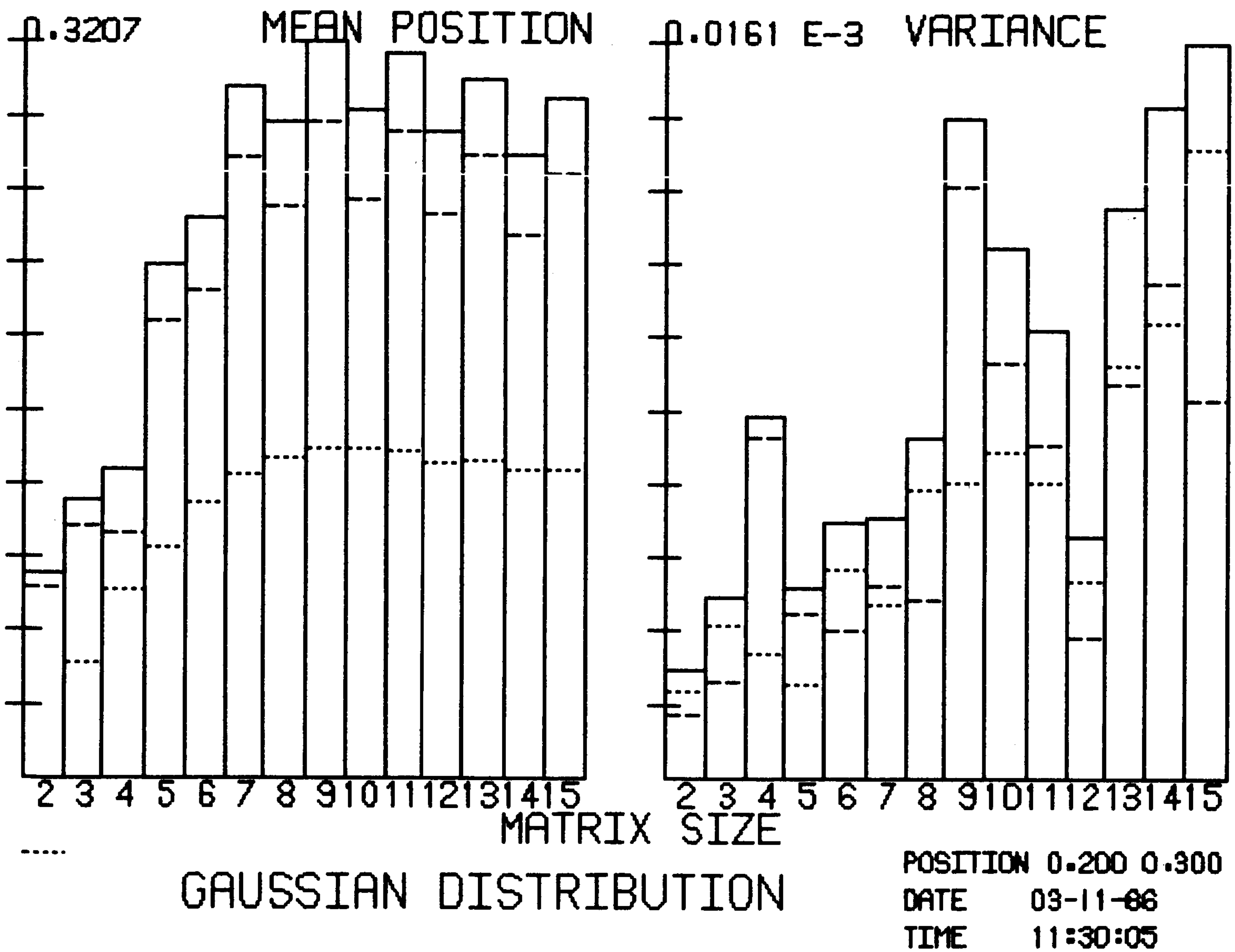

Fig. 36 Position Estimate as a Function of Matrix Size - Noisy CCD

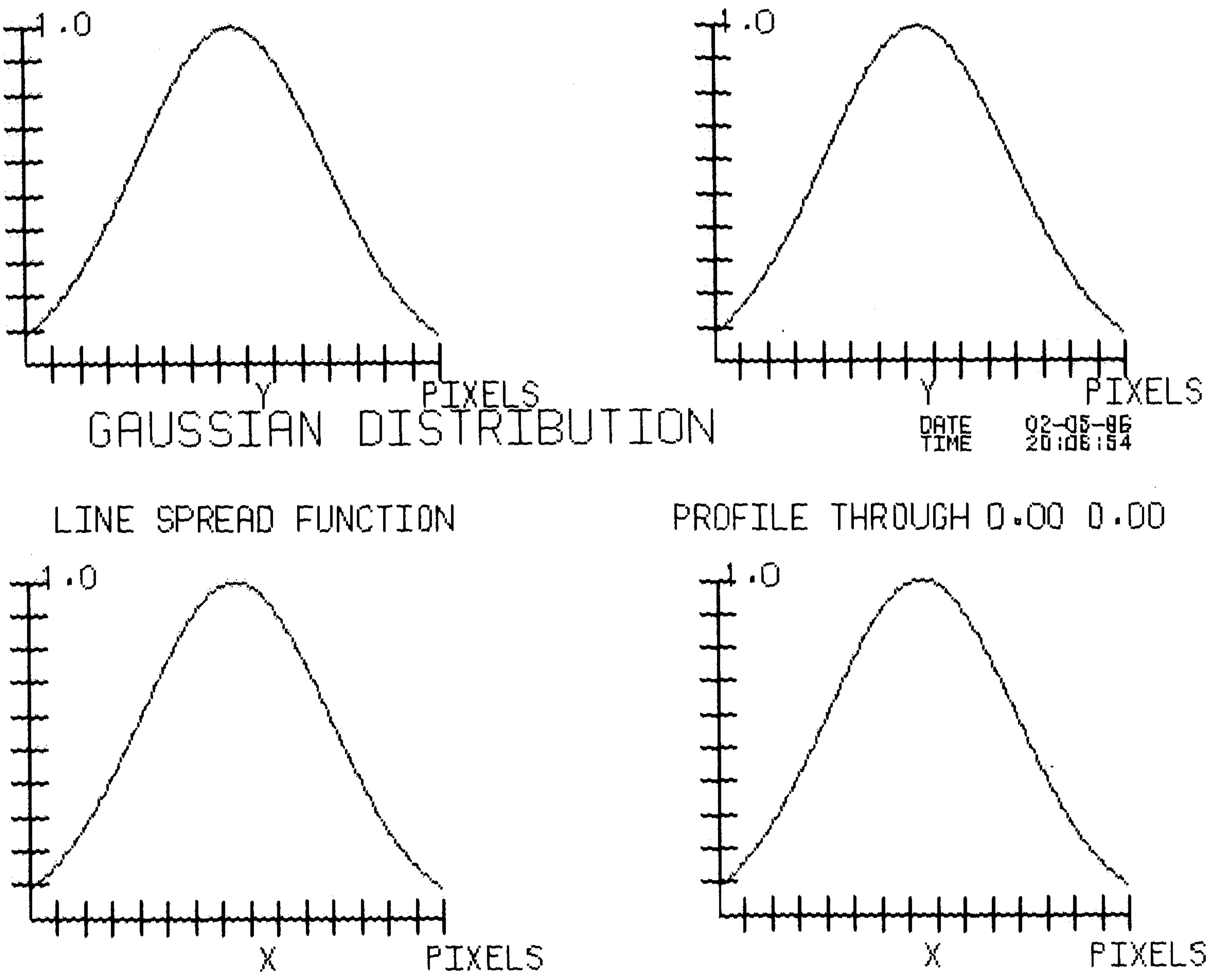

Fig. 37 Line Spread Functions - Large Gaussian PSF

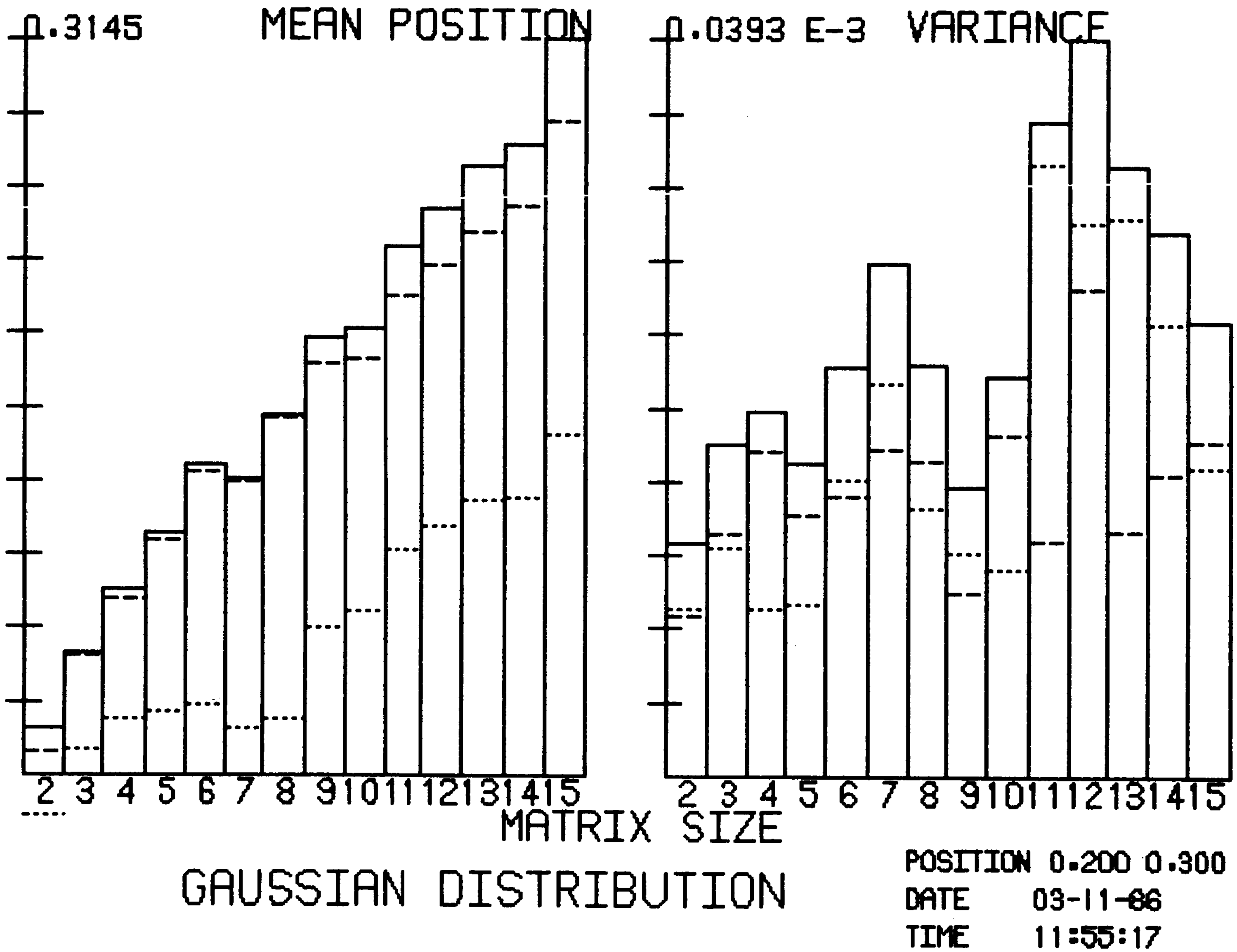

Fig. 38 Position Estimate as a Function of Matrix Size - Good CCD

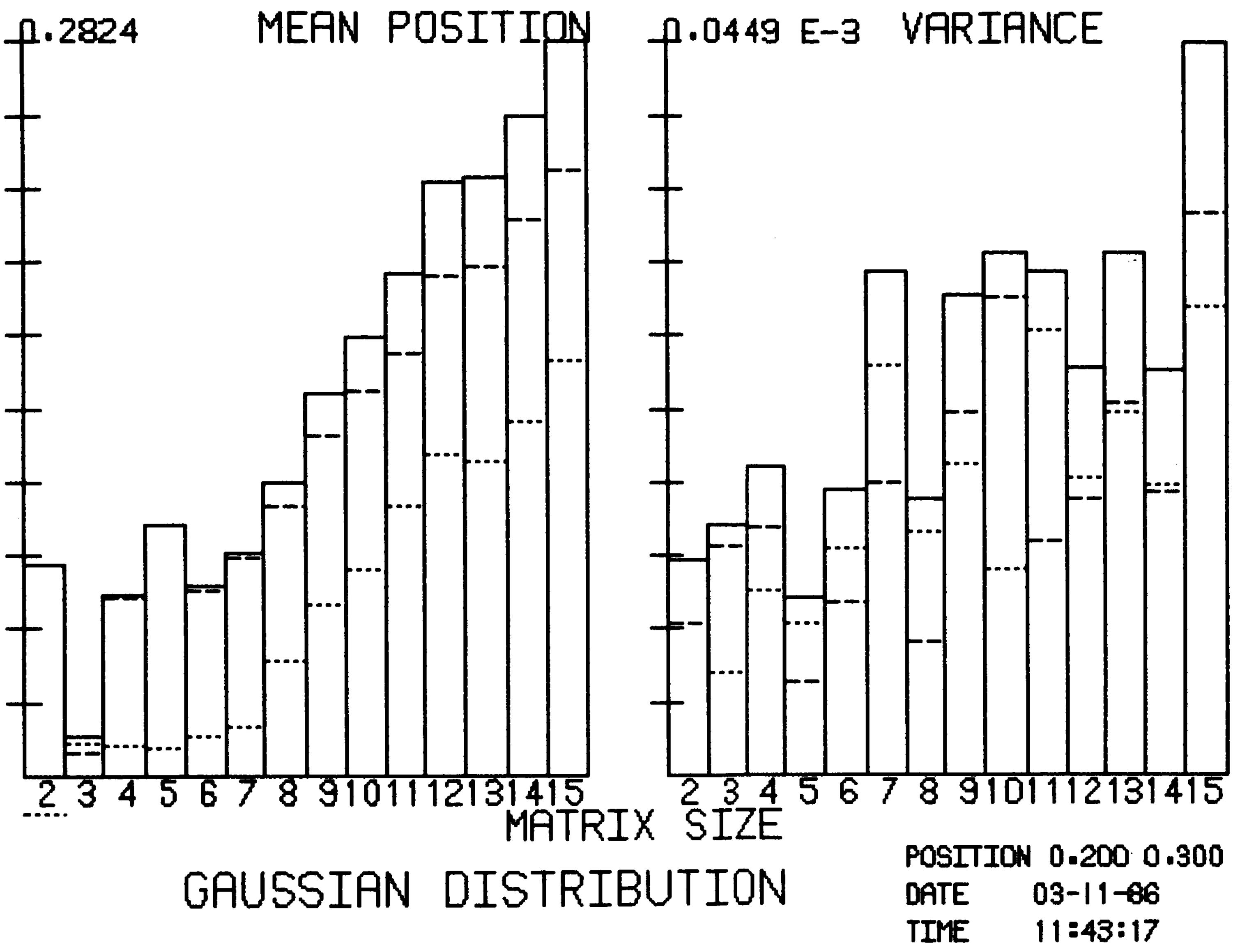

Fig. 39 Position Estimate as a Function of Matrix Size - Noisy CCD

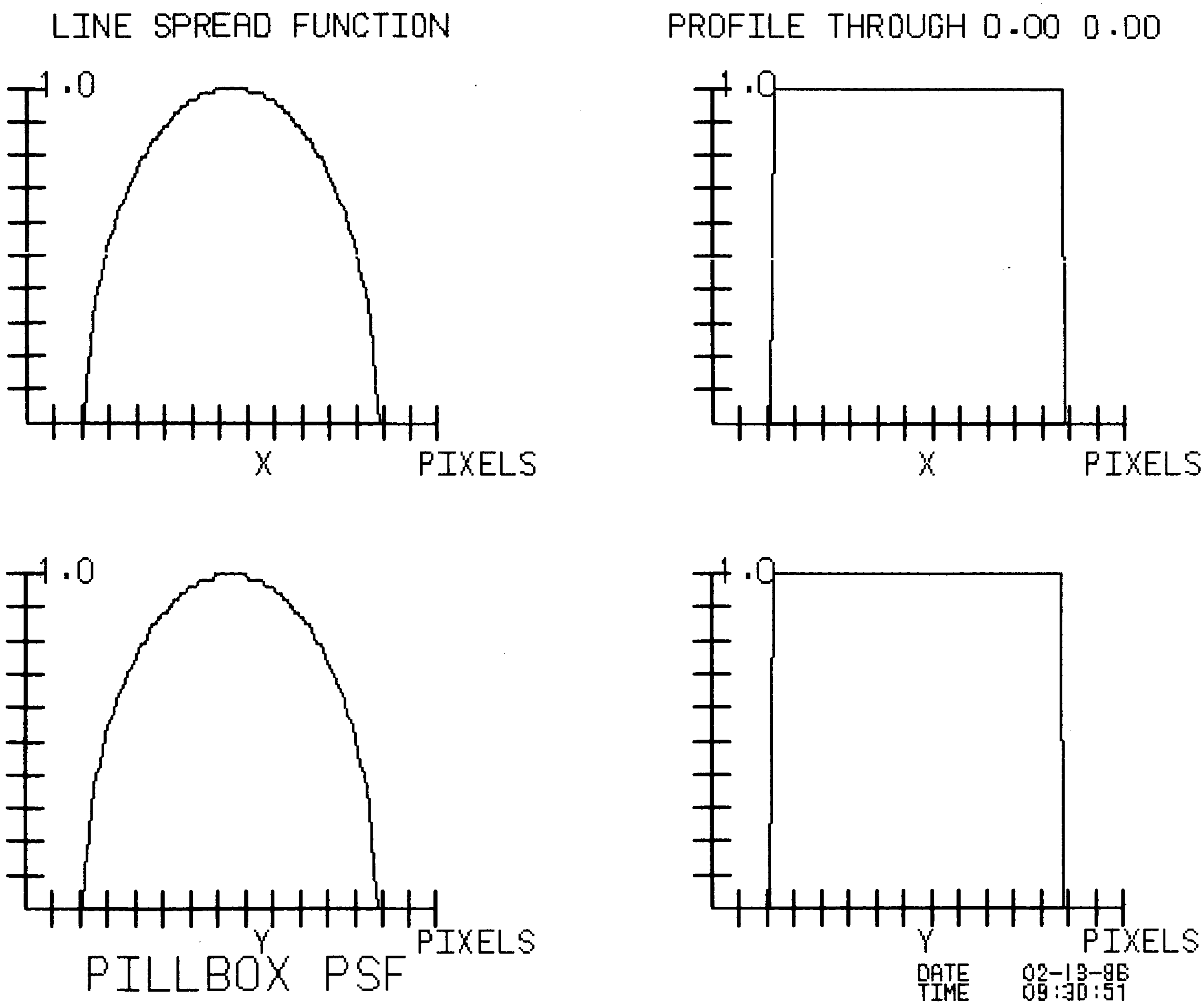

Fig. 40 Line Spread Functions - Pillbox PSF

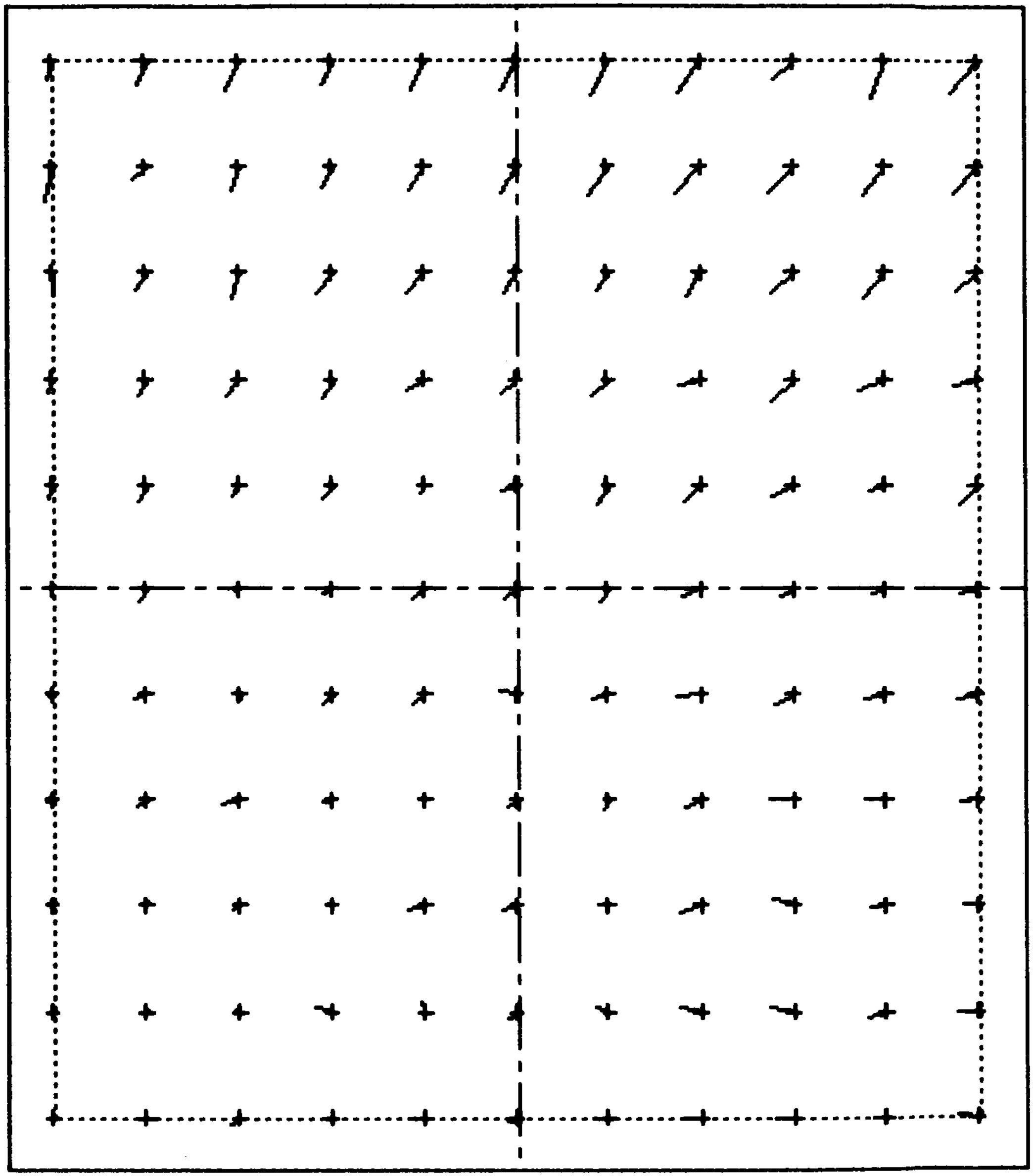

PILLBOX PSF
SCALE 1.0
MATRIX SIZE 15
ALGORITHM TYPE 2
CENTROID ORDER 1

RMS ERRORS

X	0.018
Y	0.014
RAD	0.023
ANG	34.239

DETECTOR PARAMETERS
SIGNAL 100000
DARK CURRENT 10
READ NOISE 10
RESP IRREGULARITY 0.010
CTE 0.99999 0.99999
PIXEL LOCATION 200 300
SATURATION LEVEL 250000
DARK SHADING OFF
RESP SHADING OFF
THRESHOLD TYPE NONE

DATE 02-13-86
TIME 11:49:32

Fig. 41 Pixel Performance Map - Pillbox PSF and Good CCD

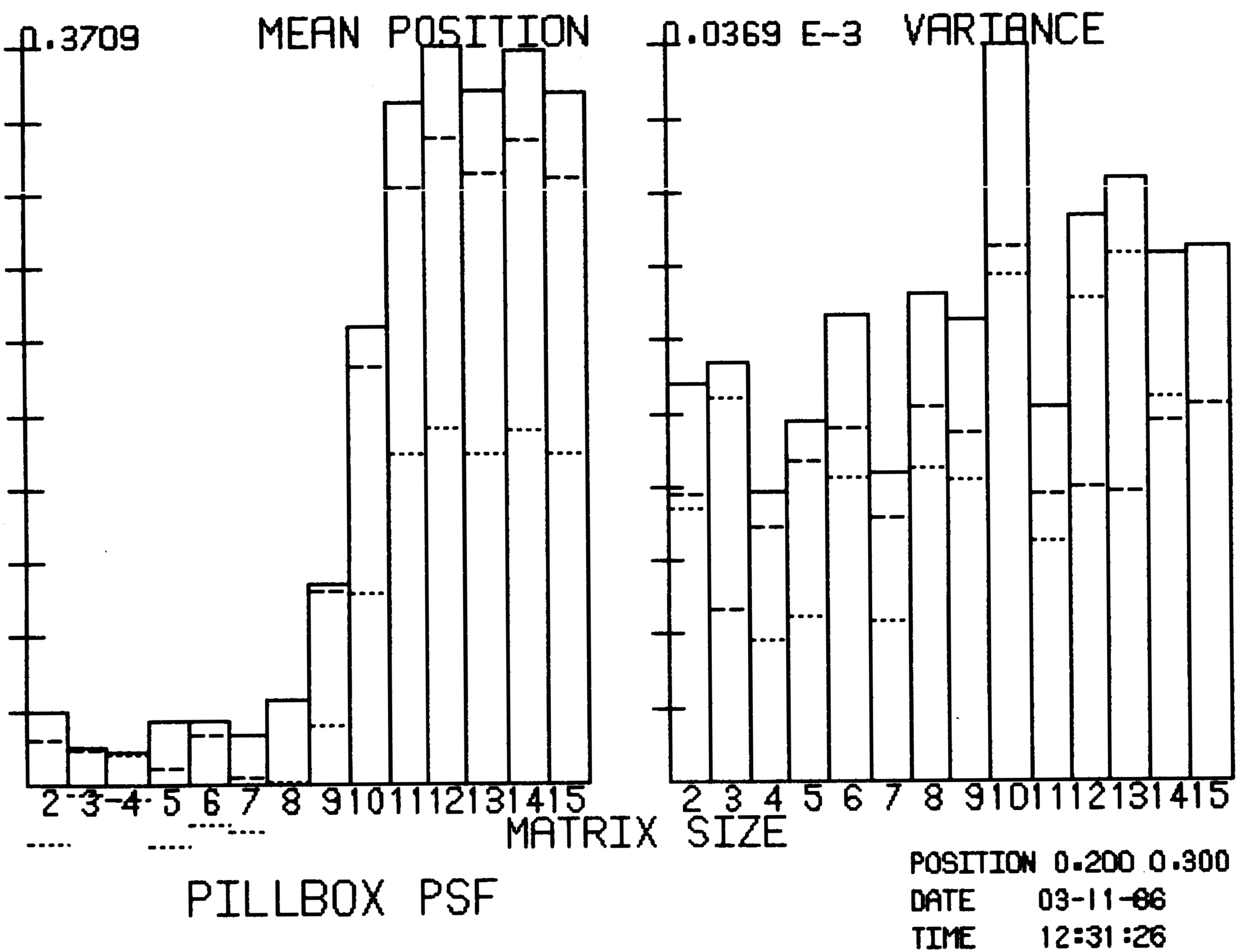

Fig. 42 Position Estimate as a Function of Matrix Size - Good CCD, Pillbox PSF

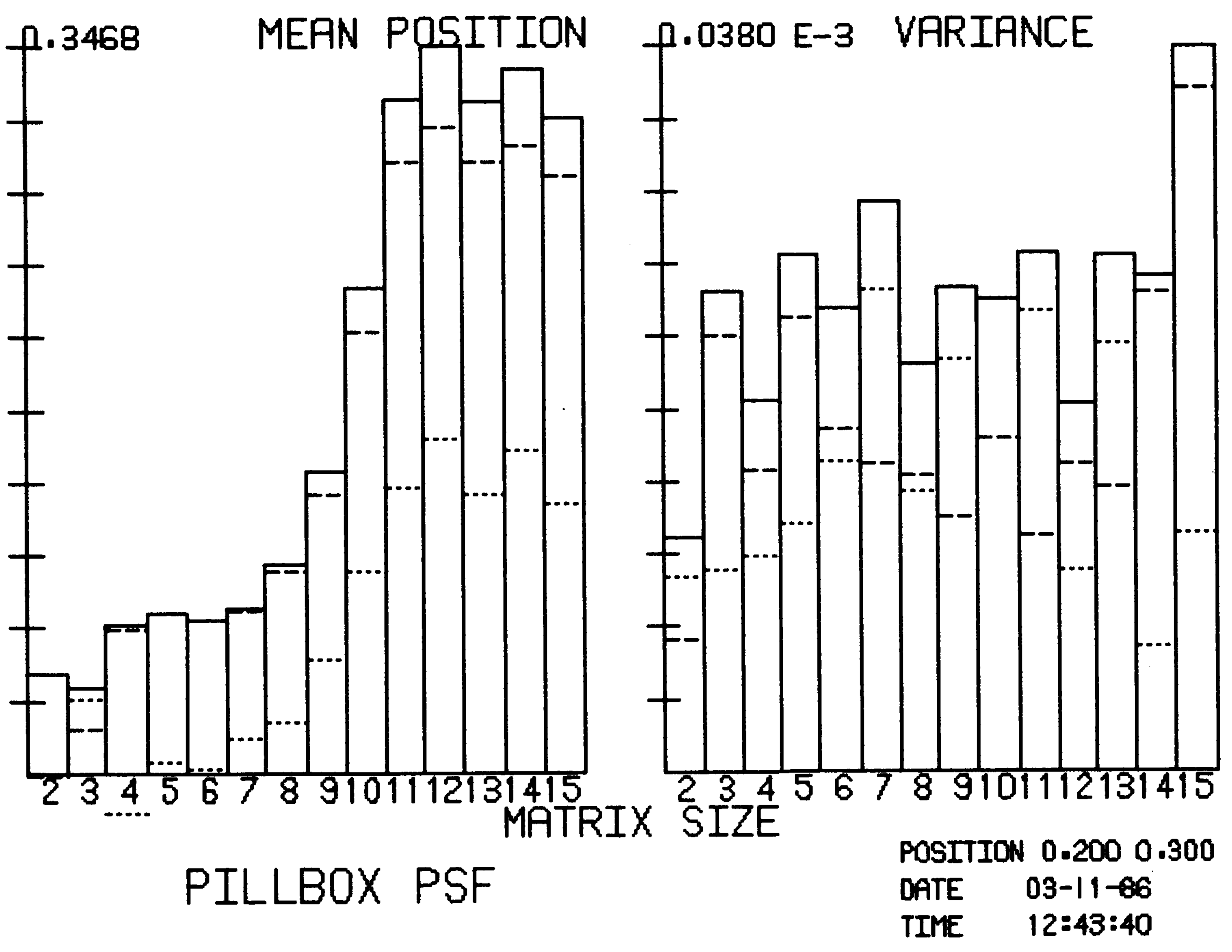

Fig. 43 Position Estimate as a Function of Matrix Size - Noisy CCD, Pillbox PSF

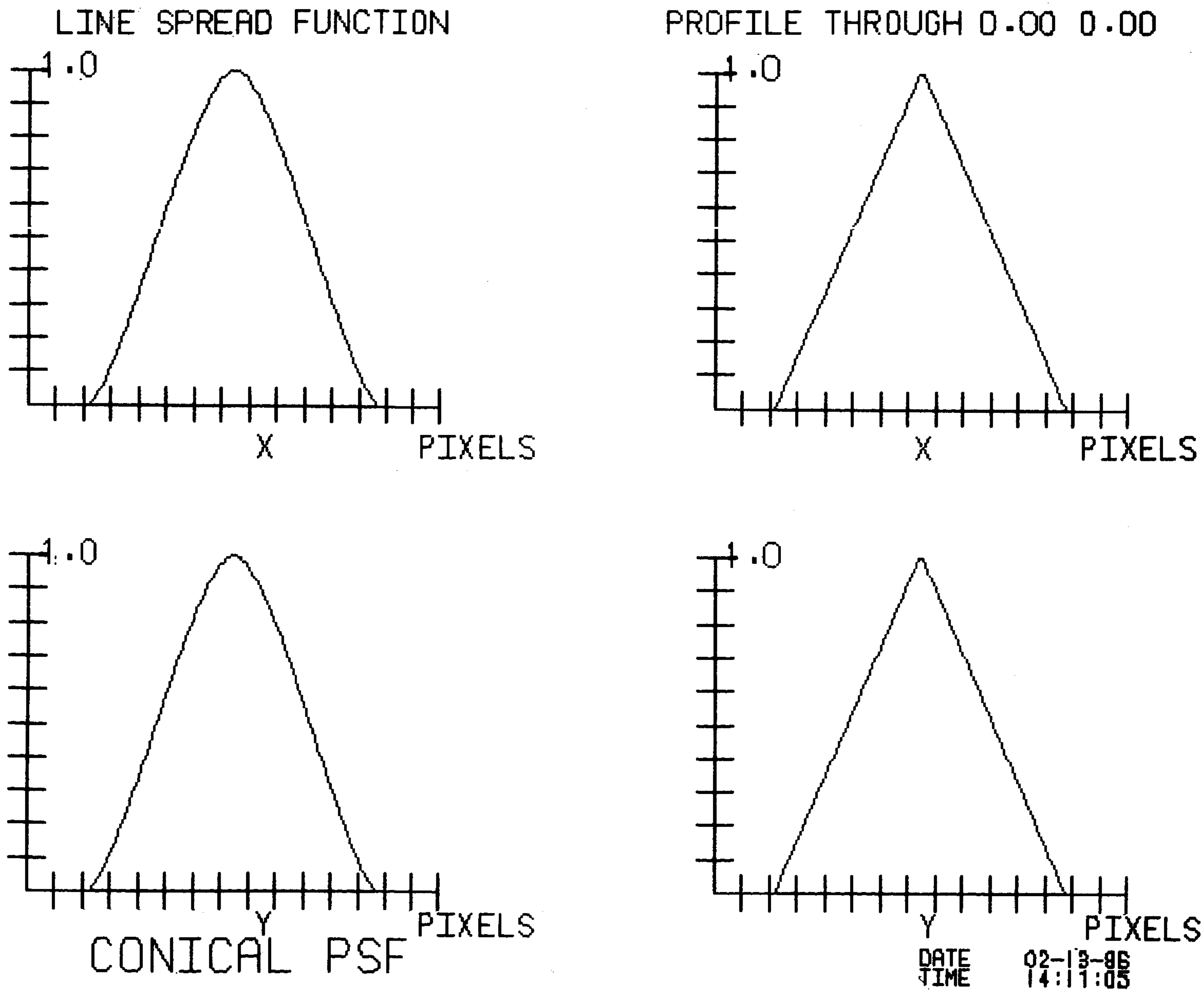

Fig. 44 Line Spread Functions - Conical PSF

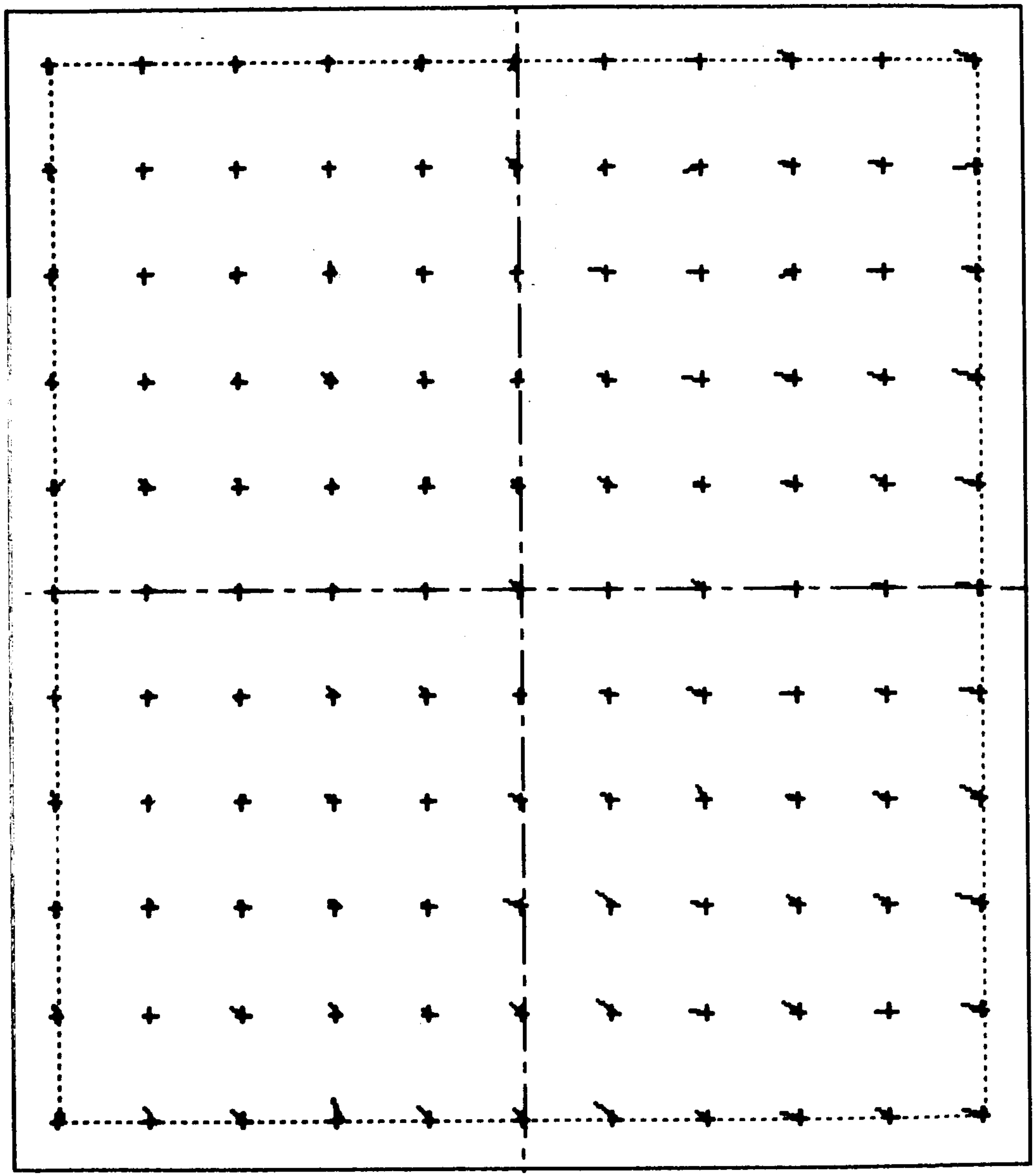

CONICAL PSF

SCALE 1.0
MATRIX SIZE 15
ALGORITHM TYPE 2
 CENTROID ORDER 1

RMS ERRORS

X	0.015
Y	0.006
RAD	0.016
ANG	29.532

DETECTOR PARAMETERS
 SIGNAL 100000
 DARK CURRENT 10
 READ NOISE 10
 RESP IRREGULARITY 0.010
 CTE 0.99999 0.99999
 PIXEL LOCATION 200 300
 SATURATION LEVEL 250000
 DARK SHADING OFF
 RESP SHADING OFF
 THRESHOLD TYPE NONE

DATE 02-13-86
TIME 14:41:28

Fig. 45 Pixel Performance Map - Conical PSF and Good CCD

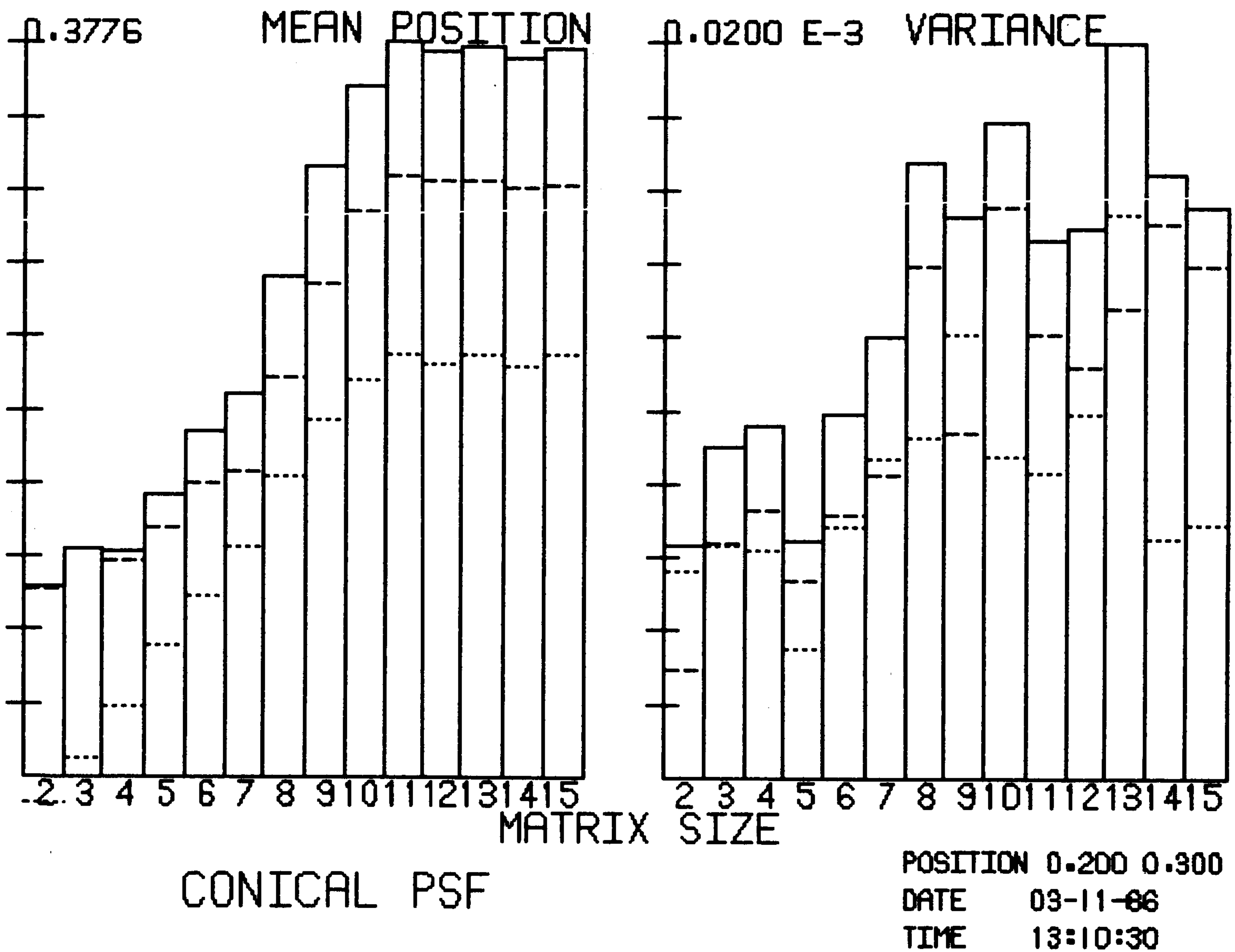

Fig. 46 Position Estimate as a Function of Matrix Size - Good CCD, Conical PSF

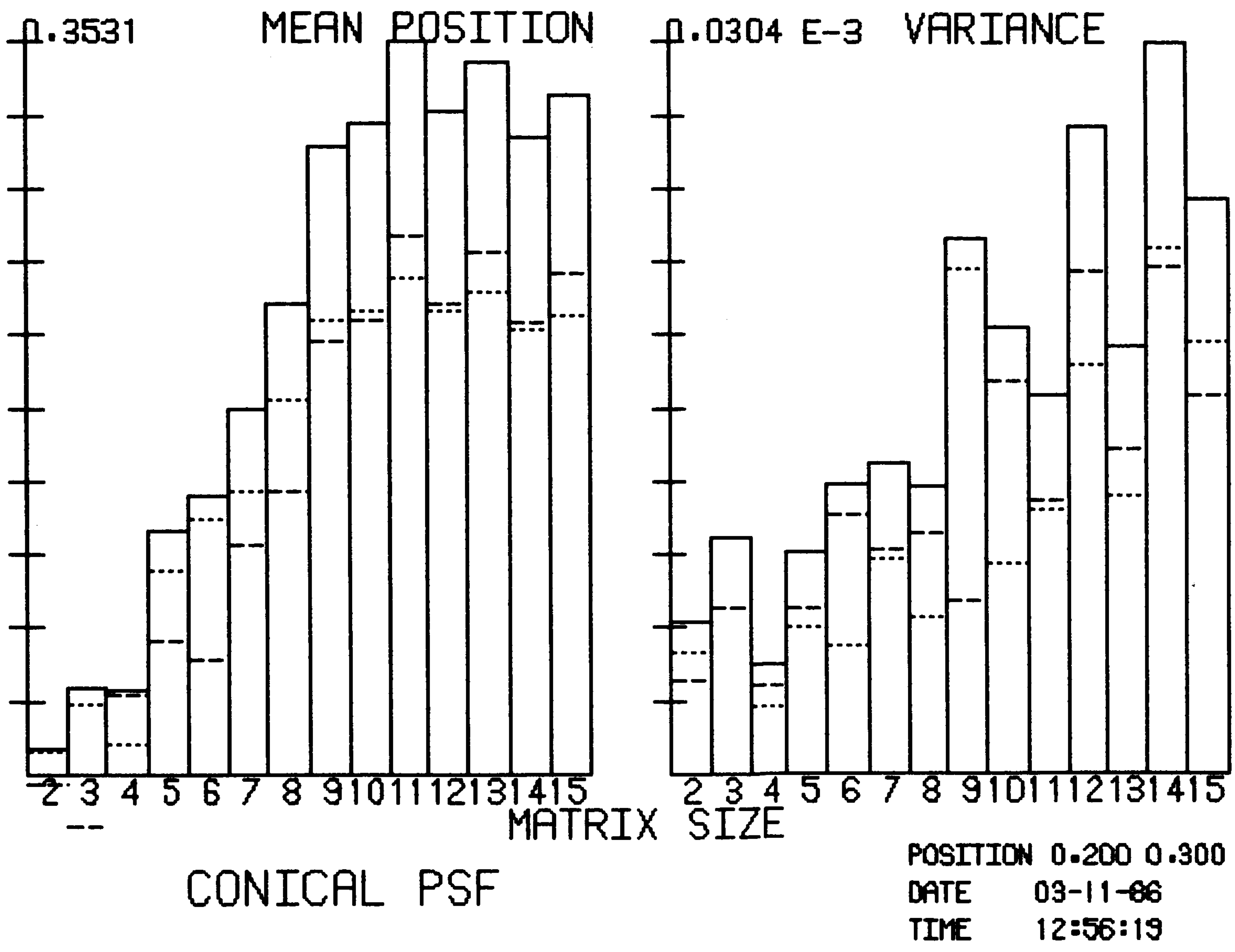

Fig. 47 Position Estimate as a Function of Matrix Size - Noisy CCD, Conical PSF

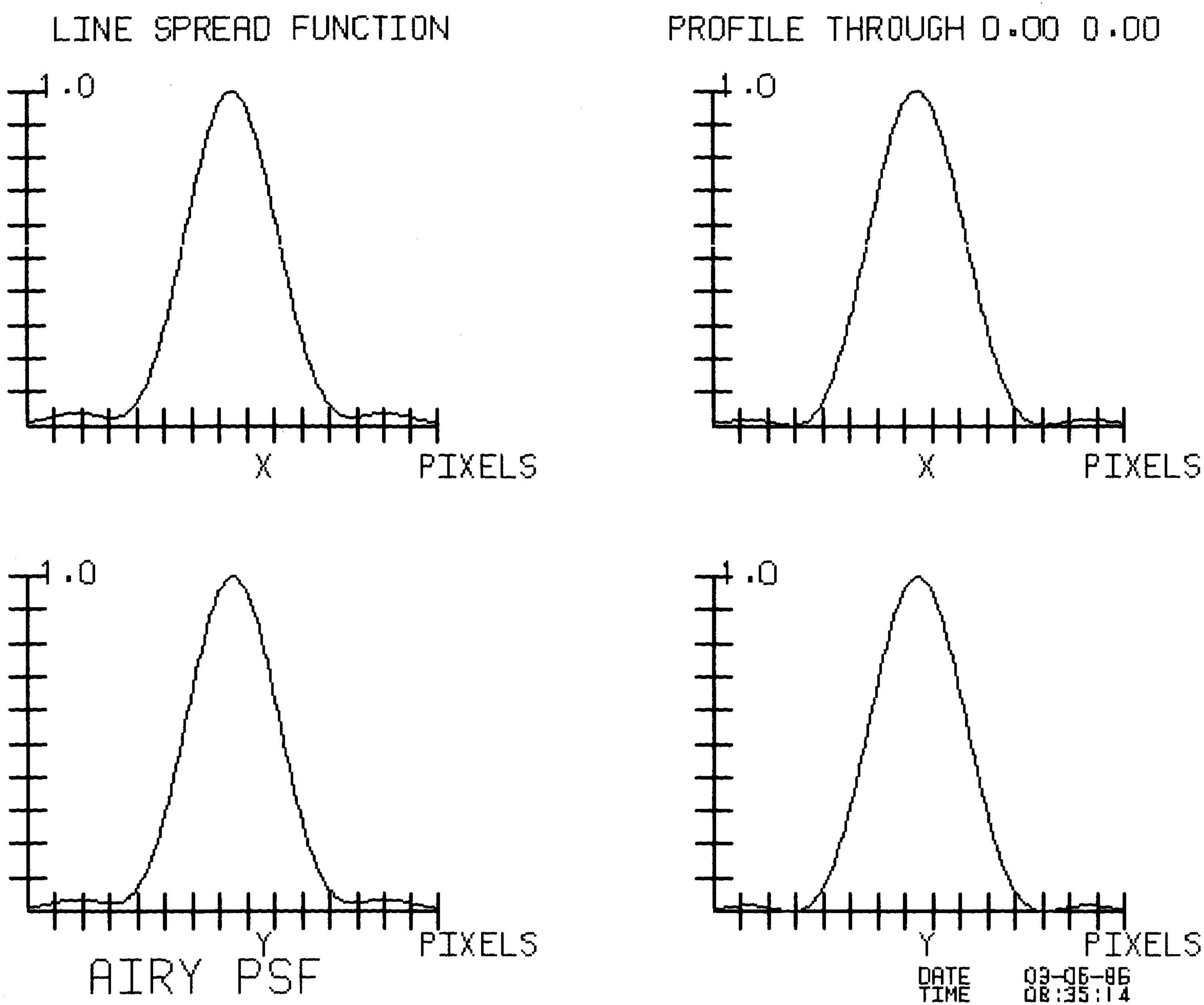

Fig. 48 Line Spread Functions - Airy.PSF

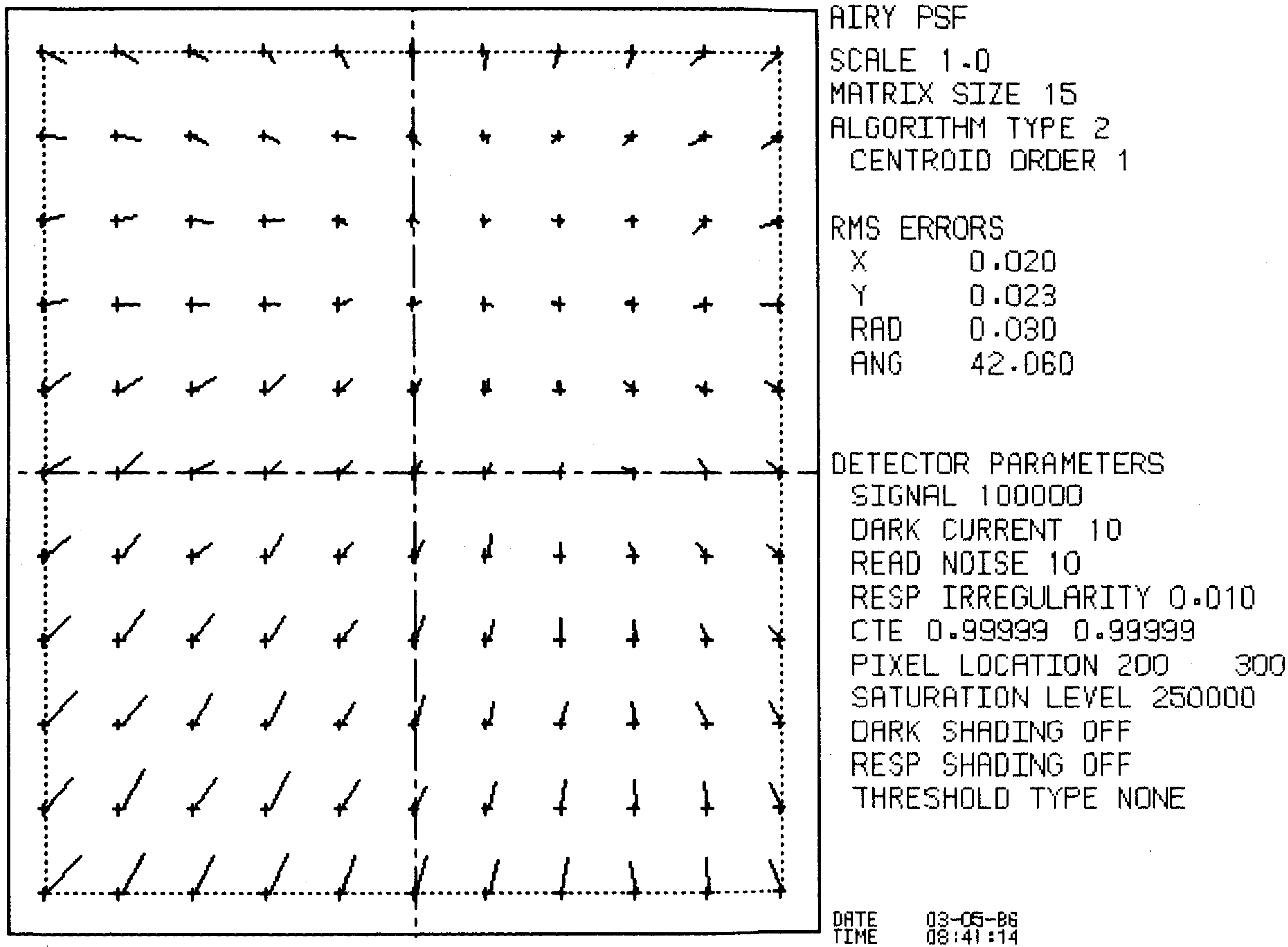

Fig. 49 Pixel Performance Map - Airy PSF and Good CCD

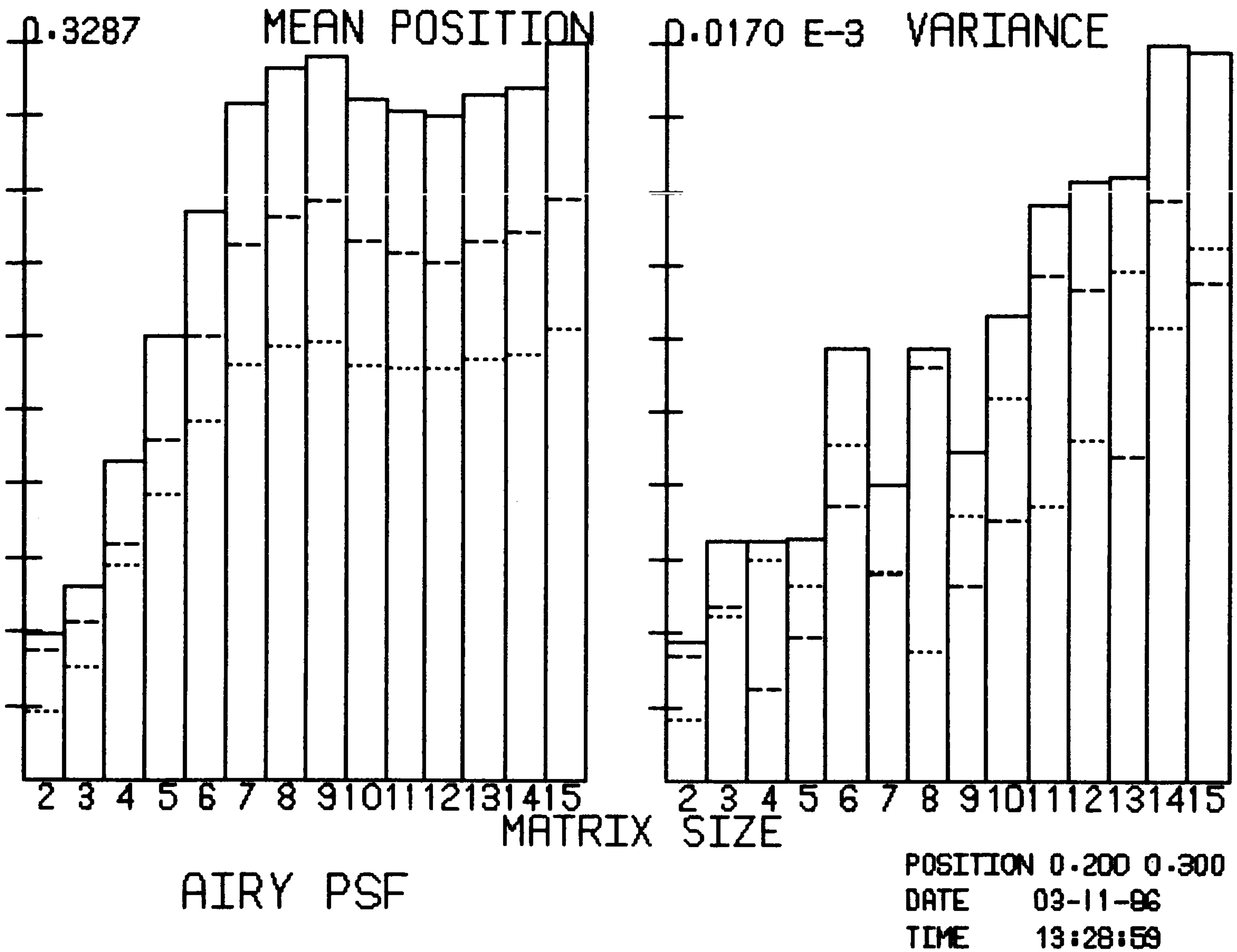

Fig. 50 Position Estimate as a Function of Matrix Size - Good CCD

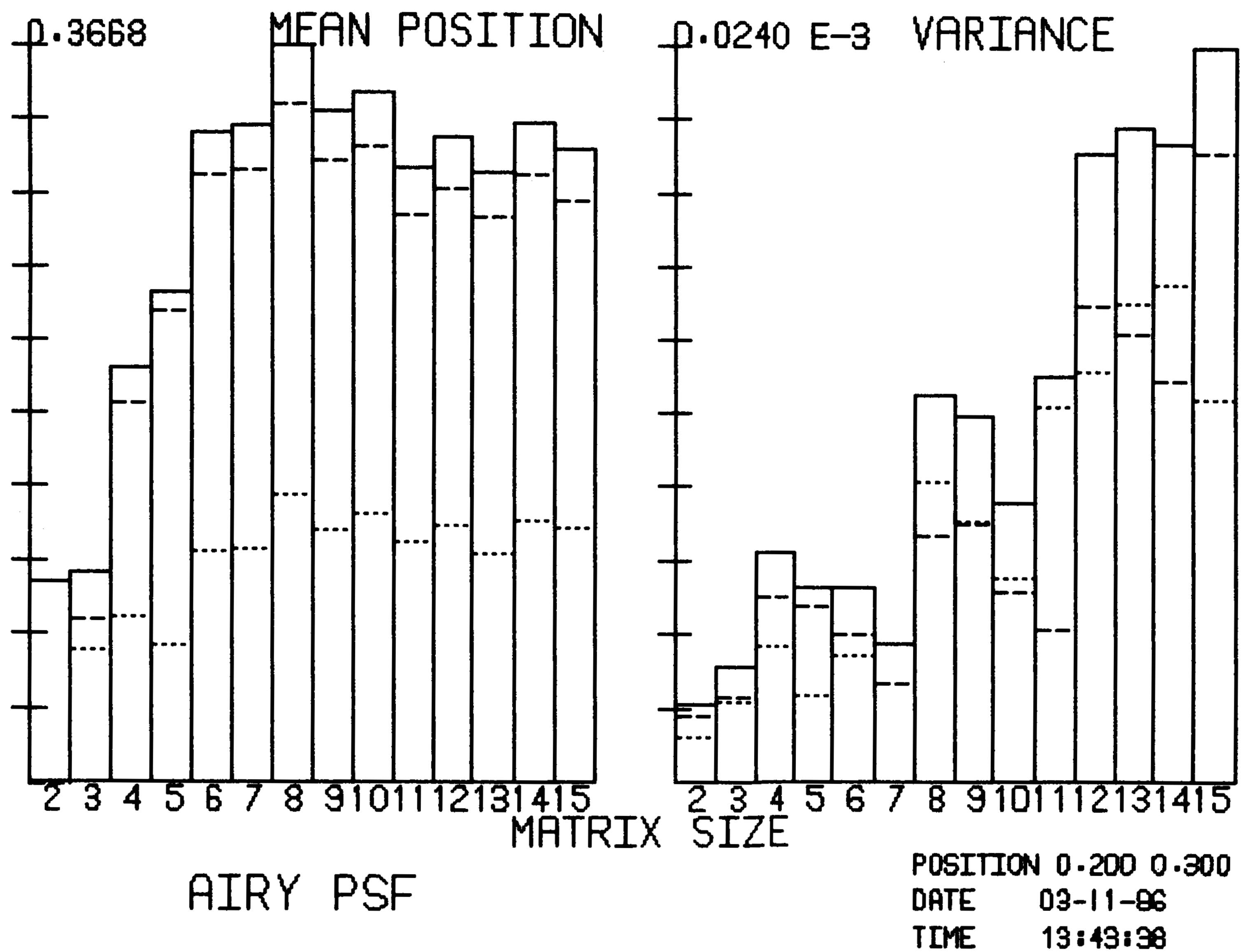

Fig. 51 Position Estimate as a Function of Matrix Size - Noisy CCD

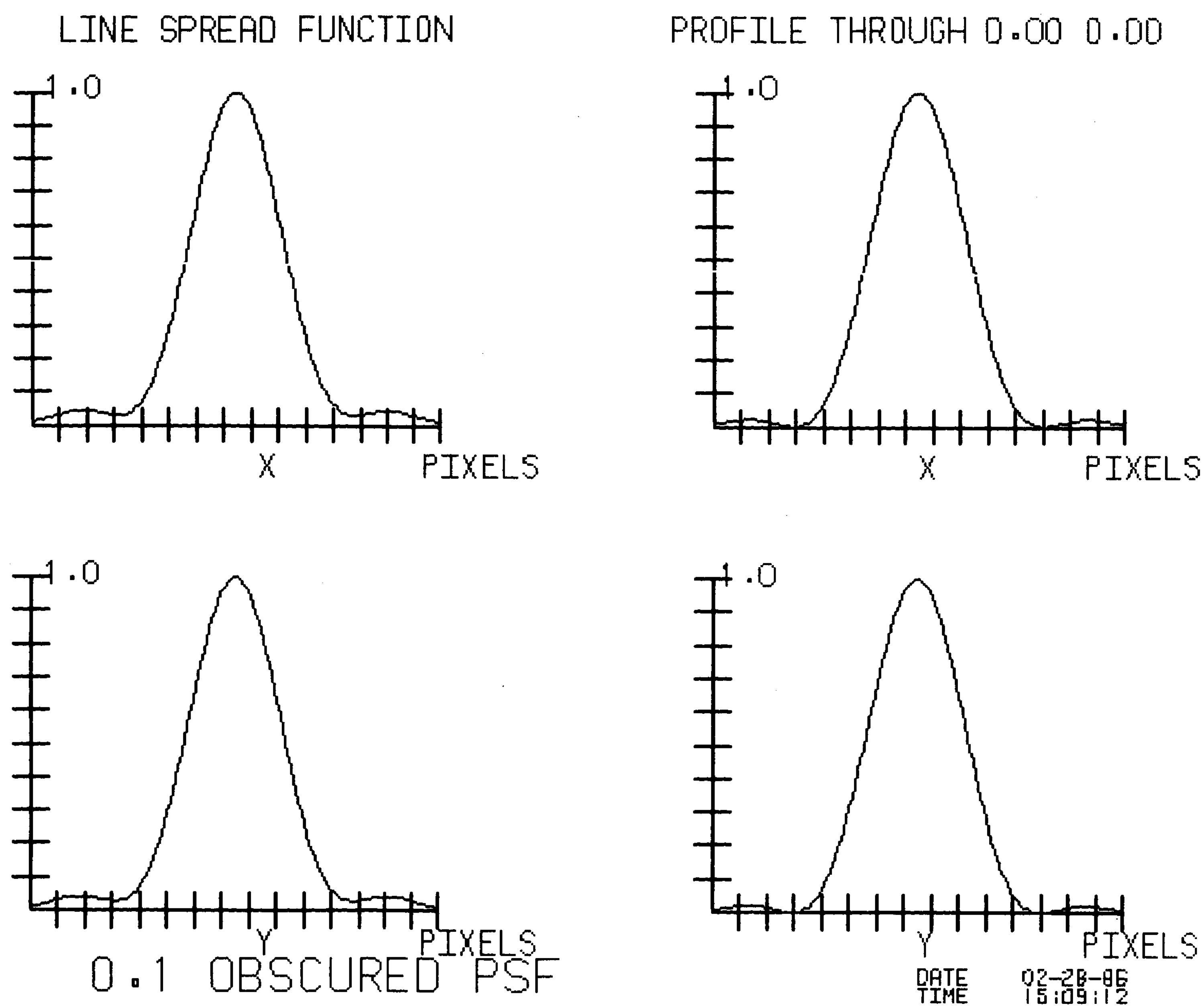

Fig. 52 Line Spread Functions - 10% Obscured PSF

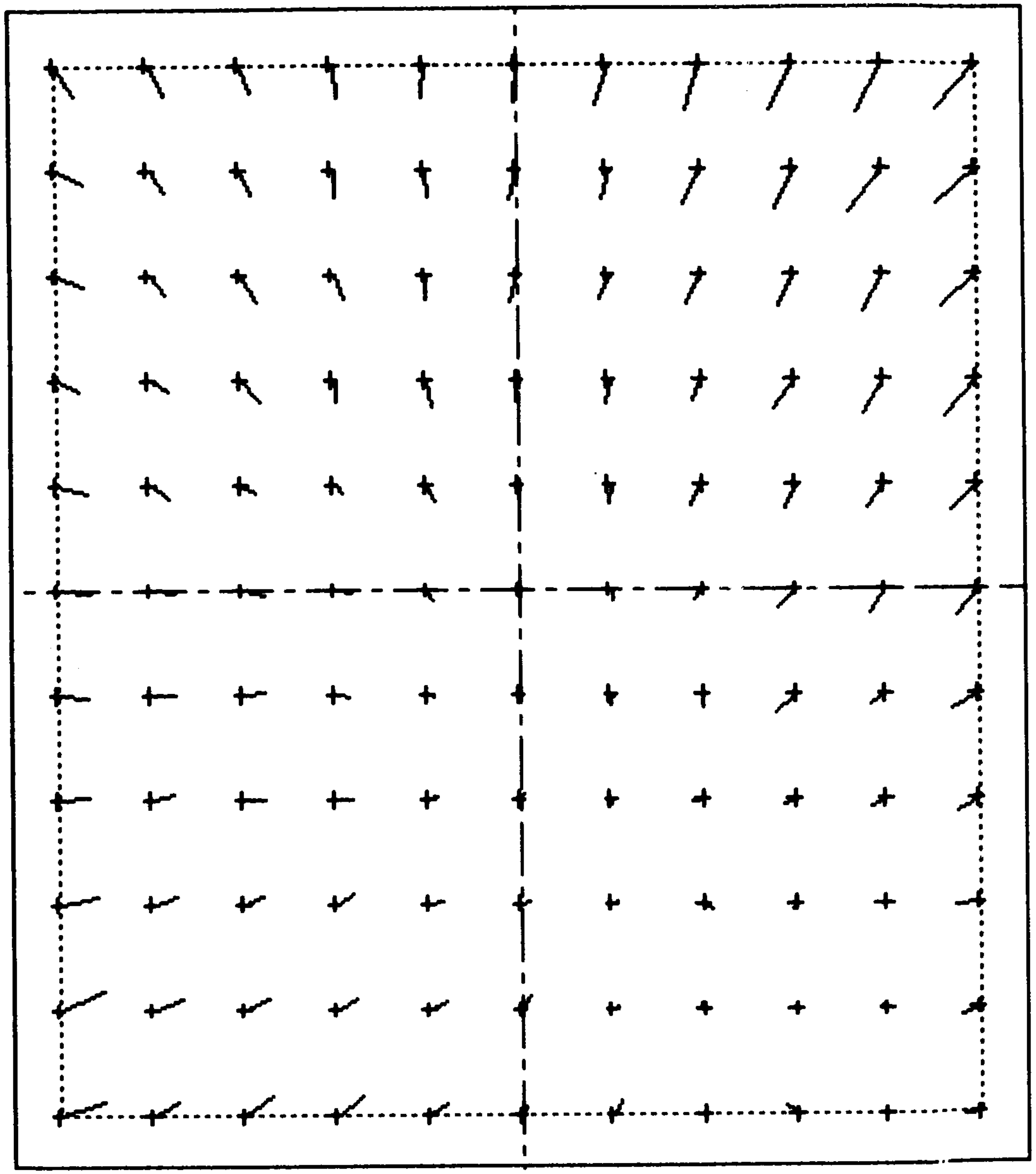

0.1 OBSCURED PSF

SCALE 1.0
MATRIX SIZE 15
ALGORITHM TYPE 2
CENTROID ORDER 1

RMS ERRORS

X	0.020
Y	0.020
RAD	0.028
ANG	41.084

DETECTOR PARAMETERS
SIGNAL 100000
DARK CURRENT 10
READ NOISE 10
RESP IRREGULARITY 0.010
CTE 0.99999 0.99999
PIXEL LOCATION 200 300
SATURATION LEVEL 250000
DARK SHADING OFF
RESP SHADING OFF
THRESHOLD TYPE NONE

DATE 02-28-88
TIME 15:27:42

Fig. 53 Pixel Performance Map - 10% Obscured PSF

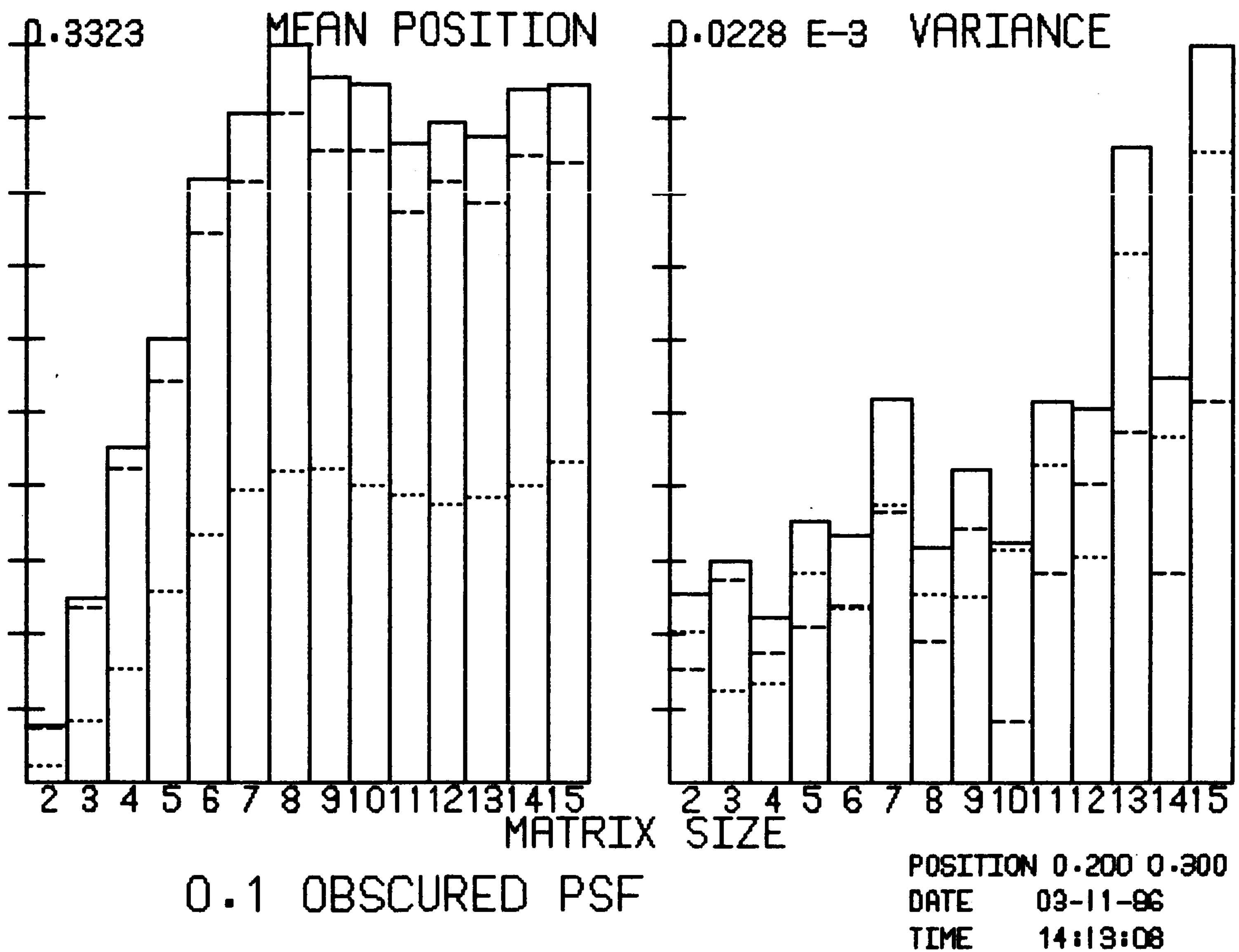

Fig. 54 Position Estimate as a Function of Matrix Size - Good CCD, 10% Obscured PSF

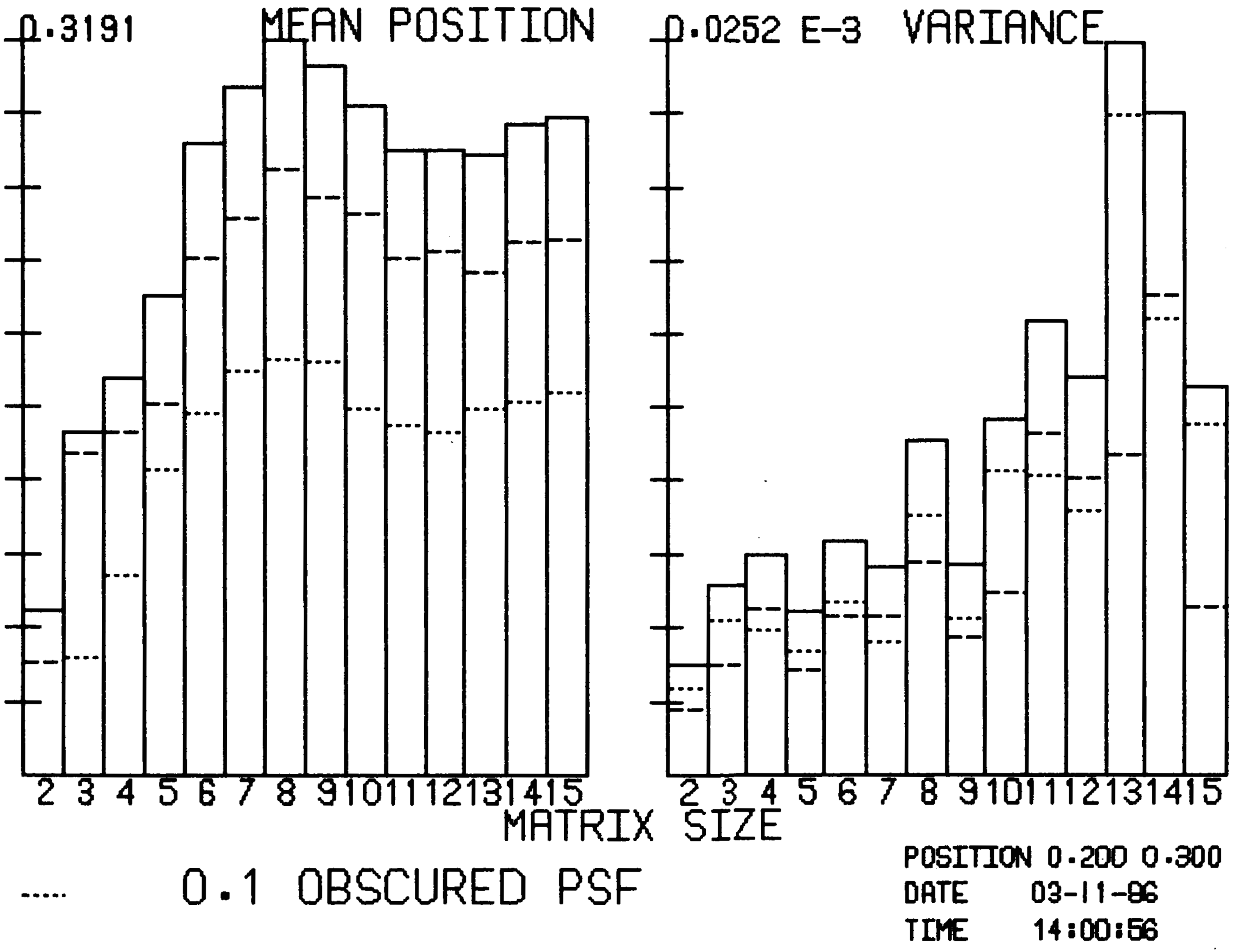

Fig. 55 Position Estimate as a Function of Matrix Size - Noisy CCD, 10% Obscured PSF

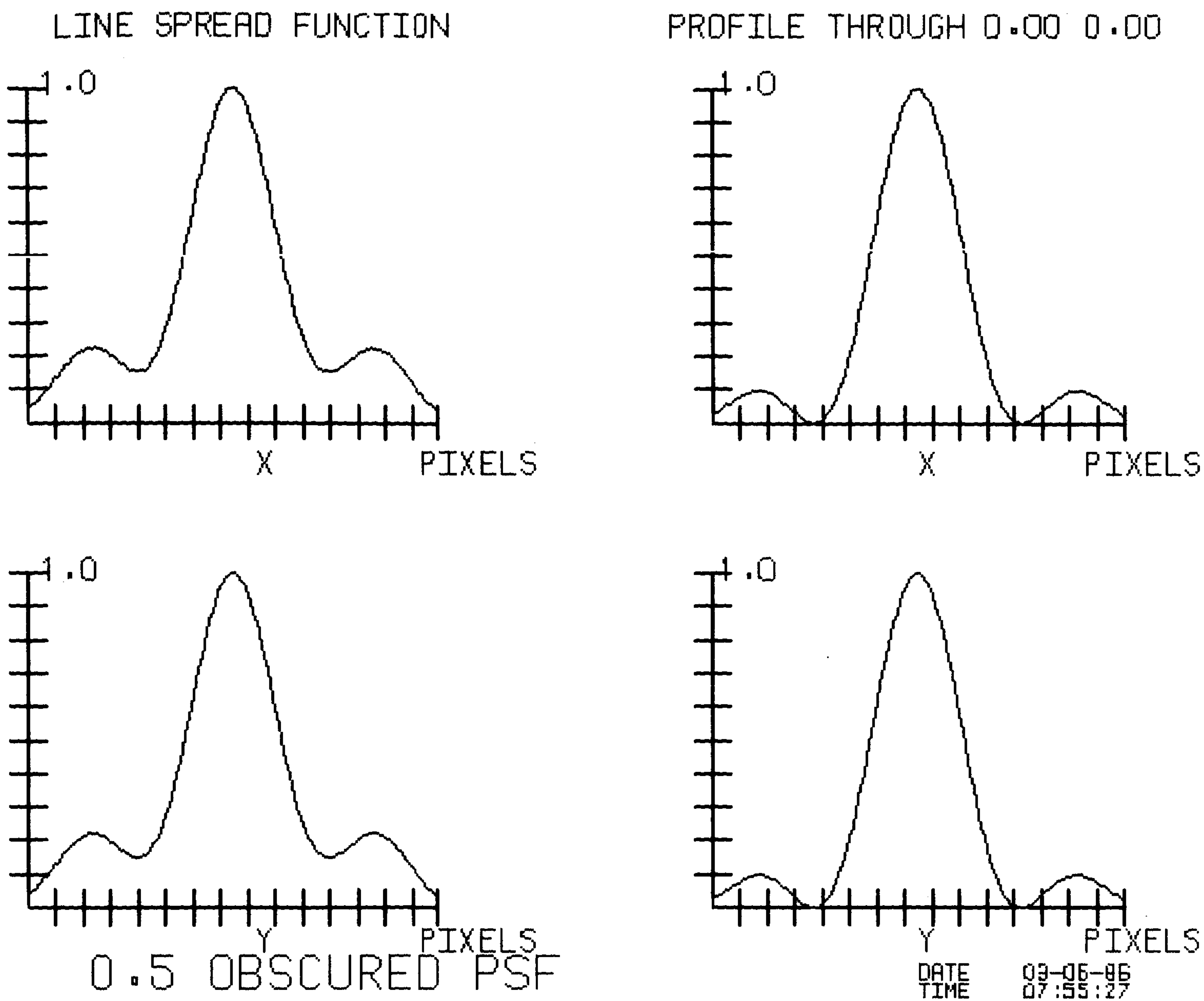

Fig. 56 Line Spread Functions - 50% Obscured PSF

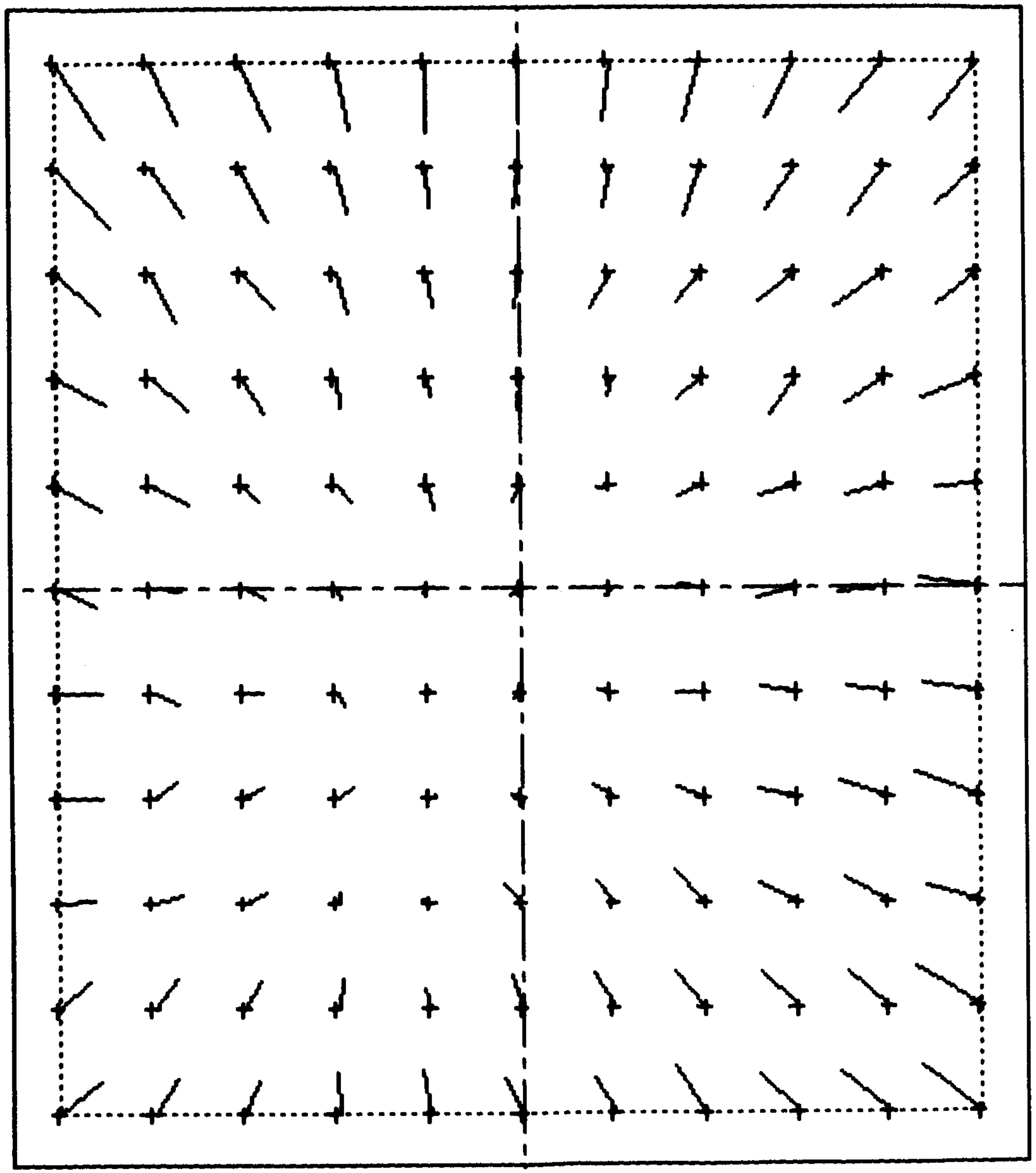

0.5 OBSCURED PSF

SCALE 1.0
MATRIX SIZE 15
ALGORITHM TYPE 2
CENTROID ORDER 1

RMS ERRORS

X	0.034
Y	0.031
RAD	0.046
ANG	40.505

DETECTOR PARAMETERS
SIGNAL 100000
DARK CURRENT 10
READ NOISE 10
RESP IRREGULARITY 0.010
CTE 0.99999 0.99999
PIXEL LOCATION 200 300
SATURATION LEVEL 250000
DARK SHADING OFF
RESP SHADING OFF
THRESHOLD TYPE NONE

DATE 03-05-86
TIME 08:03:37

Fig. 57 Pixel Performance Map - 50% Obscured PSF

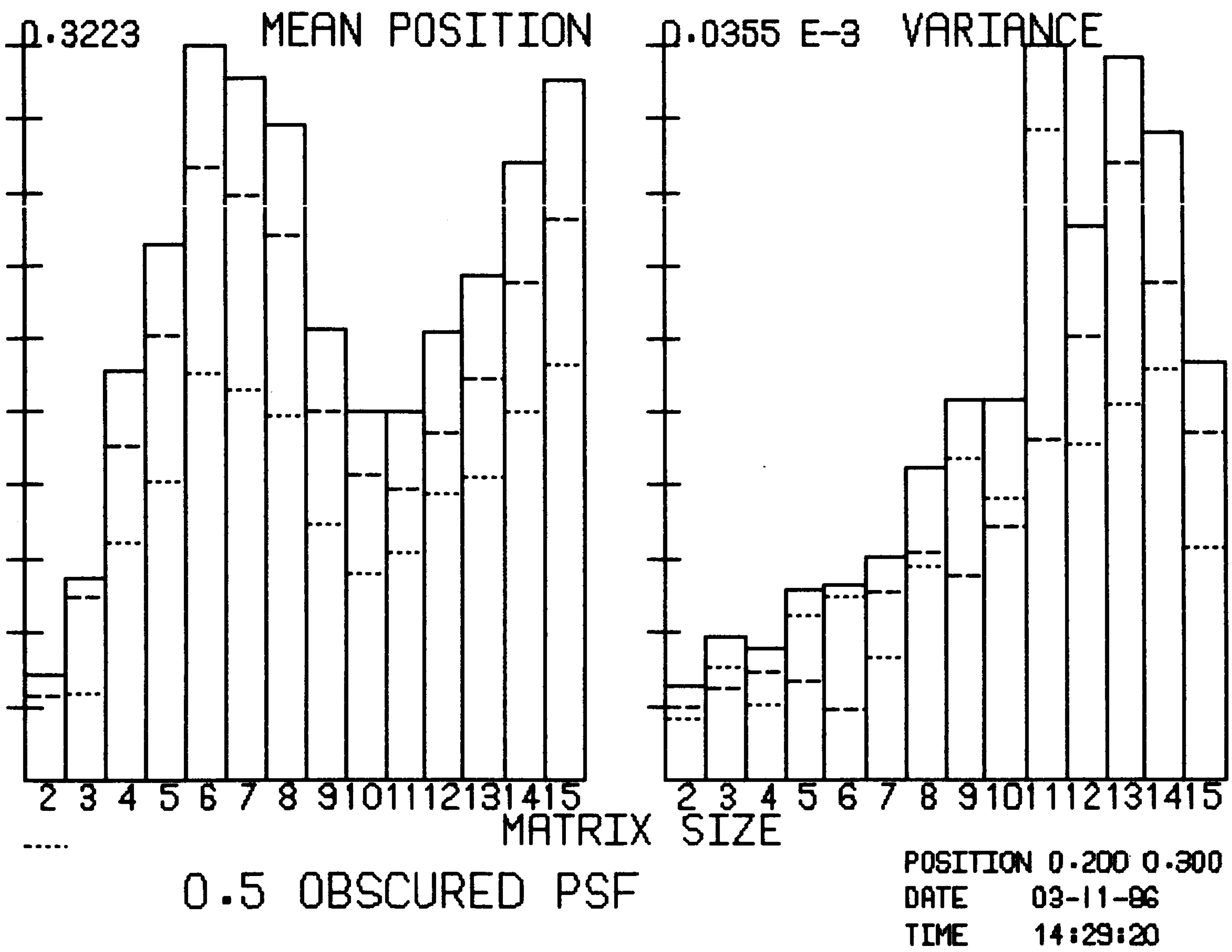

Fig. 58 Position Estimate as a Function of Matrix Size - Good CCD, 50% Obscured PSF

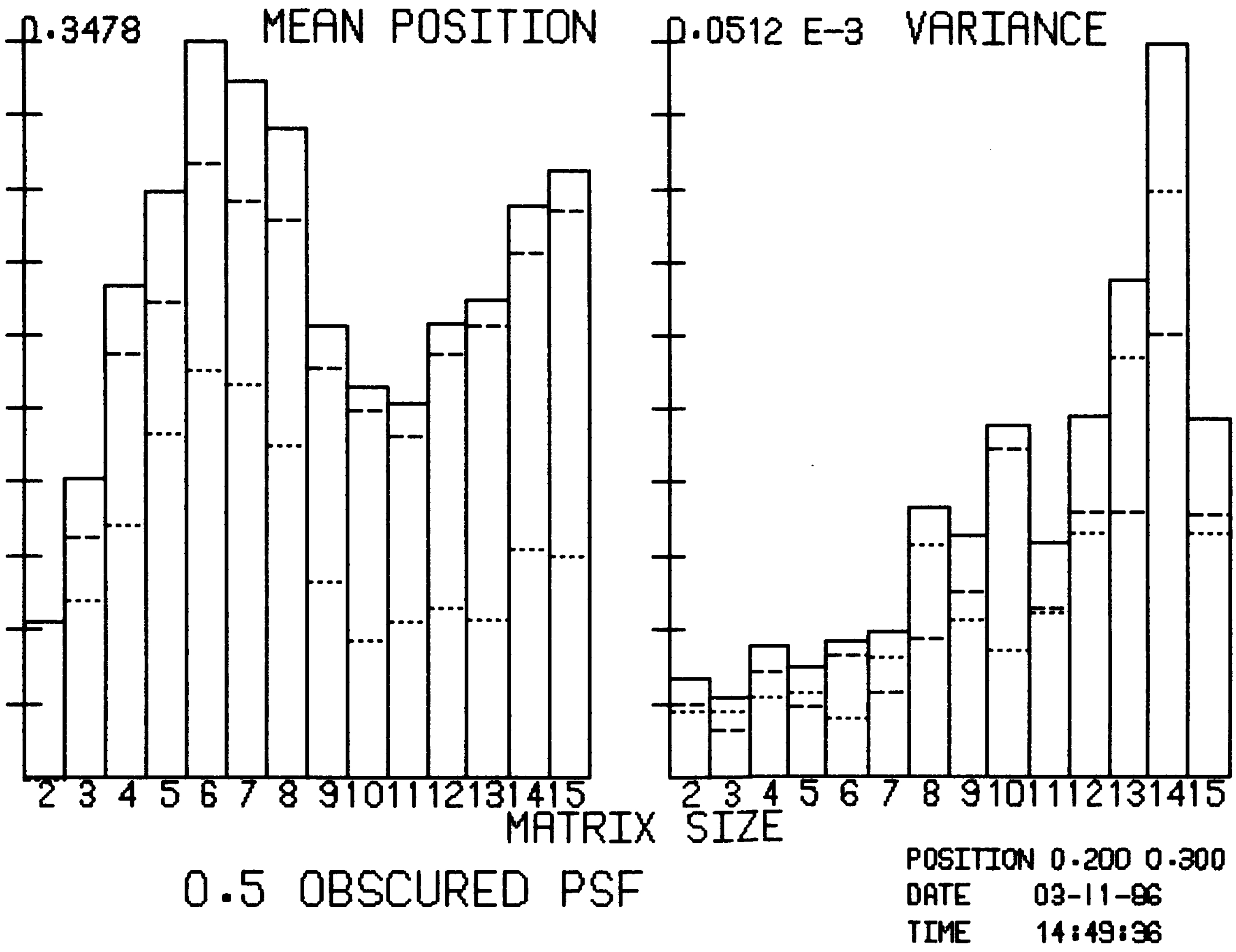

Fig. 59 Position Estimate as a Function of Matrix Size - Noisy CCD, 50% Obsucred PSF

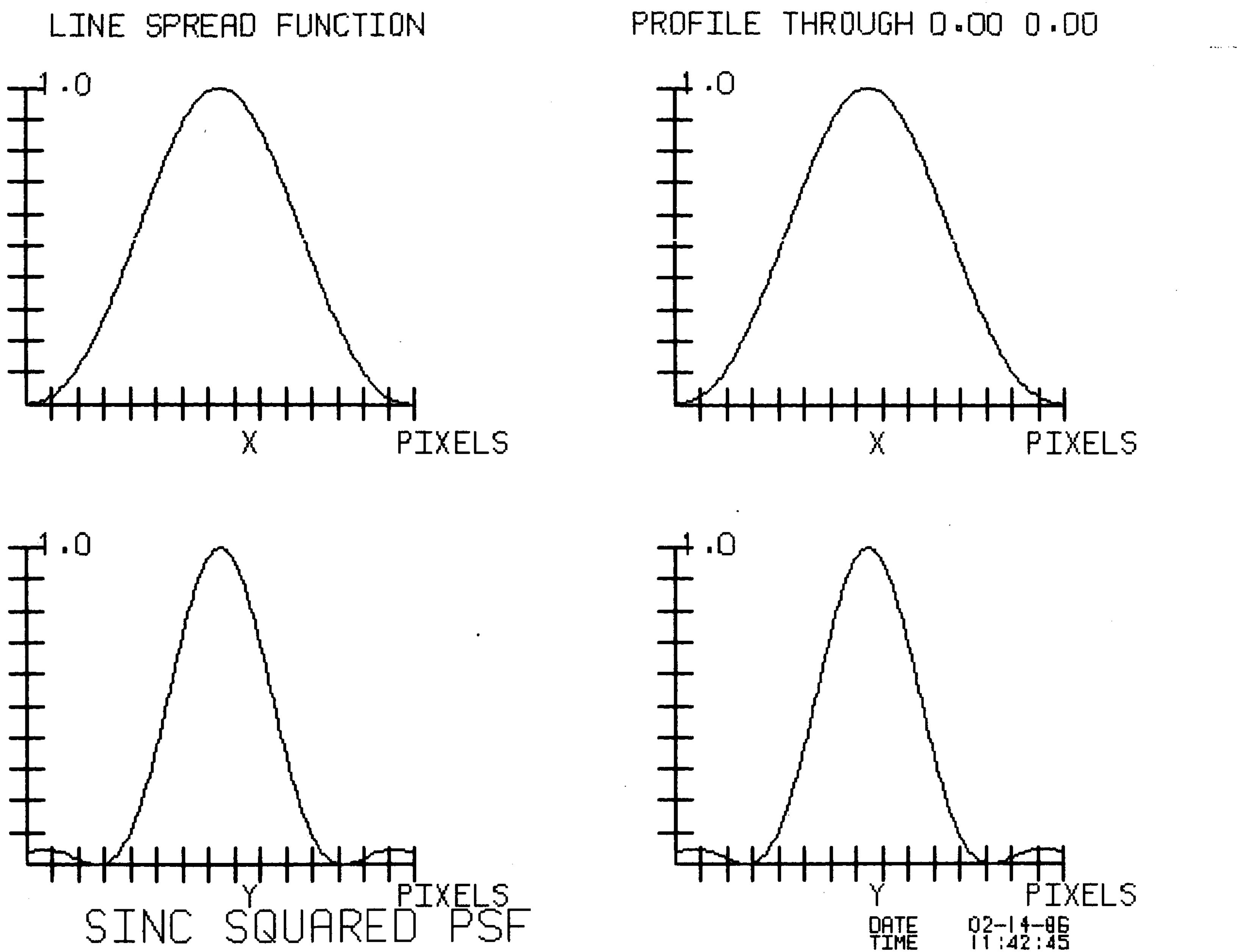

Fig. 60 Line Spread Functions - $Sinc^2$ PSF

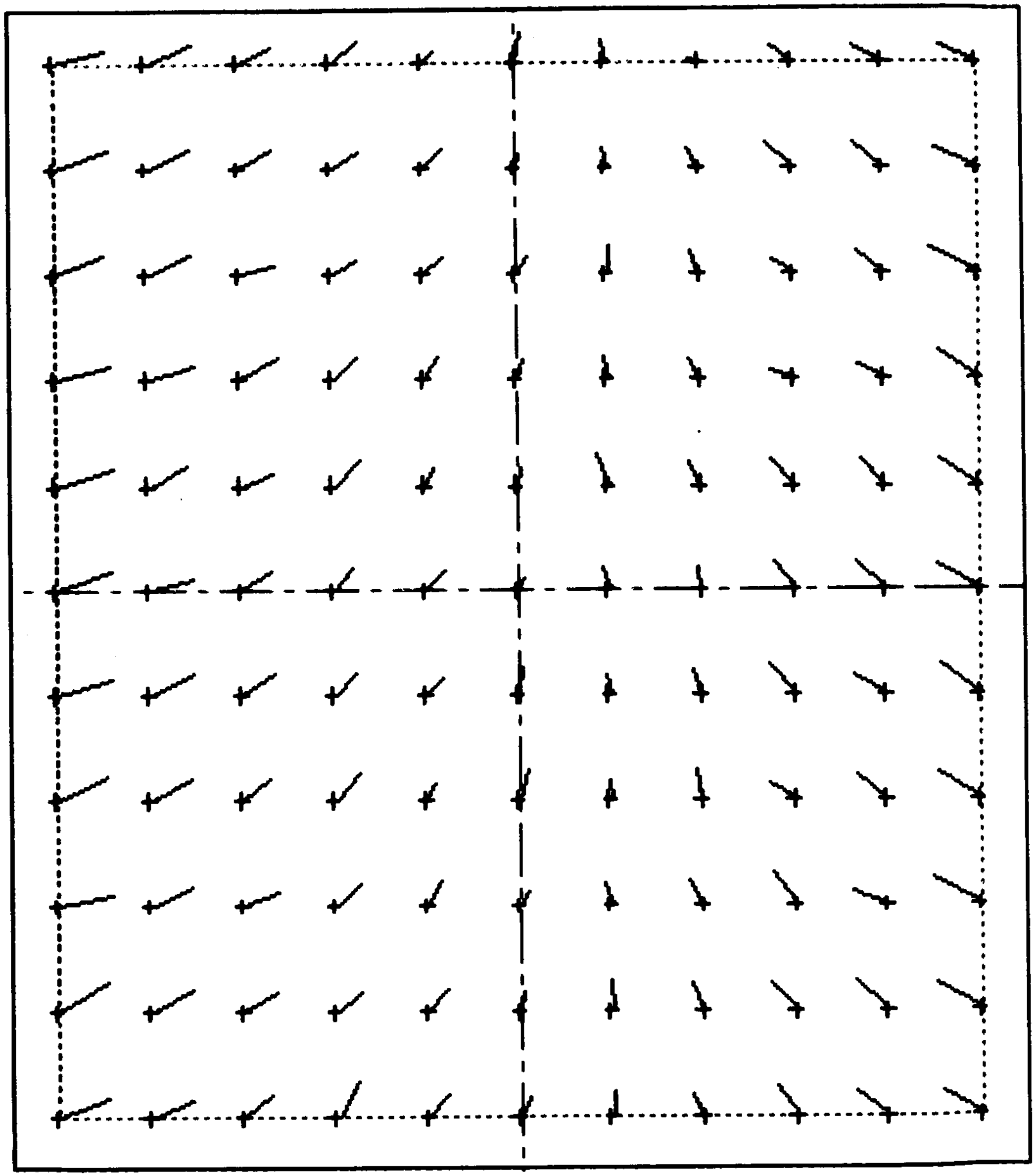

Fig. 61 Pixel Performance Map - Sinc^2 PSF

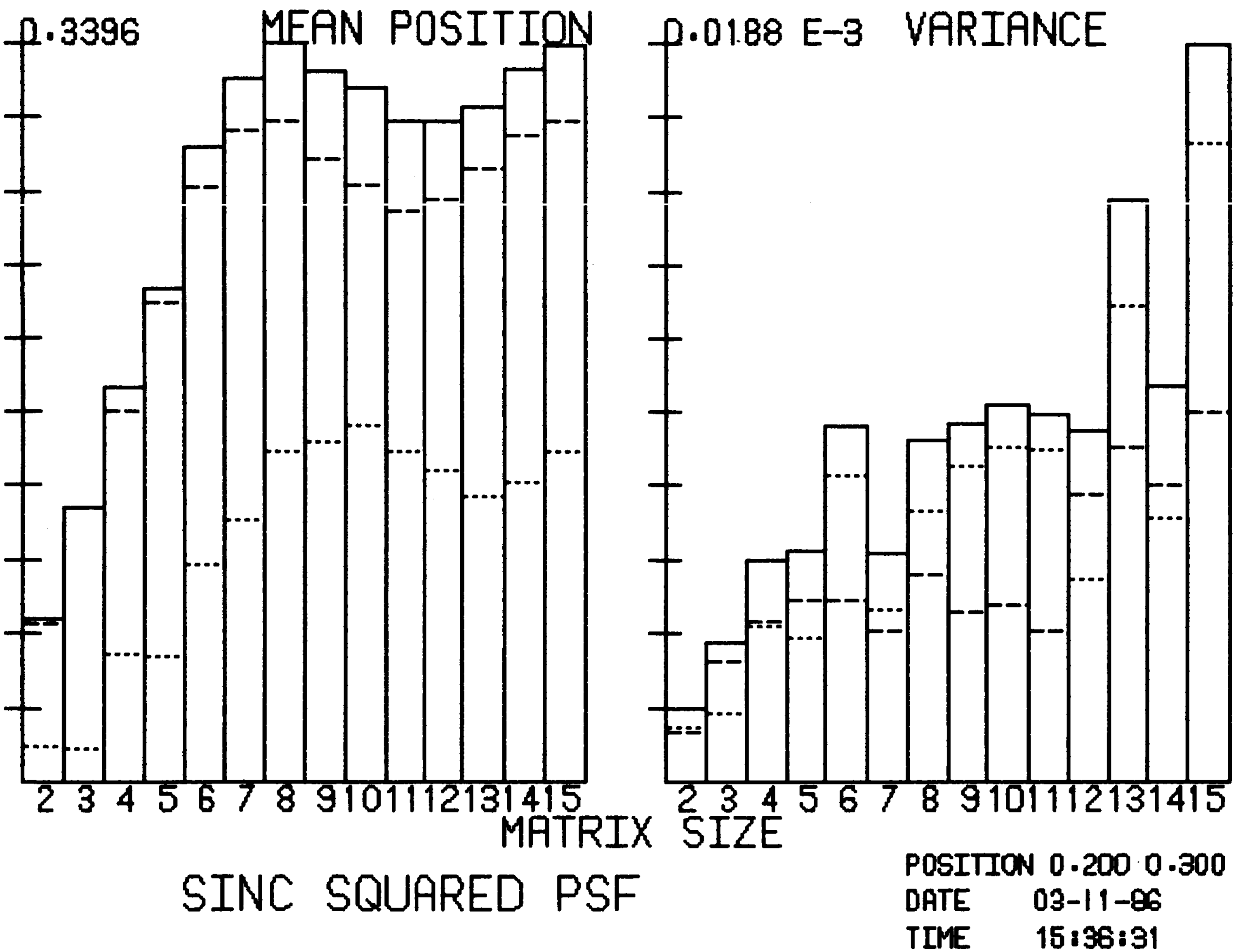

Fig. 62 Position Estimate as a Function of Matrix Size - Good CCD, $sinc^2$ PSF

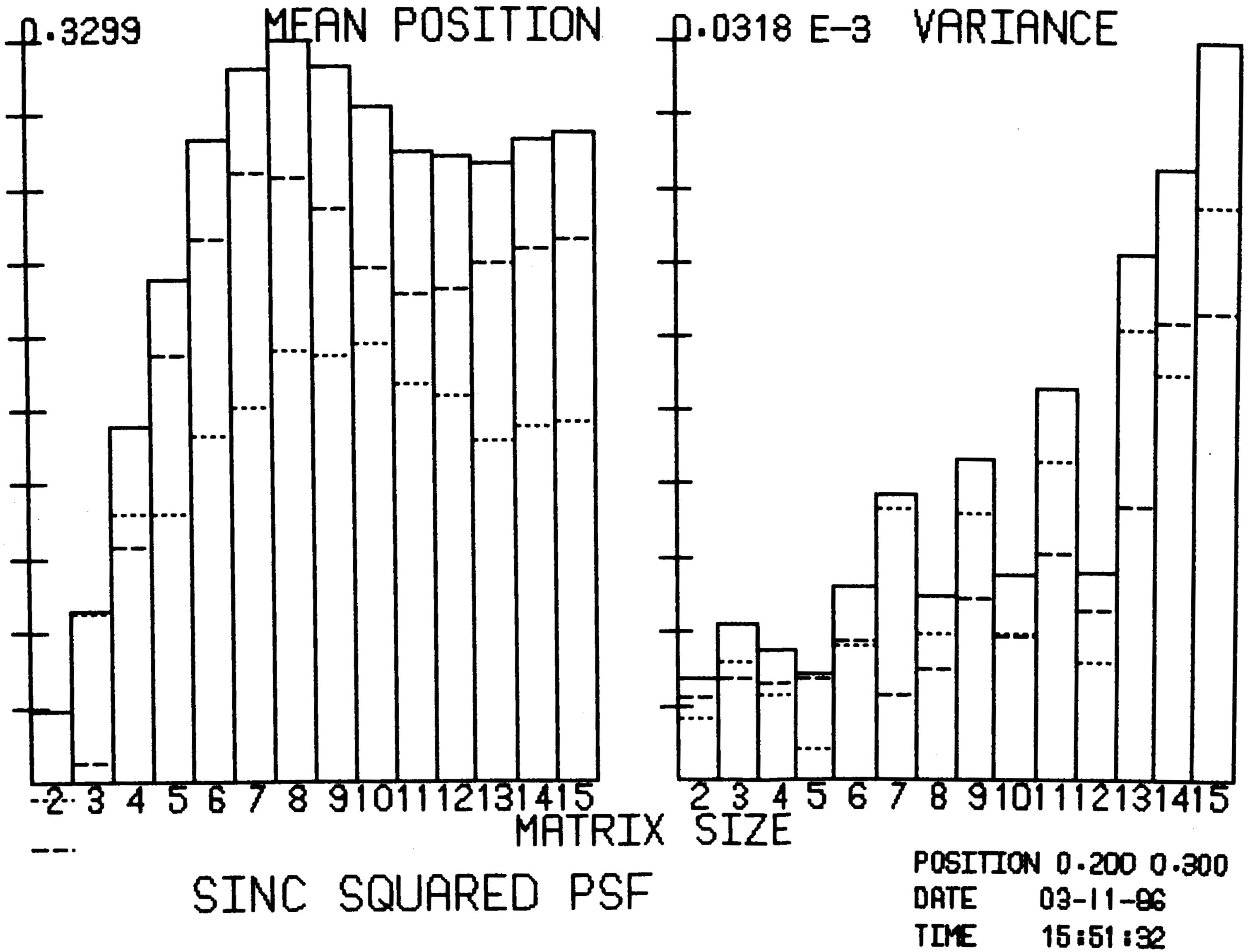

Fig. 63 Position Estimate as a Function of Matrix Size - Noisy CCD, sinc^2 PSF

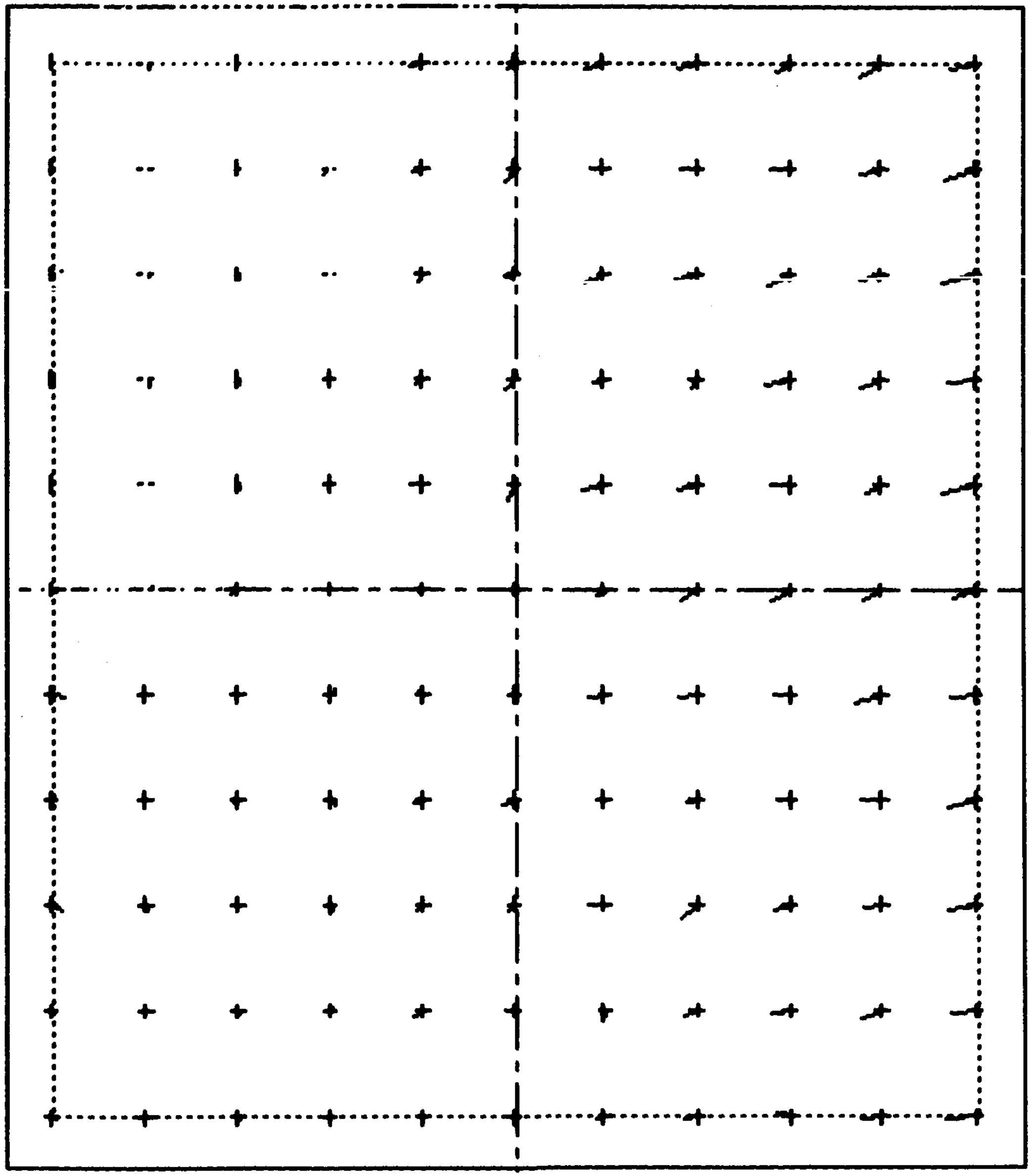

GAUSSIAN DISTRIBUTION

SCALE 1.0
MATRIX SIZE 15
ALGORITHM TYPE 2
CENTROID ORDER 1

RMS ERRORS

X	0.017
Y	0.006
RAD	0.018
ANG	30.410

DETECTOR PARAMETERS
SIGNAL 100000
DARK CURRENT 10
READ NOISE 10
RESP IRREGULARITY 0.010
CTE 0.99999 0.99999
PIXEL LOCATION 200 300
SATURATION LEVEL 250000
DARK SHADING OFF
RESP SHADING OFF
THRESHOLD TYPE 2
THRESHOLD FACTOR 20.0000

DATE 09-07-88
TIME 08:31:12

Fig. 64. Pixel Performance Map - Constant Threshold

c-2

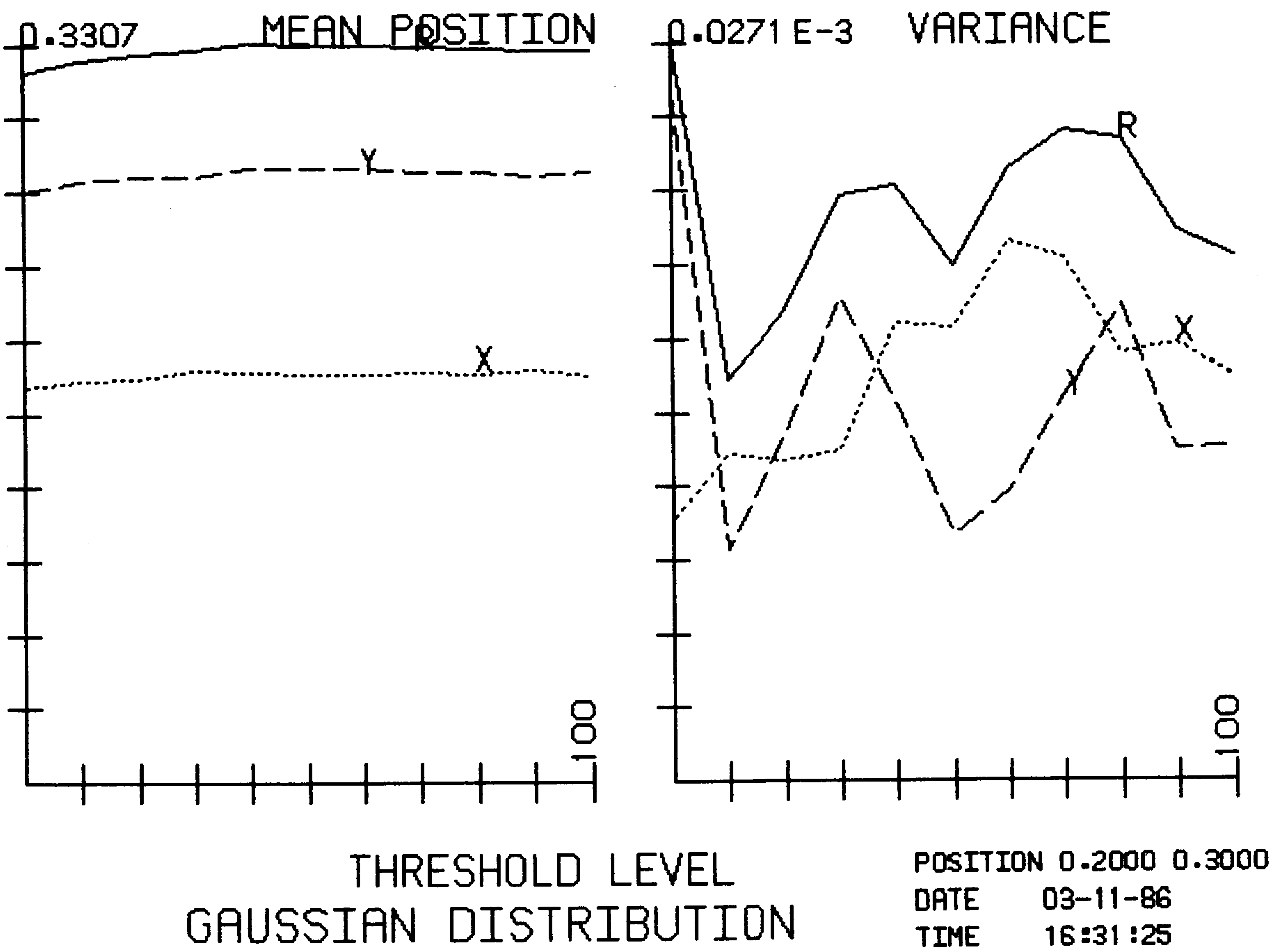

Fig. 65 Position Estimate as a Function of Threshold Value - Good CCD

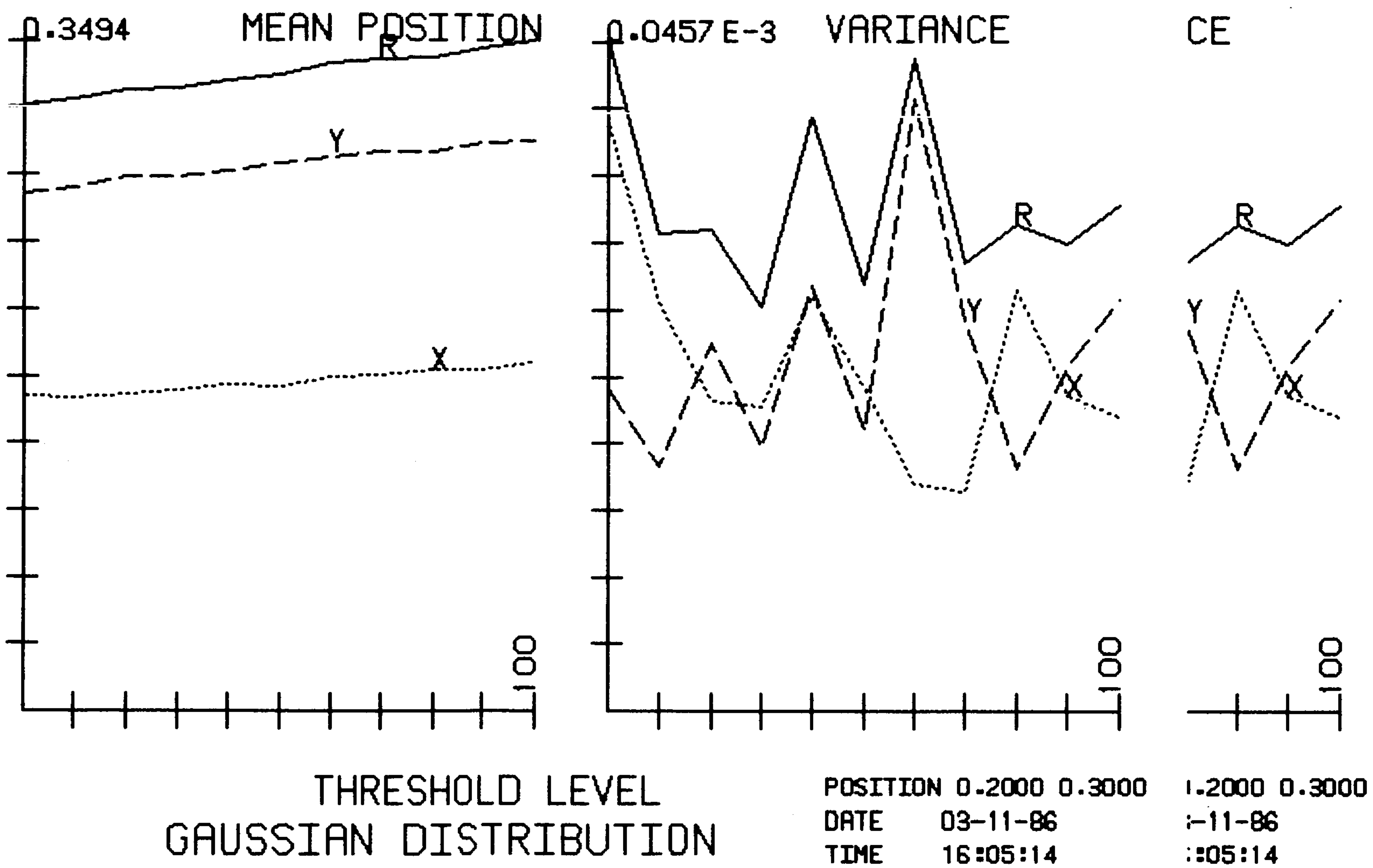

Fig. 66 Position Estimate as a Function of Threshold Value - Noisy CCD, Matrix Size 15

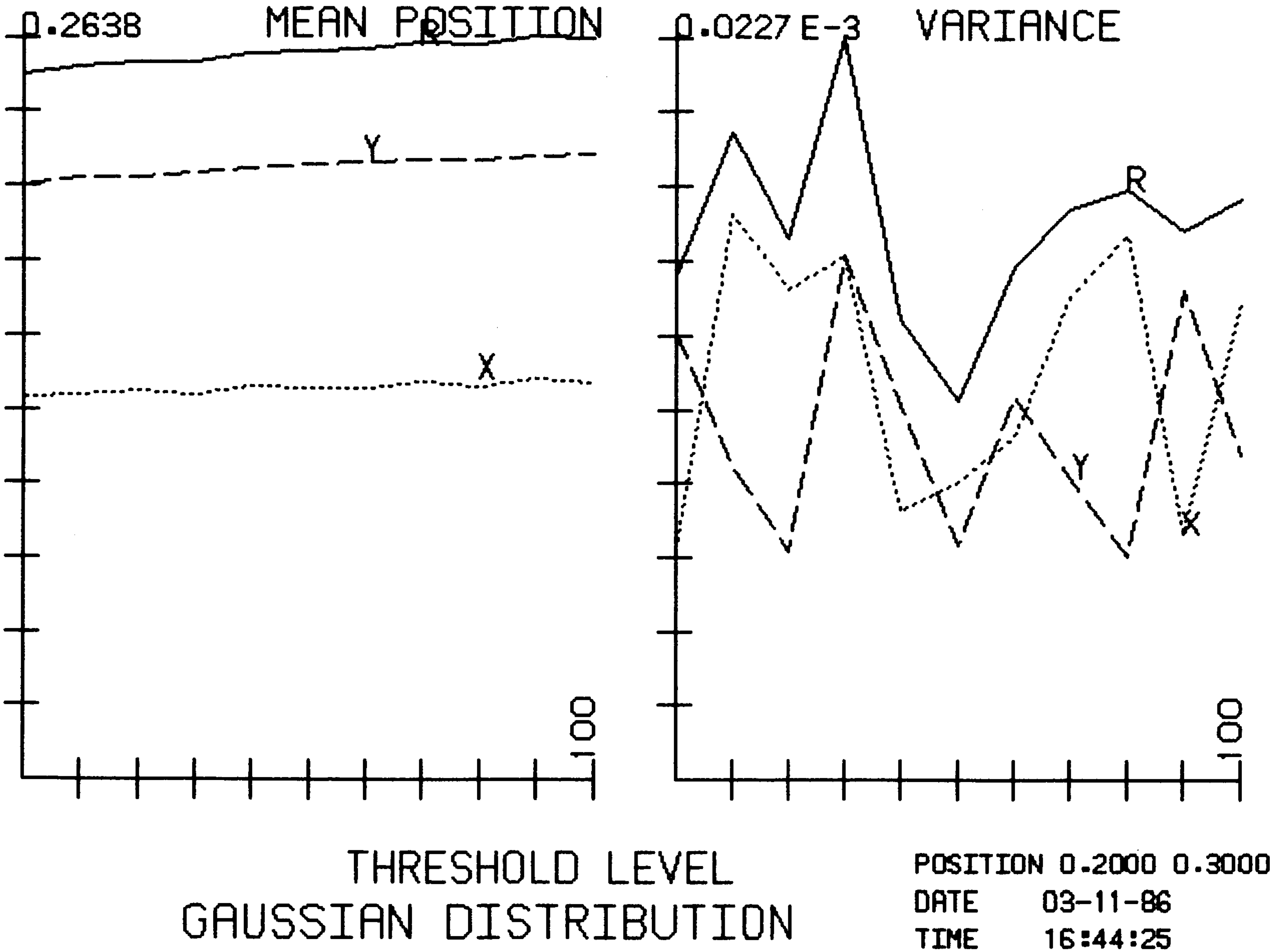

Fig. 67 Position Estimate as a Function of Threshold Value - Noisy CCD, Matrix Size 10

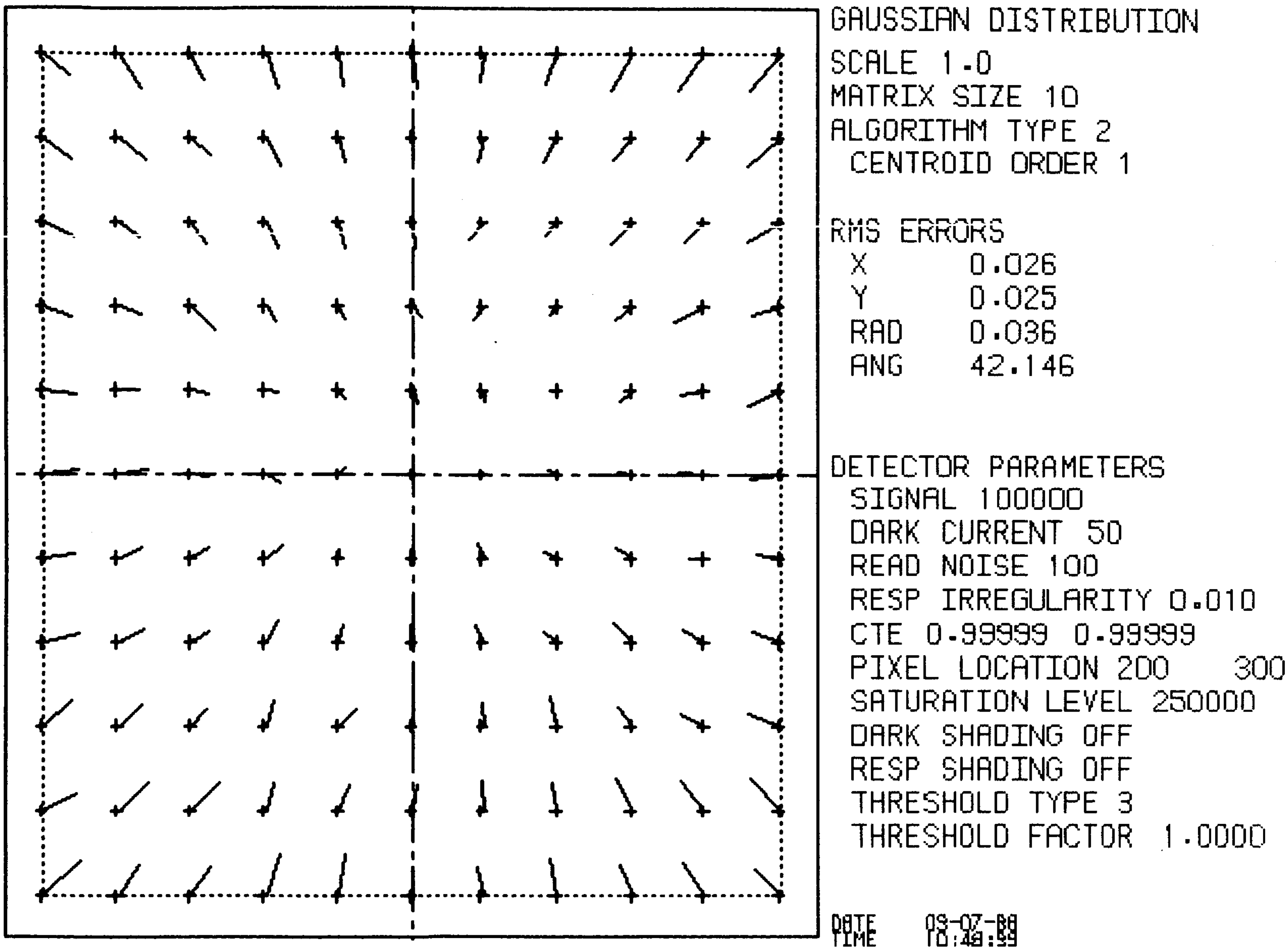

Fig. 68 Pixel Performance Map - Gaussian PSF - Guard Band Threshold

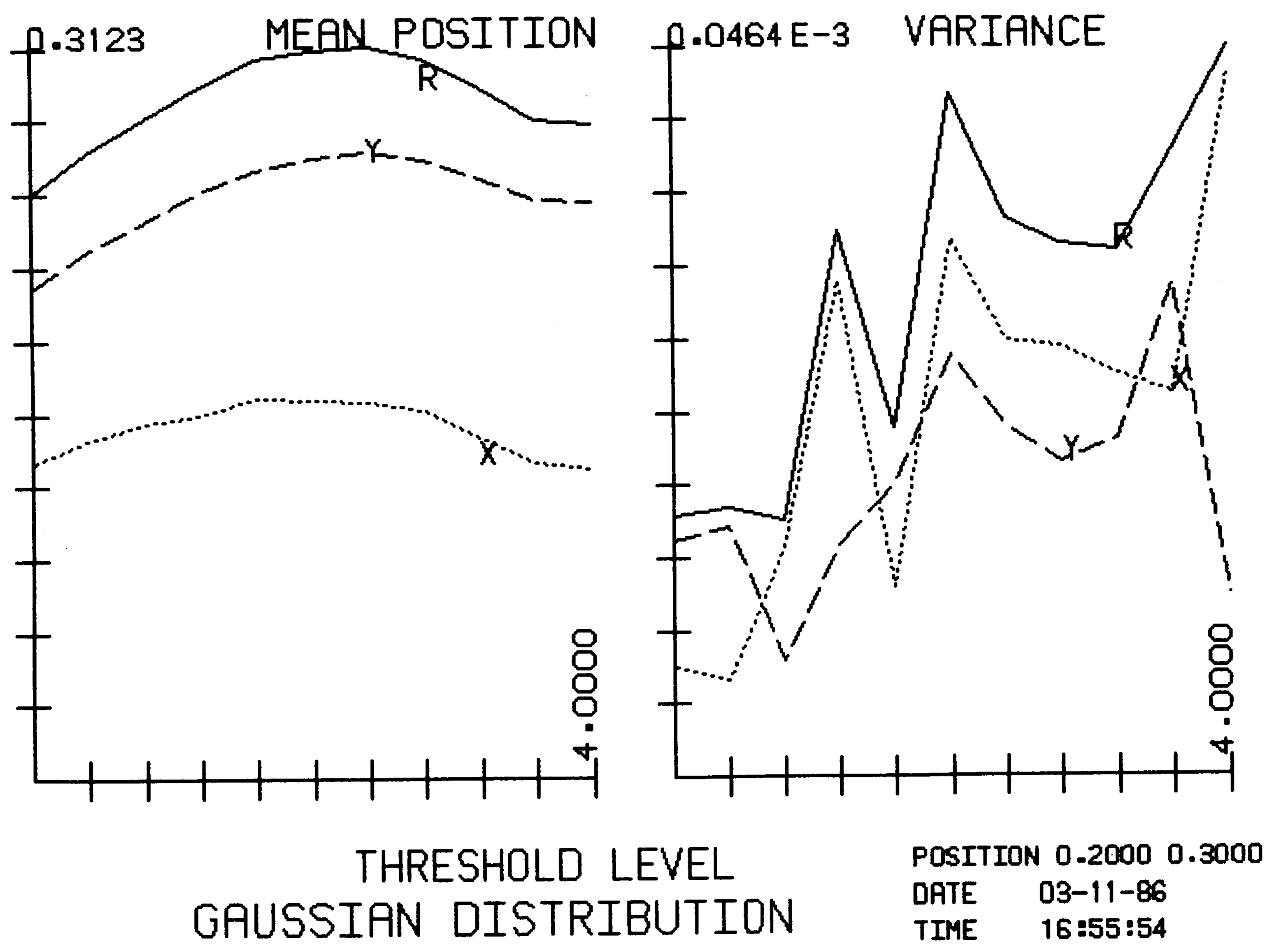

Fig. 69 Position Estimate as a Function of Threshold Value, RMS Guard Band Threshold

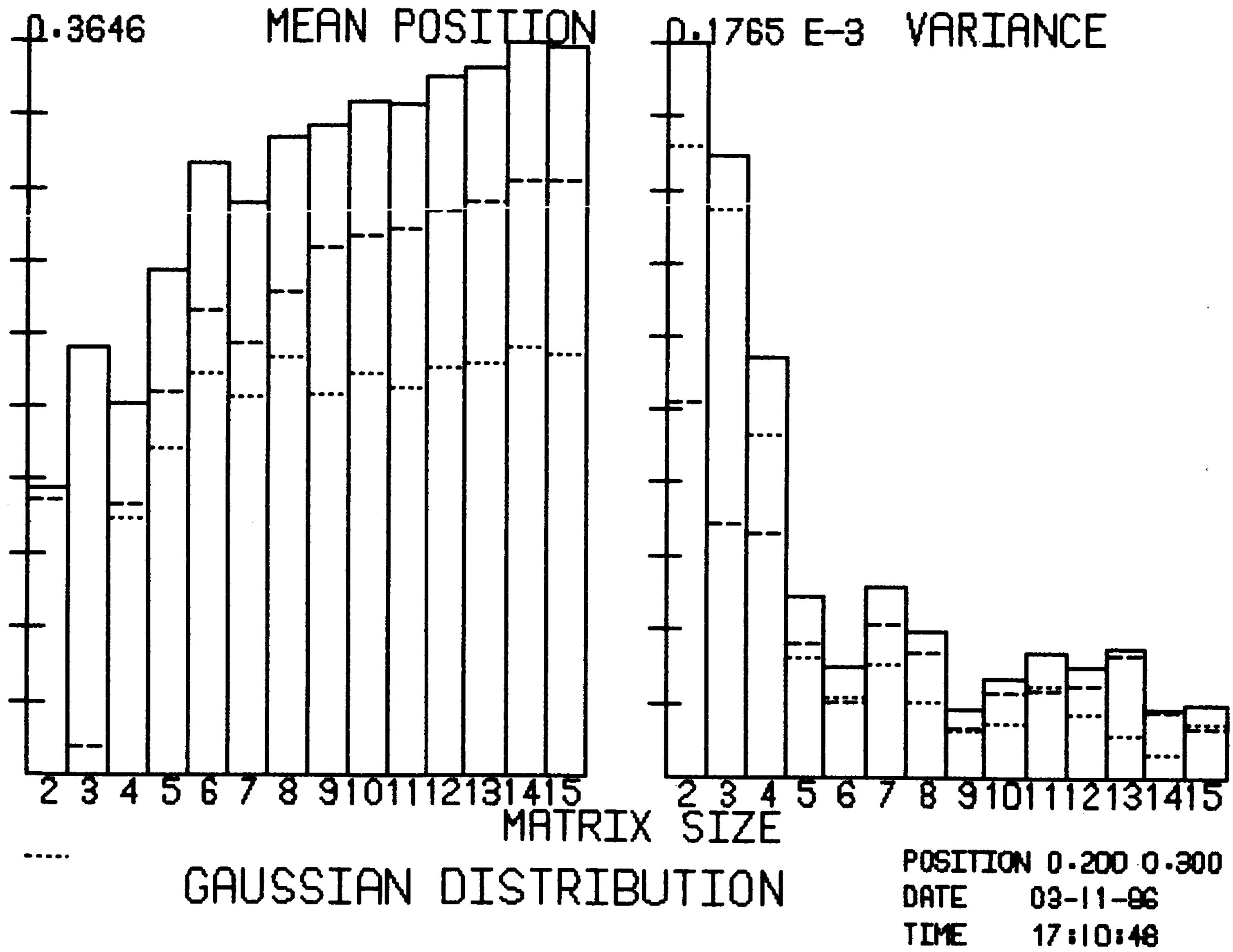

Fig. 70 Position Estimate as a Function of Matrix Size, RMS Guard Band Threshold

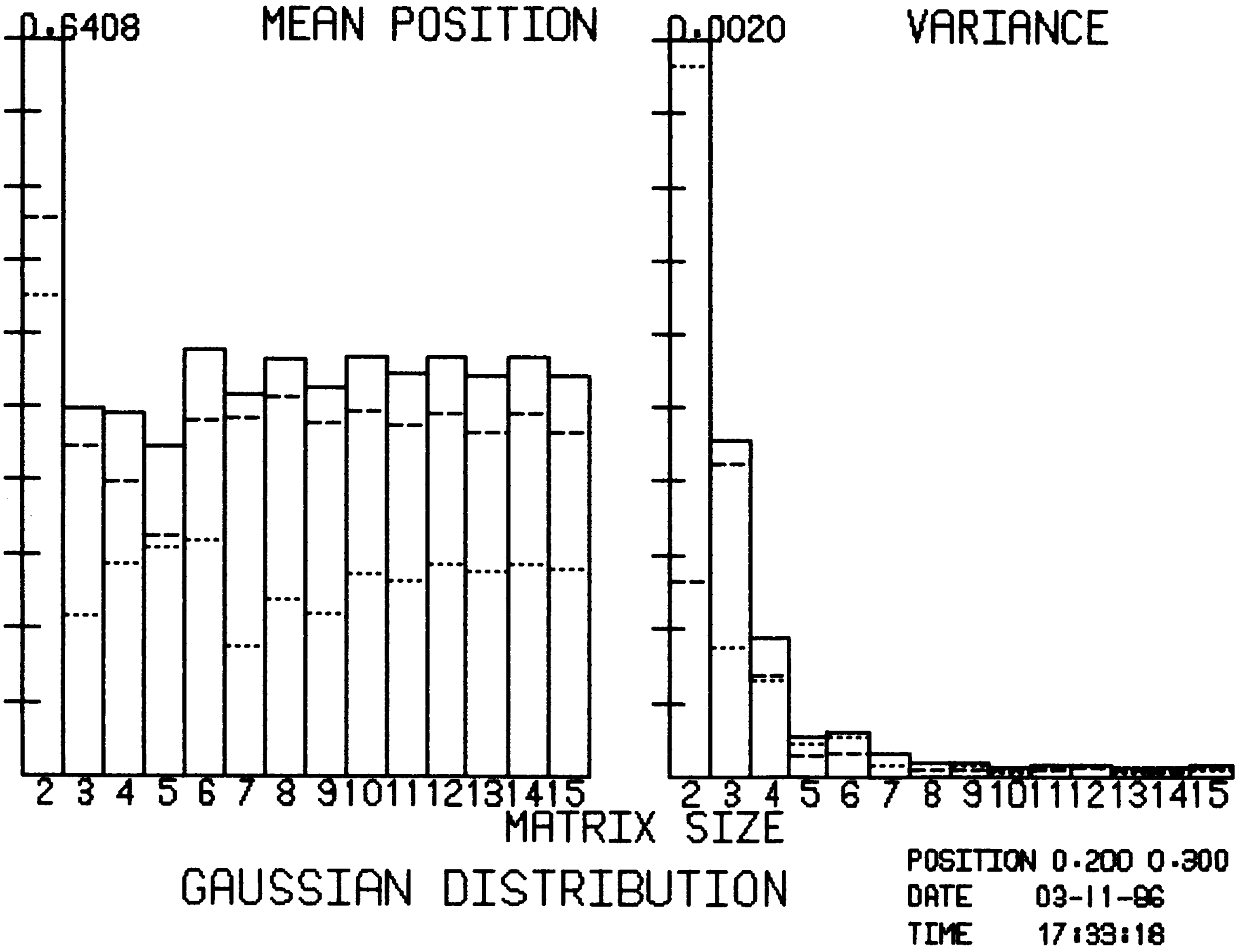

Fig. 71 Position Estimate as a Function of Threshold Value, Maximum Guard Band

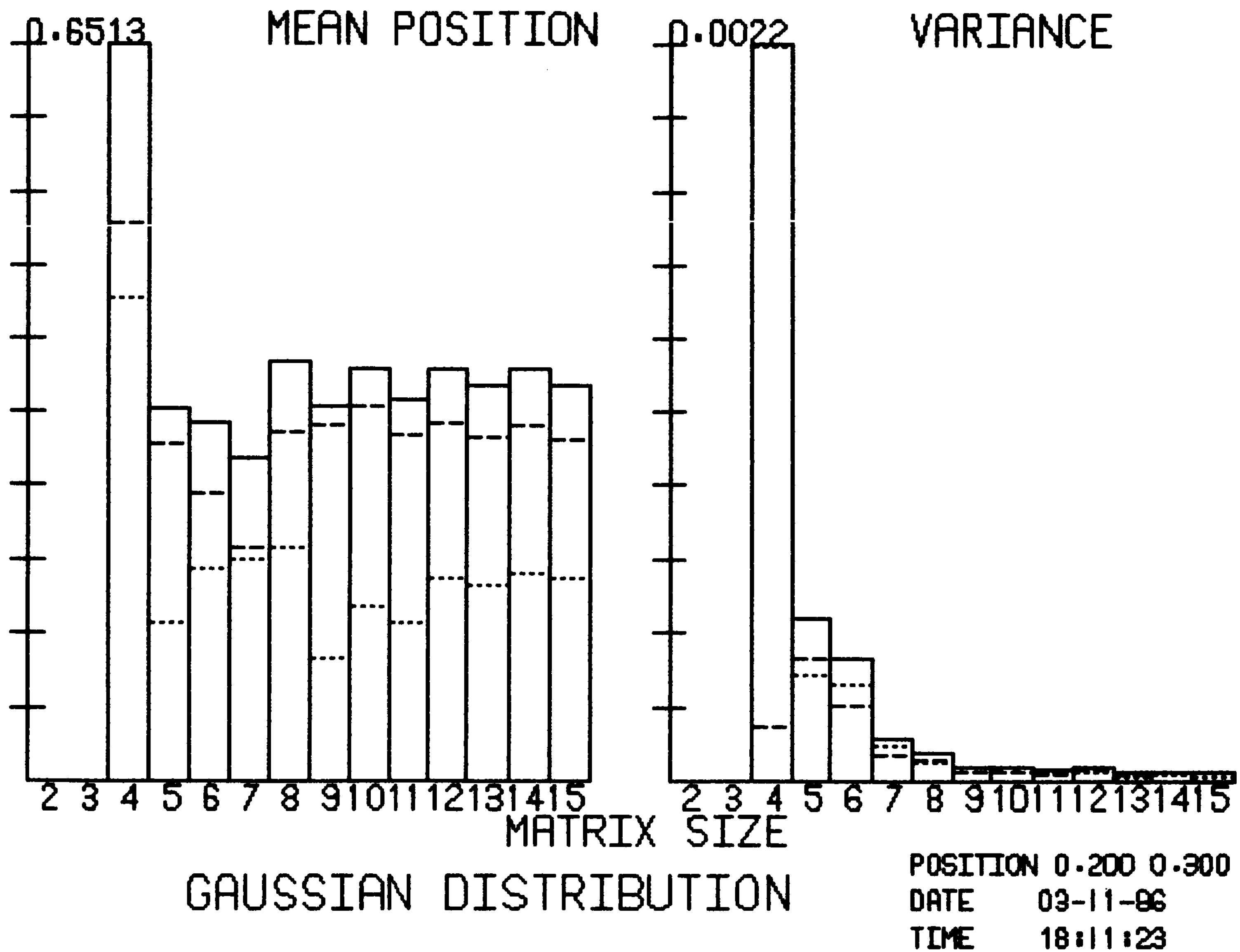

Fig. 72 Position Estimate as a Function of Matrix Size, RMS Matrix Outer Band Threshold

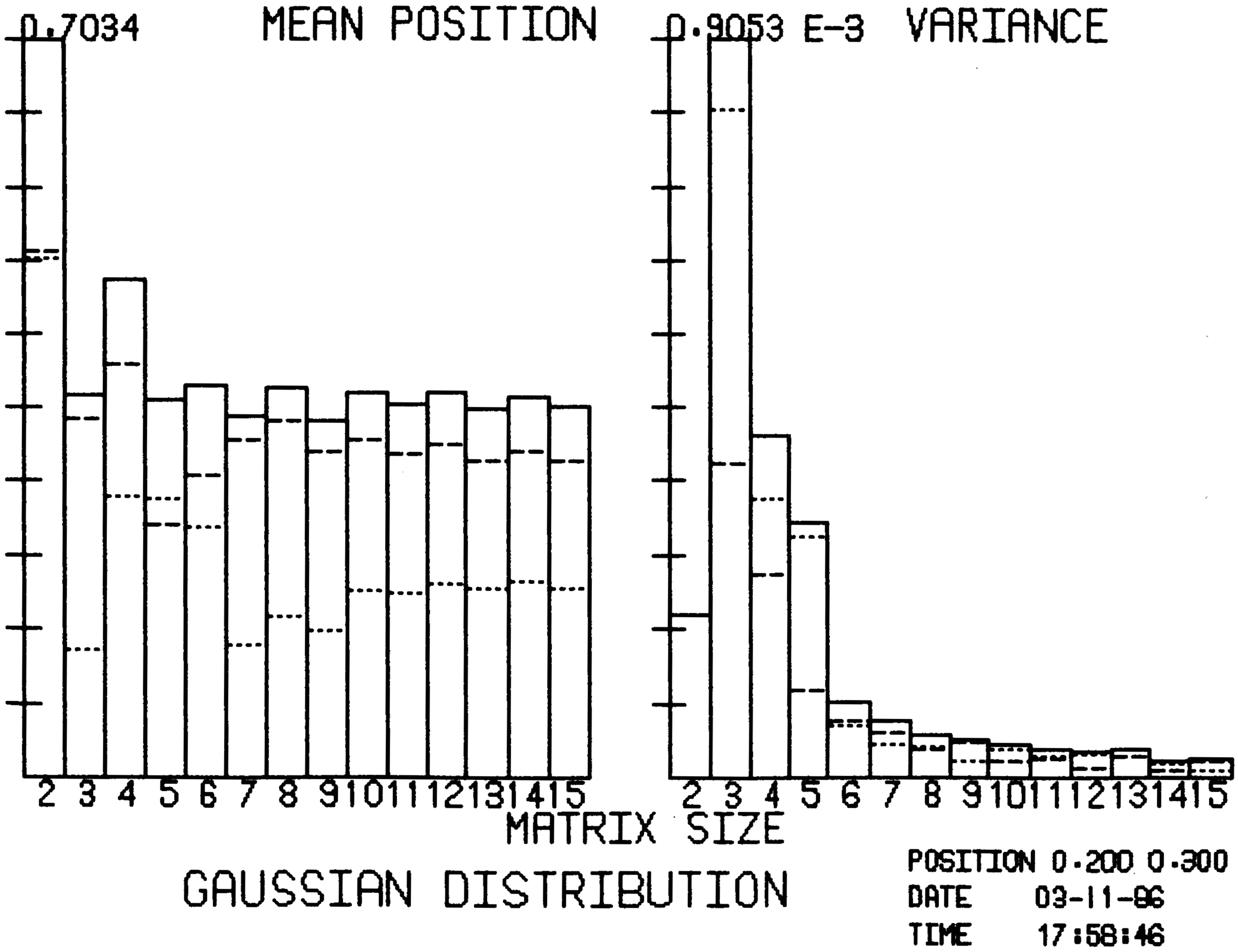

Fig. 73 Position Estimate as a Function of Matrix Size, Maximum Outer Band Threshold

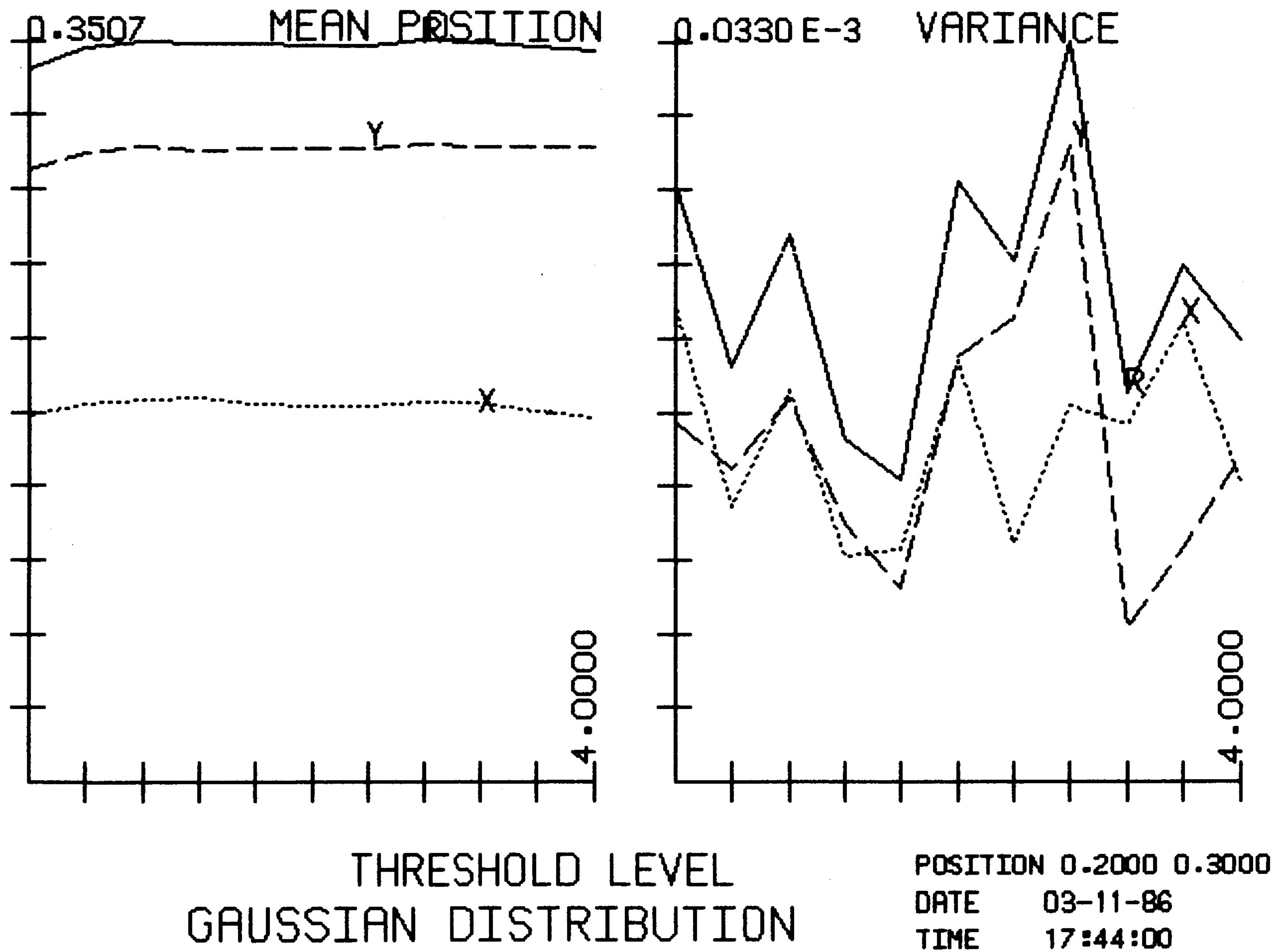

Fig. 74 Position Estimate as a Function of Threshold Value, Maximum Outer Band Threshold

TECHNICAL REPORT STANDARD TITLE PAGE

1. Report No. JPL Pub. 86-21	2. Government Accession No.	3. Recipient's Catalog No.
4. Title and Subtitle Centroid Tracking With Area Array Detectors		5. Report Date June 1, 1986 6. Performing Organization Code
7. Author(s) T.A. Glavich		8. Performing Organization Report No.
9. Performing Organization Name and Address JET PROPULSION LABORATORY California Institute of Technology 4800 Oak Grove Drive Pasadena, California 91109		10. Work Unit No. 11. Contract or Grant No. NAS7-918 13. Type of Report and Period Covered JPL Publication
12. Sponsoring Agency Name and Address NATIONAL AERONAUTICS AND SPACE ADMINISTRATION Washington, D.C. 20546		14. Sponsoring Agency Code RE 182 PX 644-11-000-407
15. Supplementary Notes		

16. Abstract

A computer program (ALGEVAL) has been developed to simulate the position estimating behavior of a centroid estimator algorithm using data typical of optical point spread function data recorded by an area array detector. Typical results are shown of varying detector properties and optical point spread function types. The detector parameters currently available for study include read noise mean value, dark current mean value and spatial variation, charge transfer efficiency and point spread function location, saturation level, signal level and pixel size. The program is capable of calculating any order centroid using an array size from 2 x 2 to 15 x 15 pixels. The output of the program is either a performance map, histogram data or tabluar data. A number of further developments are recommended.

17. Key Words (Selected by Author(s))	18. Distribution Statement
Computer Programming and Software Optical Detection	Unclassified -- Unlimited

19. Security Classif. (of this report)	20. Security Classif. (of this page)	21. No. of Pages	22. Price
Unclassified	Unclassified	viii + 99	

JPL 0184 R 9/83